NSF GRANT
GA - 32589X3

TROPICAL CYCLONE GENESIS

BY

WILLIAM M. GRAY

Atmospheric Science
PAPER NO.
234

DEPARTMENT OF ATMOSPHERIC SCIENCE
COLORADO STATE UNIVERSITY
FORT COLLINS, COLORADO

TROPICAL CYCLONE GENESIS

by

William M. Gray

Preparation of this report

has been financially supported by

National Science Foundation Grant GA-32589X3

Department of Atmospheric Science

Colorado State University

Fort Collins, Colorado

March, 1975

Atmospheric Science Paper No. 234

ABSTRACT

A new global observational and theoretical study of tropical cyclone genesis is made. This is an extension of the author's previous study (Gray, 1968) on this subject. Cyclone initial genesis locations have been stratified by season for the 20-year period of 1952-1971. Wind, temperature and moisture information are averaged by season and by 5-degree latitude-longitude Marsden squares. It is observationally shown and physical reasons are given why seasonal cyclone genesis frequency is related to the product of the seasonally averaged parameters of: 1) low level relative vorticity, 2) Coriolis parameter, 3) inverse of the vertical shear of the horizontal wind from lower to upper troposphere, 4) ocean's thermal energy to 60 meters' depth, 5) moist stability from the surface to 500 mb, and 6) middle troposphere relative humidity. A seasonal forecast potential of cyclone genesis frequency is derived. This forecast potential very well specifies the location and frequency of global cyclone genesis. A general theory on cyclone frequency is advanced.

TABLE OF CONTENTS

TABLE OF CONTENTS (cont'd)

1. INTRODUCTION

One of the most challenging subjects in meteorology is that of understanding why and how tropical cyclones form. A consensus of opinion on the environmental conditions and the physical mechanisms which bring about tropical cyclone formation is not present. Among meteorologists who have studied this subject there exist a wide variety of opinions. Yanai (1964) has previously made an attempt to summarize some of the prevailing opinions and physics on this subject up until that date. A consensus of opinions is lacking. Each researcher appears to emphasize and discuss different onset and development criteria, yet the basic physical processes which accompany the development of these warm-core cyclones must be very similar. This lack of general agreement, while partly due to semantical differences, is primarily due to fragmentary observational evidence and lack of a solid physical basis for understanding the early transformation of the tropical disturbance to a closed cyclone extending through the depth of the troposphere.

Since tropical cyclones form over tropical oceans where upper air observations are rare, definitive descriptions of the genesis characteristics of 'individual' tropical cyclones are grossly deficient. In order to obtain enough observations to understand cyclogenesis we are obliged to composite, or average, many cases of genesis together. If the physical processes of genesis are basically similar for all cyclones (as we believe) then some meaningful insights may be gained. At present we have no physical or observational reasons for thinking otherwise.

This paper attempts to establish a physical basis for understanding the processes of cyclone genesis and the variations in the seasonal climatology of genesis location and frequency. This is accomplished through an integration of our present observational information and through consideration of the likely relevant physical processes.

The first part of this paper presents statistical information on the seasonal frequency of tropical cyclone genesis and discusses what the author believes are the major physical requirements of genesis. The second part shows how these hypothesized requirements are specified by an index formed from the product of six seasonally averaged meteorological parameters. The last part of the paper shows how well the product of these seasonally averaged parameters is related to cyclone genesis location and frequency. A seasonal cyclone forecast index is proposed. A theory of cyclone genesis frequency is advanced.

It will be shown that the feature of hurricane formation which is least understood is that of how the weak precursor cyclone extending through most of the troposphere is formed from a disturbance with little initial vorticity. This very early stage in the hurricane formation process will be termed 'cyclone genesis'. By contrast the question of 'cyclone intensification' or growth of an already formed tropospheric cyclone is much better understood. Extensive numerical modeling of 'cyclone intensification' has already been accomplished with reasonable success. This latter topic is not the subject of this paper. This paper addresses only the question of initial cyclone formation. It is important to make this distinction. Very few tropical disturbances or cloud clusters develop closed circulations which extend through the troposphere. The vortex or closed circulation which is sometimes associated with a tropical disturbance is typically confined to a shallow layer. No significant net tropospheric warming or surface pressure fall occurs. On the other hand, a weak cyclone which extends throughout the troposphere possesses a weak upper tropospheric warming and a small surface pressure decrease. This type of deep tropospheric vortex or cyclone is nearly as rare as the hurricane. Hurricanes form only from these latter types of systems.

Numerical Modeling. In the last decade extensive efforts have gone into the numerical modeling of tropical cyclone intensification. These modeling efforts have been primarily directed towards obtaining realistic simulations of tropical cyclone growth rates from already existing cyclones whose inner 100-200 km radius vorticity is of an order of magnitude larger than that of the typical pre-cyclone cloud cluster as described by Williams and Gray (1973), see Table 1. These modeling efforts have shed light on the role of frictional convergence, condensation heating, ocean energy exchange, etc. to the growth process. Although very laudable advancements have been made by the models in increasing our knowledge of such physical processes, these numerical modeling efforts have not dealt with the crucial question of specifying how the tropical cyclone from which they start the calculations is itself formed. Cyclones of the strengths and vertical depths initially assumed by most of the modelers are rare.

Should not the primary question of cyclone genesis be that of ascertaining how a vortex with maximum winds of 5-10 m/sec at radii of 100-200 km and extending through most of the troposphere is able to form from a pre-cyclone cluster? In the author's view this is a much more difficult physical question than understanding the later cyclone intensification processes. Once a circular cyclone of the strength assumed by the modelers has formed, the horizontal energy dispersion processes (to be discussed) are greatly reduced and energy can readily

Table 1

Summary of Recent Numerical Modeling Papers on Hurricane Development and Their Assumed Initial Cyclone Strengths

Modelers	Assumed Initial Maximum Wind Velocity and Radial of Maximum Wind		Vortex Vorticity Inside the Radius of Maximum Winds ($10^{-6}sec^{-1}$)	Type of Vortex
Kuo (1965)	10 m/sec,	141 km	142	Symmetrical
Yamasaki (1968)	4.7m/sec,	100 km	94	Symmetrical
Ooyama (1969)	10 m/sec,	50 km	400	Symmetrical
Miller (1969)	10 m/sec,	200 km	100	Real Vortex
Rosenthal (1970)	7 m/sec,	250 km	56	Symmetrical
Sundquist (1970)	15 m/sec,	200 km	150	Symmetrical
Carrier (1971)	21 m/sec,	50 km	840	Symmetrical
Anthes, <u>et al.</u> (1971a,1971b)	18 m/sec,	240 km	150	A-symmetrical
Anthes (1972)	18 m/sec,	240 km	150	A-symmetrical
Mathur (1972)	15 m/sec,	200 km	150	A-symmetrical
Harrison (1973)	∿10 m/sec,	∿120* km	∿170	A-symmetrical
Kurihara and Tuleya (1974)	12 m/sec,	200 km	120	Symmetrical
Ceselski (1974)	17 m/sec,	∿100-150 km	∿200	Real Vortex
Typical pre-cyclone cloud cluster			∿10-15	

*Estimated from initial height field

accumulate within the central region. The frictionally forced convergence processes of the boundary layer produce momentum, vapor, and energy import into the cyclone center. Further intensification should take place.[1] Thus, intensification of an already developed cyclone is no great physical mystery. About two-thirds of all cyclones of the strength assumed by the intensification modelers (Table 1) reach hurricane strength. The processes responsible for formation of the initial cyclone from which the modelers start their integrations, however, is much less understood. Very few cloud clusters grow into tropical cyclones which extend through most of the troposphere. In a study of six years of satellite-observed Atlantic tropical weather systems, Frank and Hebert (1974) indicate that only 50 of 608, or 8 percent, of these systems become named or developed cyclones. These ratios are not much different in the other oceans.

Definitions. Meteorologists will often see or infer closed circulations or vortices at various levels associated with different classes of tropical weather systems (Aspliden, et al., 1966; Frank, 1969, 1970a, 1970b, 1971, 1972, 1973; Frank and Johnson, 1969; Riehl, 1954; Sadler, 1967a, 1967b, 1974a; Yanai, 1961, 1968). In this paper these closed

---

[1] It is of interest to note that of all the cyclone modelers Rosenthal (1970) assumed the weakest vortex. His vortex grew very slowly for the first 3-4 days as the water vapor content of the middle levels slowly increased. After the water vapor contents reached values typical of those of the pre-cyclone cloud cluster (Ruprecht and Gray, 1974), a rapid and unstable growth occurred. Rosenthal started with moisture contents of Jordan's (1958) mean tropical atmosphere. Thus, the lack of rapid growth of the Rosentahl model in the first 3-4 days was not due to a lack of any innate vortex instability but most likely due to the unrealistically low water vapor content with which he started. The Jordan mean summer time tropical atmosphere gives 700 to 500 mb relative humitidies of 56 and 46 percent, respectively. Ruprecht and Gray's observations of pre-cyclone cloud clusters show that the relative humidities at these levels are rather 78 and 76 percent.

circulations are not considered to be tropical cyclones unless they can be detected through an appreciable depth of the troposphere. This is rare. Seldom do tropical closed circulations extend through more than half of the troposphere. When this does happen, a hurricane typically results.

This paper will distinguish between vortices and cyclones as follows:

1. Tropical vortex. Any closed circulation at any level whose inner 100-200 km relative vorticity is less than 100 x $10^{-6}sec^{-1}$ and whose vertical depth is less than half of the troposphere. ITCZ vortices, middle level easterly wave vortices, and vortices which result from traveling waves superimposed on a zonal current, etc. all fall into this category.
2. Tropical cyclone. A closed circulation warm-core system of at least 5^{o} diameter which extends vertically through most of the troposphere with little vertical slope and whose relative vorticity at lower levels and inner 100-200 km radius is greater than 100 x $10^{-6}sec^{-1}$. This requires horizontal wind speeds at 100 and 200 km to be 5 m/sec and 10 m/sec. This is the strength of the typical cyclone from which the numerical models begin their intensification calculations.

Tropical cyclones which extend through most of the troposphere and which have 5-10 m/sec winds at radii of but 100-200 km are not just a natural result of the vorticity or shear configuration across a strong doldrum equatorial trough within the ITCZ region - see Fig. 1. Even though these cyclones' natural genesis location is just on the poleward side of or within the doldrum equatorial trough (see Gray, 1968 and Sadler, 1967a) the wind shears across such troughs are much weaker than

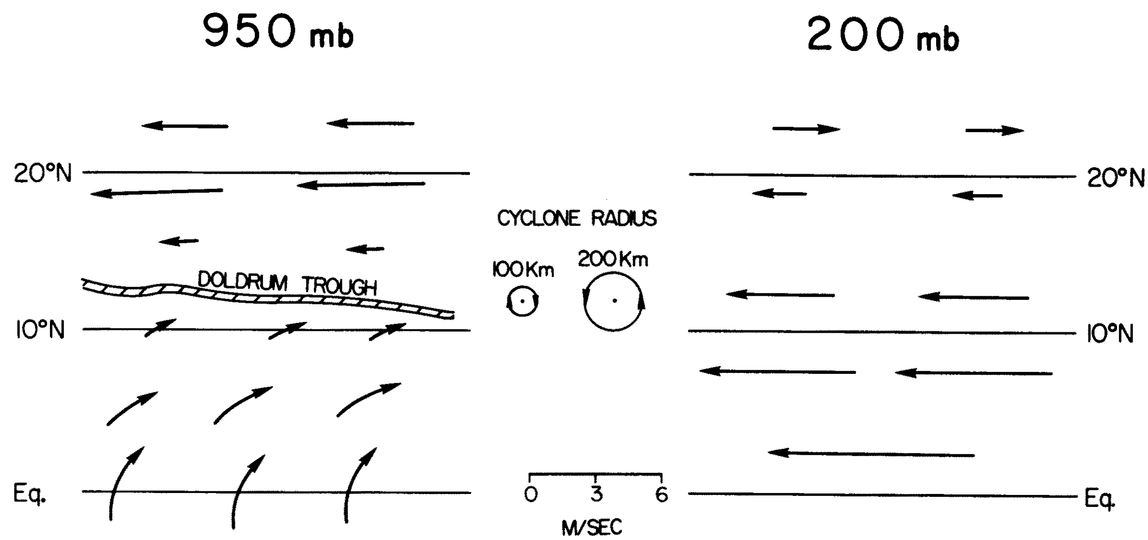

Fig. 1. Comparison of 100 and 200 km radii closed circulations (center) with typical gradient level (left) and 200 mb flow patterns (right) surrounding a doldrum equatorial trough on whose poleward side tropical cyclones typically originate.

those of the early stage tropical cyclone from which the numerical modelers begin their intensification calculations. In addition, these wind shears across the equatorial trough are seldom present above the 400-500 mb levels. Upper tropospheric flow above the ITCZ is typically from the east (right side of Fig. 1). When non-cyclone upper tropospheric vortices occur they seldom are associated with low level vortices.

Conclusion. To understand the formation of deep tropospheric cyclones with maximum winds at 100-200 km radius, one must hypothesize a genesis mechanism which is able to greatly accentuate the naturally occurring low level vorticity along the equatorial trough and vertically stack this vorticity through most of the troposphere. The doldrum trough and weak large-scale vortices confined to shallow vertical layers are present nearly every day in the tropics. The tropical cyclone with 5-10 m/sec maximum winds at 100-200 km radius and extending through most of the troposphere is a rare phenomenon. Something unusual must take place near the doldrum trough (or in the trade wind current) in order for a cyclone system to be formed. The doldrum equatorial trough does not naturally give us these cyclones. Although the tropical vortex is common, the tropical cyclone (as here defined) is nearly as rare as the hurricane. The greatest difficulty in understanding hurricane formation is not that of cyclone intensification but rather that of initial cyclone genesis.

2. CYCLONE ORIGIN STATISTICS

The dots on Figs. 2 - 6 show cyclone origin points by season for all tropical cyclone formations during the 20-year period of 1952-1971. These initial cyclone origin points were obtained from the author's tropical cyclone data files with recent updating and checking from the U. S. Navy tropical cyclone data tapes (see Appendix). Information is less reliable before the early 1950's. A longer data sample would likely not change or improve these statistics. Figure 7 portrays the regions of cyclone genesis and gives information on regional genesis frequency per 20 years. Table 2 stratifies the genesis information by region and season, and gives 20- and 1-year frequencies. Most of these nearly 2000 disturbance formations (∿ 100 per year) produced cyclones with sustained winds of ∿ 20 m/sec or greater.

The dots show the first reported detection point of intensifying disturbances which later became developed cyclones with maximum sustained winds of at least 20-25 m/sec. About two-thirds of these cyclones reached hurricane intensity - having maximum sustained winds greater than ∿ 33 m/sec. These dots can be taken as the approximate location where the developing disturbance system first became a cyclone (as defined in this paper). In some cases the observations were ∿ 12-36 hours too late to detect this initial cyclone genesis location and the origin points represent an already formed cyclone. In other cases the initial points shown are those 12-36 hours prior to the time of cyclone origin. These initial cyclone location errors are of opposite sign. In the 20-year average it is believed that these initial cyclone origin errors largely cancel each other and that the statistics shown are representative.

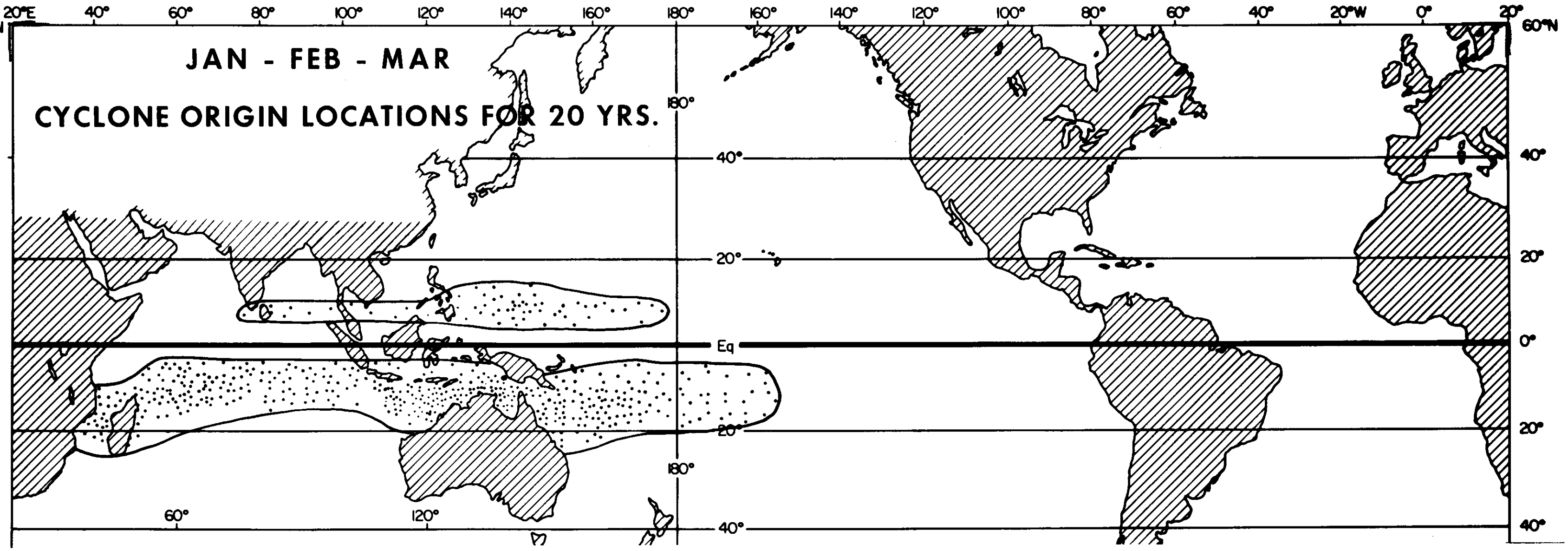
JAN - FEB - MAR
CYCLONE ORIGIN LOCATIONS FOR 20 YRS.
20°E 40° 60° 80° 100° 120° 140° 160° 180° 160° 140° 120° 100° 80° 60° 40° 20°W 0° 20°
60°N 40° 20° 0° 20° 40°
Eq

Fig. 2.

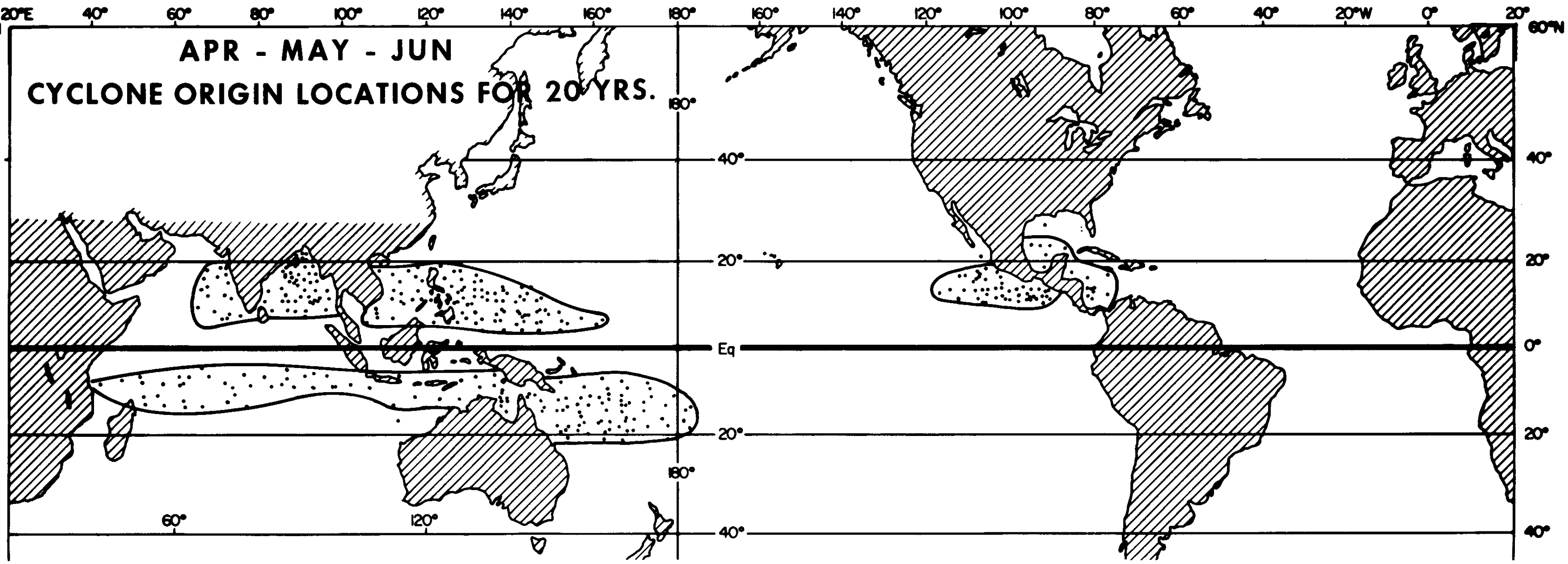
APR - MAY - JUN
CYCLONE ORIGIN LOCATIONS FOR 20 YRS.
20°E 40° 60° 80° 100° 120° 140° 160° 180° 160° 140° 120° 100° 80° 60° 40° 20°W 0° 20°
60°N 40° 20° 0° 20° 40°
Eq

Fig. 3.

Fig. 4

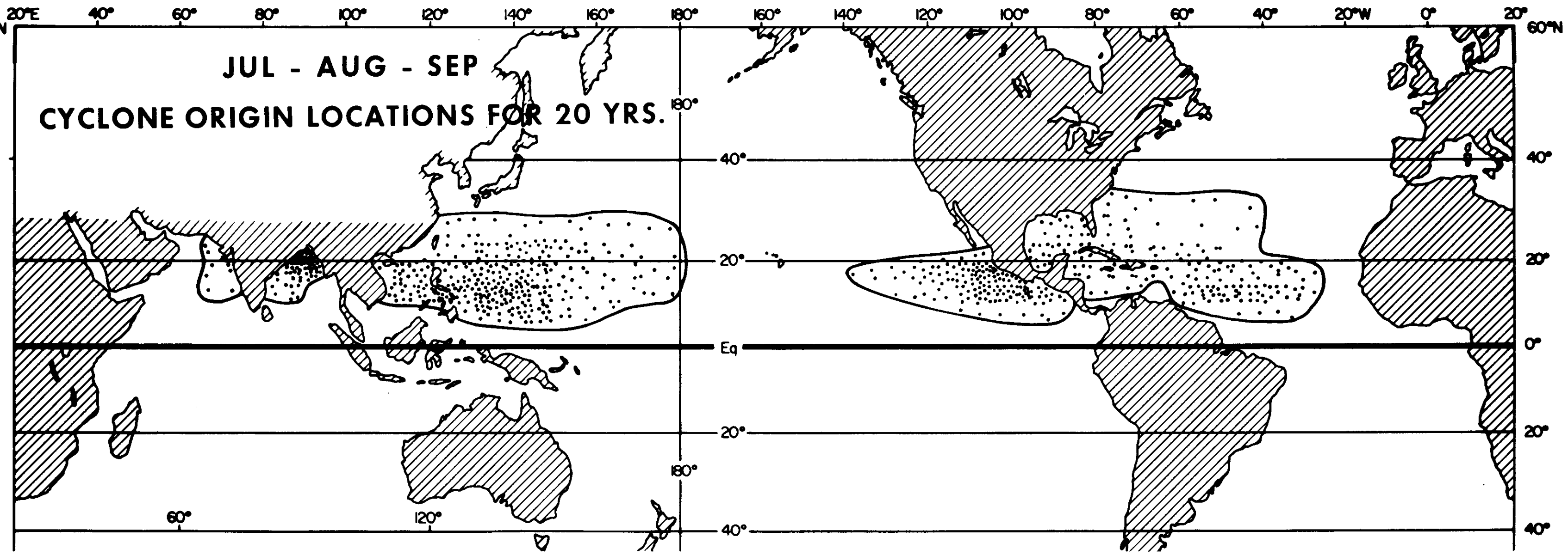
JUL - AUG - SEP
CYCLONE ORIGIN LOCATIONS FOR 20 YRS.
20°E 40° 60° 80° 100° 120° 140° 160° 180° 160° 140° 120° 100° 80° 60° 40° 20°W 0° 20°
60°N 40° 20° 0° 20° 40°
Eq
180°
60° 120°

Fig. 5

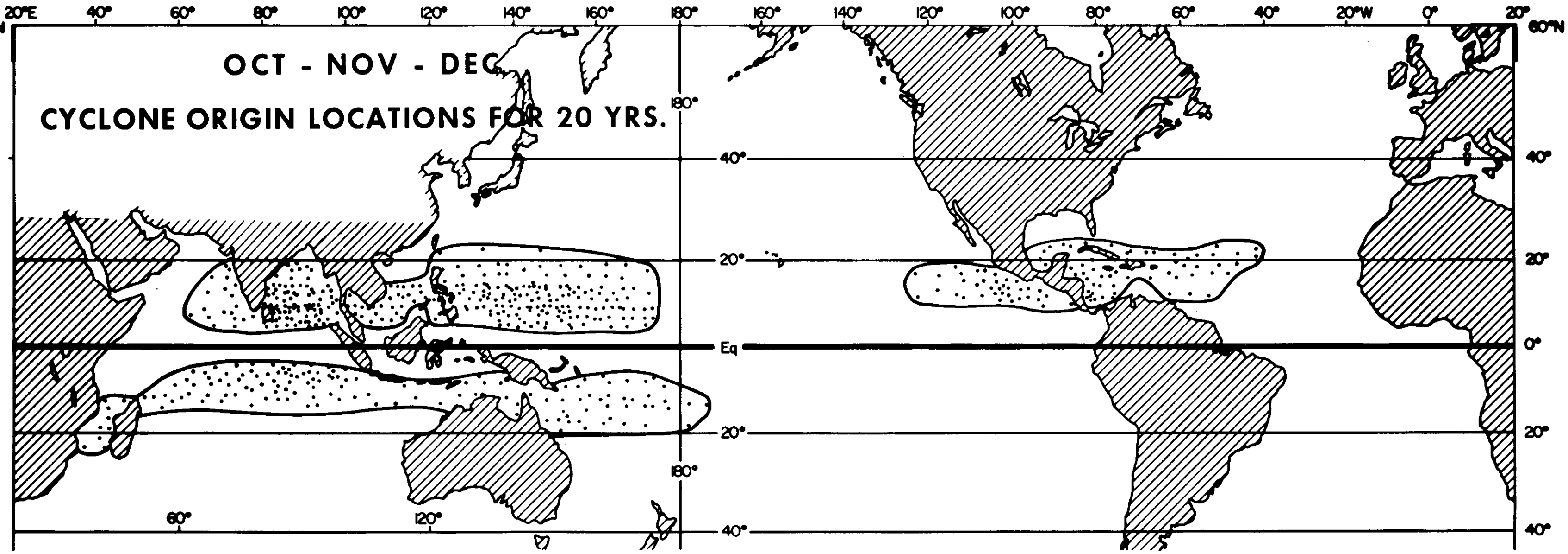
OCT - NOV - DEC
CYCLONE ORIGIN LOCATIONS FOR 20 YRS.
20°E 40° 60° 80° 100° 120° 140° 160° 180° 160° 140° 120° 100° 80° 60° 40° 20°W 0° 20°
60°N 40° 20° 0° 20° 40°
Eq
180°
60° 120°

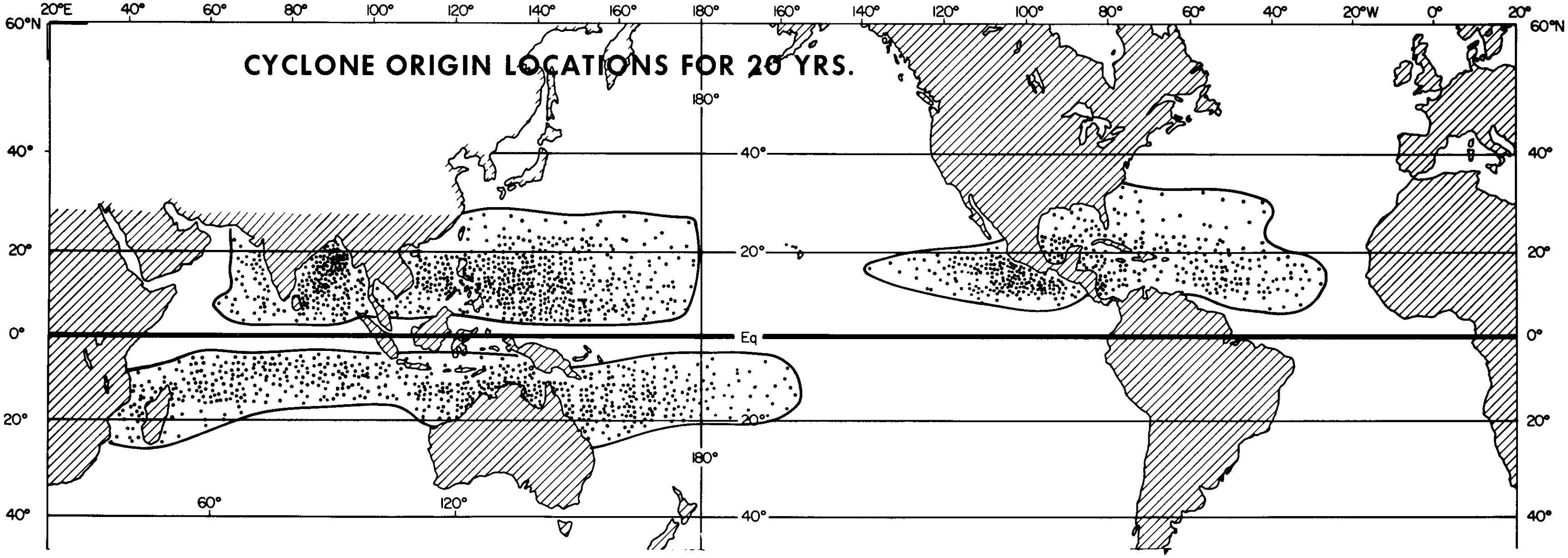

CYCLONE ORIGIN LOCATIONS FOR 20 YRS.
20°E
40°
60°
80°
100°
120°
140°
160°
180°
160°
140°
120°
100°
80°
60°
40°
20°W
0°
20°
60°N
40°
20°
0°
Eq
20°
40°
180°
60°
120°

Fig. 6

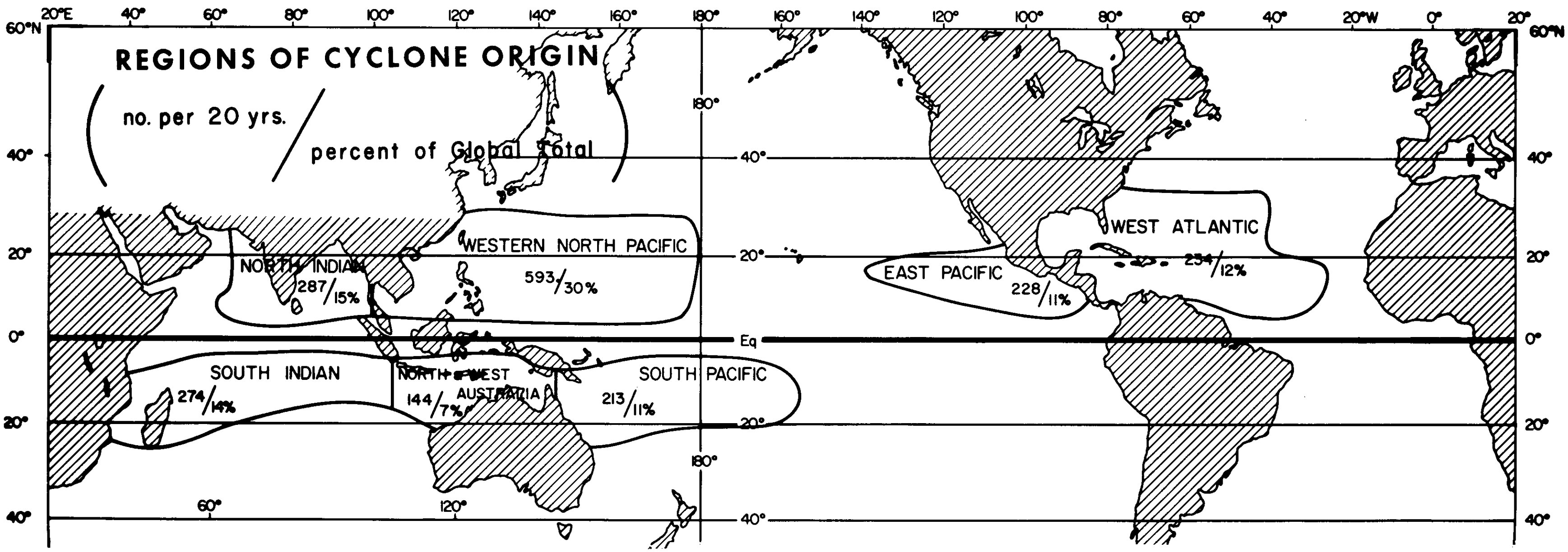

REGIONS OF CYCLONE ORIGIN
no. per 20 yrs.
percent of Global Total
NORTH INDIAN
287/15%
WESTERN NORTH PACIFIC
593/30%
EAST PACIFIC
228/11%
WEST ATLANTIC
234/12%
SOUTH INDIAN
274/14%
NORTH-WEST AUSTRALIA
144/7%
SOUTH PACIFIC
213/11%
Eq
180°
60°
120°

Fig. 7

Table 2

Number of Cyclone Genesis Cases per 20 Years and 1 Year by Season and by Genesis Area. Percentage of Genesis by Season and Area Also Shown.

	Jan-Mar	Apr-Jun	Jul-Sept	Oct-Dec	No. per 20 Year Regional Percent	No. per Year
N. Atlantic & West Indies	0	11	169	54	234/12%	∿12
Eastern Pacific	0	38	154	36	228/11%	∿11
Western N. Pacific	29	81	234	249	593/30%	∿30
North Indian Ocean	6	66	116	99	287/15%	∿14
South Indian Ocean	171	24	0	79	274/14%	∿14
North & West Australia	117	15	0	12	144/7%	∿ 7
South Pacific	126	46	0	41	213/11%	∿11
No. per 20 Year	449	281	673	570	1973	99
Seasonal Percent	23%	14%	34%	29%	100%	
No. per Year	∿22	∿14	∿34	∿29	99	

It is to be noted that:

1. Cyclones do not form within 4-5° of the equator. Genesis is especially favored in the latitude belts of 5-15° (see Fig. 8). Genesis does not occur poleward of 22° latitude in the Southern Hemisphere. In the Northern Hemisphere genesis occurs at latitudes as high as $\sim$ 35°.
2. Two-thirds of all cyclones form in the Eastern Hemisphere. (see Fig. 9). Regions centered around 90°E, 140°E and 105°W longitude are especially favored for genesis.
3. Although the majority of tropical cyclones form in the summer, genesis is possible in all seasons in the Western North Pacific. This region has nearly one-third of all the globe's tropical cyclones.
4. There are two seasons per year of cyclone formation in the North Indian Ocean between 5-15° latitude.
5. The Southeast Pacific and South Atlantic are devoid of cyclones.
6. Cyclone genesis is especially favored near the usual location of the ITCZ (Sadler, 1967a; Fett, 1968).

As previously discussed (Gray, 1968) about 80-85 percent of the tropical cyclones originate in or just on the poleward side of the Inter-Tropical Convergence Zone (ITCZ). Most of the remainder ($\sim$ 15 percent) form in the trade winds at a considerable distance from the ITCZ but usually in association with an upper tropospheric trough to their northwest (Sadler, 1967a, 1967b, 1974a). A few hybrid-type of warm-core cyclone systems ($\sim$ 1-2 percent) develop in sub-tropical latitudes along stagnant frontal zones. This latter type of cyclone is very

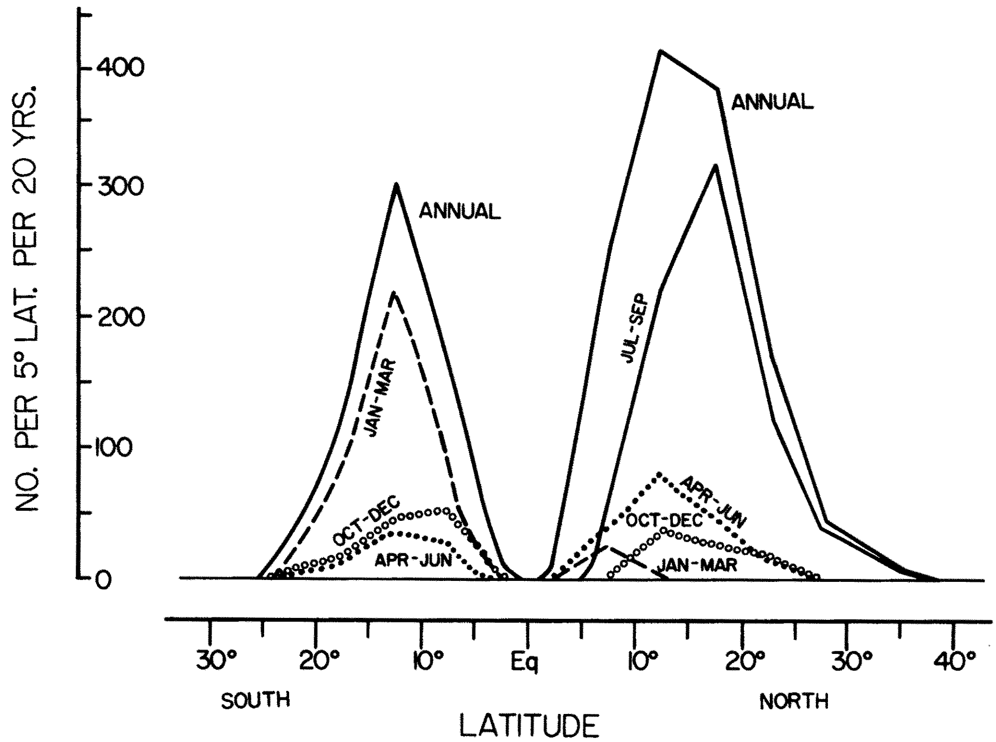

Fig. 8. Seasonal and annual distribution of tropical cyclone origin by latitude.

atypical and not part of the discussion of this paper. The author's previous paper (op.cit.) has more statistical information on cyclone genesis.

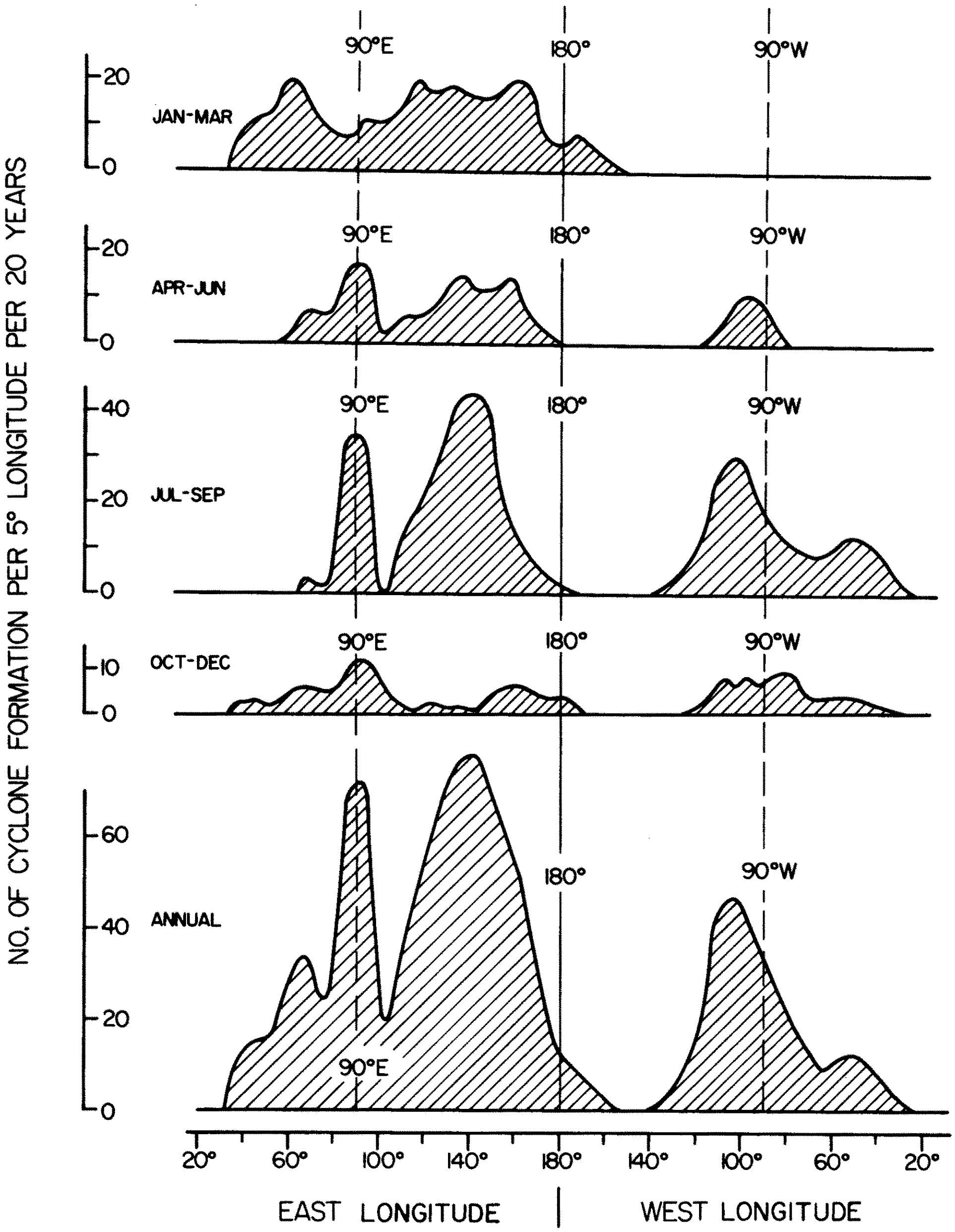

Fig. 9. Seasonal and annual distribution of tropical cyclone origin by longitude.

3. PHYSICAL REQUIREMENTS OF CYCLONE GENESIS

Over broad areas of the tropics where cyclones form, horizontal temperature gradients are practically non-existent. To understand tropical cyclone genesis one must understand how the tropical disturbance or tropical cloud cluster[2] is occasionally able to induce an upper troposphere enthalpy increase and then concentrate this enthalpy increase over a small area of ∿ 200-300 km width. This upper tropospheric enthalpy increase (or warming) produces thickness increase and (with the top of the system near 100 mb) small surface pressure decreases. Observations of early cyclone development show that this required enthalpy increase first takes place in the layers between 500-300 mb (Lopez, 1968; Yanai, 1961, 1963; Zipser, 1964) and is of the typical magnitude indicated in Fig. 10. This upper-tropospheric enthalpy increase is lacking in disturbances which do not develop into cyclones. It appears that the primary question of genesis rests with understanding how this upper tropospheric enthalpy increase (or warming) occurs and how it is concentrated and accumulated over the westward moving disturbance. This initial concentrated warming typically occurs on the side of the cloud cluster (LaSeur, 1962; Fett, 1964; Lopez, 1968), not at its center.

<u>Enthalpy Increase through Release of Latent Heat</u>. As has been previously discussed by Lopez (1973a), Gray (1973) and Yanai <u>et al</u>. (1973), precipitating cumulus clouds do not directly warm the immediate environment in which they exist. In fact, it appears that cumulus convection cools the area directly around the clouds by evaporation of liquid water

[2] In this paper the terms 'disturbance' and 'cloud cluster' (defined in GARP conference, 1968) are used synonymously. These clusters may be considered as being the 'pre-existing' disturbance from which Riehl (1954) states all tropical cyclones develop.

as the clouds die and mix with their environment. Cloud re-evaporation of liquid water is especially large in the lower troposphere.

Cumulus condensation heat goes primarily into potential energy which is exported to the regions surrounding the cumulus. Some of the compensating sinking motion for the cumulus comes in the environment not far removed from the cumulus. Other portions of this compensating sinking occur in the surrounding clear regions and/or in the distant anticyclones where the adiabatic sinking balances the atmosphere's radiational losses. For the upper tropospheric enthalpy in or near the disturbance to increase, it is necessary that a portion of the mass compensation for the upward cumulonimbus (Cb) transport occur in the local environment. In addition, it is necessary that this sinking-warming not be totally lost through the horizontal energy dispersion processes of ventilation and divergence.

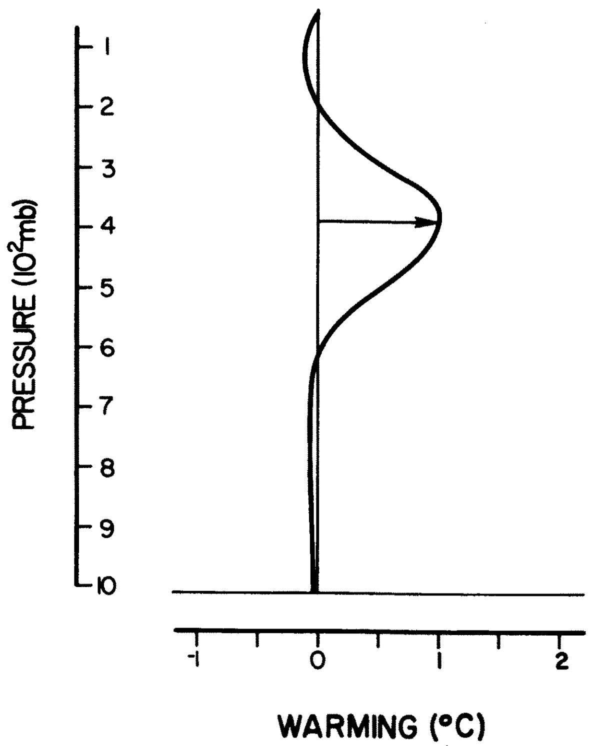

Fig. 10. Vertical distribution of the typical warming which is required to form a tropical cyclone.

This upper tropospheric warming can only be produced as a consequence of the compressional sinking motion of the downward return flow of the Cb convection. Because the gradient of potential temperature (Θ) with pressure in the tropical cloud cluster is nearly linear (see Fig. 11), equal amounts of mass subsidence at any pressure level produce equal increases of enthalpy. The vertical variation of specific humidity (q) with pressure within the typical cloud cluster is not linear, however. Equal units of mass subsidence produce greater drying in the lower troposphere. If this vapor loss due to sinking drying is entirely replaced by evaporation of liquid water, then a vertical variation in net tropospheric warming results. Assuming 100 mb/day sinking motion at all levels, Fig. 12 portrays the vertical distribution of net warming (curves W and C) which would result from a combination of sinking warming (curve W) and evaporational cooling (curve C). The sinking-warming is larger than the

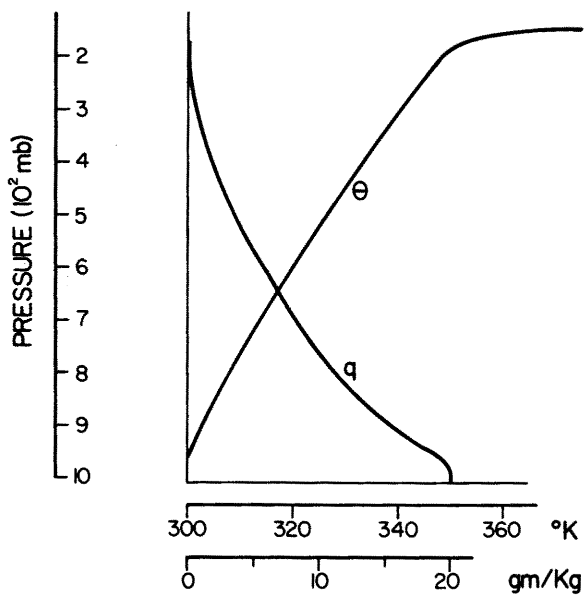

Fig. 11. Vertical distribution of potential temperature (Θ) and specific humidity (q) which is present in the typical tropical cloud cluster.

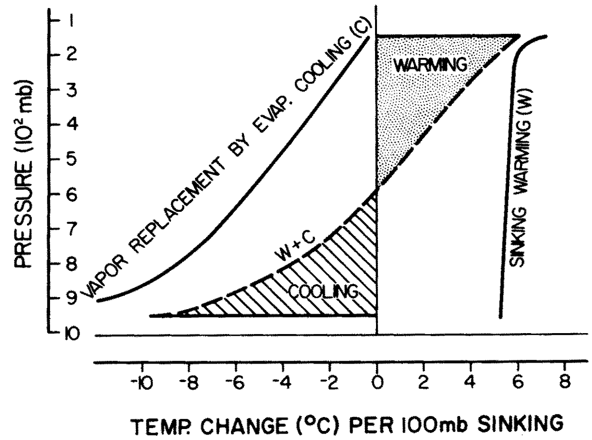

Fig. 12. Portrayal of the sinking warming (W) and evaporational cooling (C) which would result from 100 mb sinking and if the resulting sinking drying were totally made up for by evaporation. The W + C curve is an addition of the two curves.

required evaporational cooling in the upper troposphere. In the lower troposphere, however, evaporational cooling is dominant. Thus, one should not be surprised that the middle and upper troposphere are the favored levels for Cb induced enthalpy increase.

Some of the cloud cluster's enthalpy gain relative to its surroundings is due to the reduced net radiation loss of the cluster produced by its extensive layered cloud structure. This inhibits cluster long wave radiational loss (Cox, 1968, 1971, 1973). Although radiation is an important influence in distinguishing between the energy budget of the cloud cluster and its environment, it cannot be (because of their similar layered cloud structure) invoked as a primary factor in distinguishing between clusters which grow into cyclones and those which do not.

Cloud Cluster Characteristics. A significant portion of the mass transported upward by cumulus in a typical tropical cloud cluster does not leave the cluster but rather sinks locally within the cluster. This up-moist and down-dry recycling circulation is typical of most tropical cloud clusters. Figure 13 portrays the typical 4^o cloud cluster average up-moist ($\overline{\omega}_m$) and down-dry ($\overline{\omega}_d$) vertical circulation which is required for moisture and energy balance. $\overline{\omega}$ portrays the upward mean cluster circulation. See the reports by Gray (1973), Ruprecht and Gray (1974) and Lopez (1973a) for more discussion of this cloud cluster vertical circulation. At lower levels the magnitude of this vertical recycling circulation ($\overline{\omega}_m$ and $\overline{\omega}_d$) is substantially larger than that of the mean upward circulation. This vertical mass recycling pattern is typical of both the pre-cyclone and the non-developing cloud clusters.

As previously discussed by the author (op.cit., 1973) the vapor replacement for the cloud cluster sinking drying motion does not all come from evaporational cooling. Much of the vapor replacement for this sinking drying comes from direct vapor transport from the cumulus as they mix with their environment and as they die. Figure 14 shows the vertical variation of the required vapor replacement of the typical 4^o cloud cluster and the parts of this sinking drying made up by evaporation and direct vapor diffusion from the cumulus. Most of the vapor replacement in the lower levels comes from direct transfer from the cumulus.

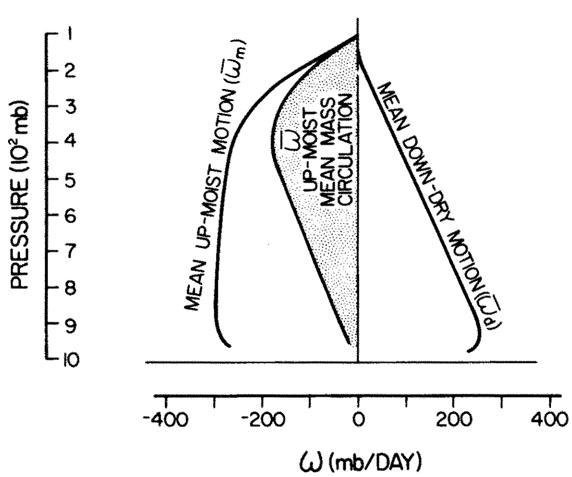

Fig. 13. Up-moist, down-dry and mean mass circulation occurring in the typical 4^o tropical cloud cluster.

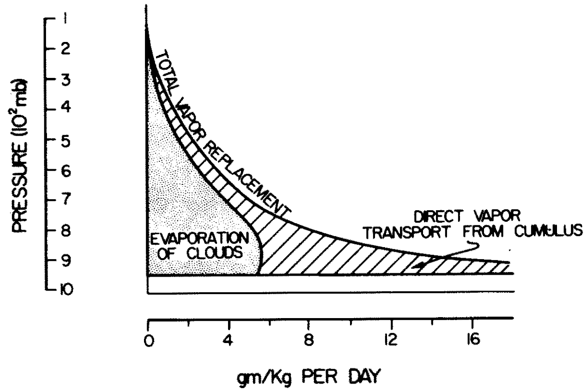

Fig. 14. Vertical distribution of required rate of water vapor replacement in the typical 4° wide cloud cluster to keep the cluster vapor content constant with the sinking drying motion as specified in Fig. 13. That portion of the vapor replacement accomplished by evaporation and that portion by direct transfer from cumulus clouds is also shown.

Figure 15 contrasts the 4° divergence pattern (see Williams and Gray, 1973) of the pre-cyclone cloud cluster and the non-developing cloud cluster. Note that these divergence patterns are very similar. The magnitude of their up-moist and down-dry vertical recycling circulations are also very similar. To explain the differences in cloud cluster cyclone genesis potential, one must look to other distinguishing cloud cluster features besides the mean divergence and vertical mass recycling fields. Cloud cluster rainfall is not well correlated with cluster cyclone genesis potential. Clusters which produce massive amounts of rainfall often do not form into cyclones, while other clusters with lesser amounts of precipitation do.

Nature of the Cloud Cluster's Upper Tropospheric Warming. Figure 16 portrays the hypothesized warming and cooling processes which are acting in the typical 4° pre-cyclone and non-developing cloud clusters in the absence of any horizontal energy advection or dispersion processes. There is no difference in the net vertical divergence of energy

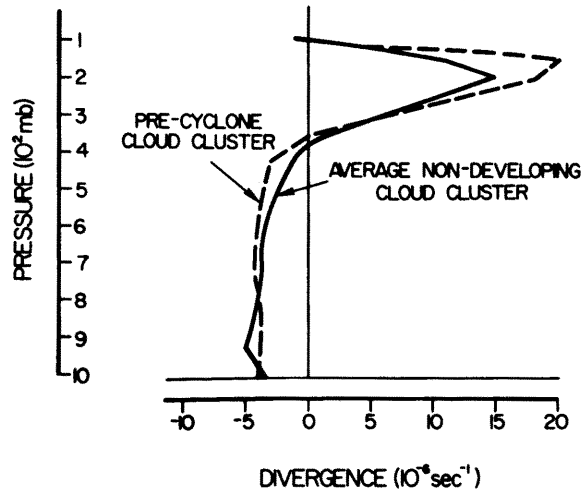

Fig. 15. Comparison of the vertical distribution of the average divergence occurring in the 4^{o} wide pre-cyclone cloud cluster with the 4^{o} wide non-developing cloud cluster.

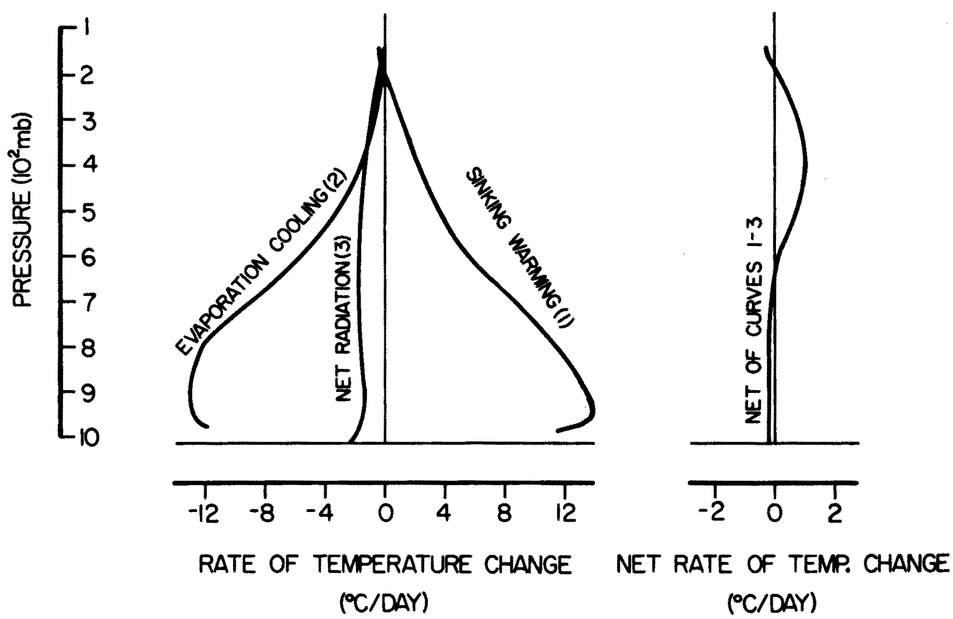

Fig. 16. Vertical distribution of typical 4^{o} wide cloud cluster rate of temperature change due to sinking warming, evaporation cooling, and radiation (left) and the residual of these heating mechanisms (right).

flux between these two systems. As shown on the right diagram of this figure, a small net accumulation of enthalpy is taking place in the upper troposphere of both systems. At upper levels the sinking warming (curve 1) is slightly greater than the sum of the evaporational (2) and radiational cooling (3) curves. This enthalpy gain, however, will not lead to cyclone genesis if the cluster's upper level horizontal energy dispersion processes are very large. This is the usual situation. Enthalpy gain is usually cancelled out by horizontal dispersion and cluster growth to a cyclone does not occur. Thus, the primary determinant for cluster growth appears not to be the existence of an upper tropospheric cluster heating source but rather the presence of environmental conditions which allow the accumulation of this energy.

Cyclone Genesis Hypothesis. The author believes that the primary determinant for cloud cluster growth to cyclone strength rests with the characteristics of the upper tropospheric energy dispersion processes. Only rarely do the upper level wind conditions relative to a moving cloud cluster act to inhibit horizontal dispersion of energy and thereby allow an upper level enthalpy accumulation within a moving system.

By horizontal energy dispersion the author means: 1) divergence, and 2) advection or ventilation. As the divergence profiles of the pre-cyclone and non-developing cloud clusters (Fig. 15) are about the same, the horizontal energy losses from divergence cannot be a distinguishing feature of cluster growth. In addition, the magnitudes of the cluster divergences between 300-500 mb where the major warming occurs are not large, being near zero around 400 mb. Thus, the horizontal energy losses due to divergence are not felt to be the primary distinguishing factor to growth. Cloud cluster upper level advection or ventilation appears, on the other hand, to be fundamental in specifying cluster cyclone formation potential.

Cluster Ventilation. As previously discussed, over 85% of all tropical cyclones form within or just on the poleward side of a Doldrum Equatorial Trough or ITCZ. As shown in the north-south vertical cross-section of zonal wind in Fig. 17, this is an especially favorable place (location C) for small tropospheric vertical wind shear (also see third profile from the left of the lower diagram) and for 200-500 mb wind and cloud cluster velocity to be very similar. Designators A, B and D correspond to the typical locations of Monsoon, GATE[3] and trade wind cloud clusters relative to the Doldrum Equatorial Trough. These locations are places where the cluster 200-500 mb wind typically blows at a velocity considerably different than that of the cluster itself. Thus, the ventilation, or blow-through component of the zonal wind past these clusters is typically large. The lower diagram of this figure shows the typical vertical shear of the zonal wind (U) and the vertical distribution of the zonal wind component ($U - U_d$) relative to the typical moving (U_d) cloud cluster at these four locations. Most oceanic cloud clusters move at velocities of 6-8 m/sec (Chang, 1970; Wallace, 1970). All except the monsoon clusters move toward the west. The horizontal energy dispersion rates or ventilation rates between 200-500 mb for profiles A, B and D are much greater than for profile C.

In all but the pre-cyclone clusters the environmental air between 200-500 mb is blowing through the cluster in a time interval of but

[3]GARP Atlantic Tropical Experiment conducted off West Africa between June and September in 1974.

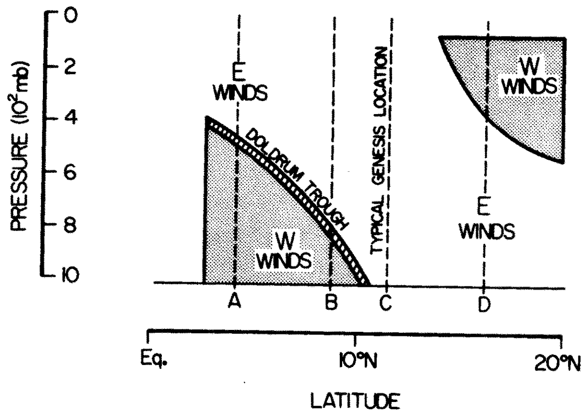

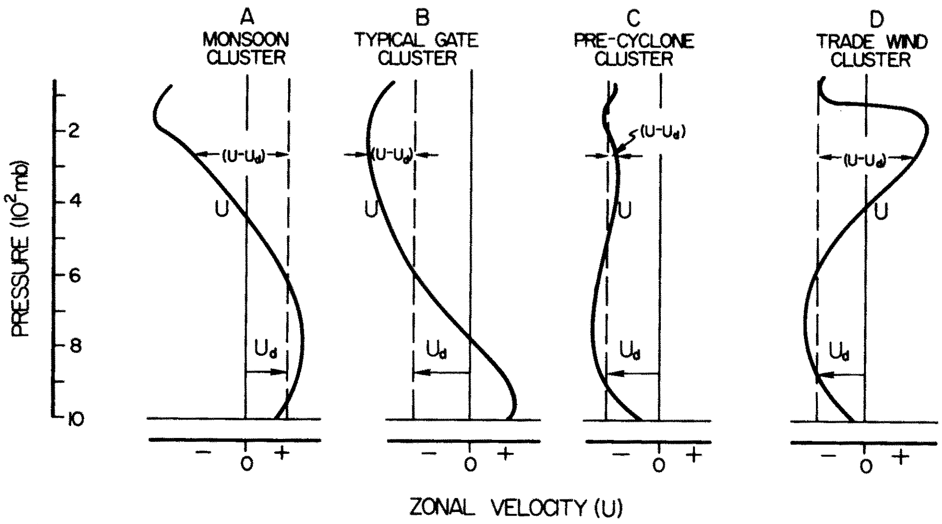

Fig. 17. North-south cross-sections of the typical locations of various classes of tropical cloud clusters relative to the doldrum equatorial trough and the usual zonal winds present with these systems (top diagram). The bottom diagram portrays the vertical distribution of typical zonal wind velocity (U) occurring with different A to D types of cloud clusters whose general location is specified in the top diagram. The usual zonal cluster velocity is designated U_d and the difference in cloud cluster and environmental wind velocity at any level is given by $(U - U_d)$.

10-20 hours. The cloud cluster induced warming (Fig. 10) which is occurring is advected or ventilated out of the cluster. An upper level energy accumulation cannot occur. In the pre-cyclone cluster, on the other hand, the 200-500 mb motion of the air is very close to that of the cloud cluster motion and upper level energy accumulation can occur. In general, it is only cloud clusters with this type of vertical wind profile which produce tropical cyclones. Figure 18 shows the vertical profile of the average zonal wind in the Western North Pacific pre-cyclone and non-developing cloud clusters. Note that the 200-500 mb zonal wind for the pre-cyclone clusters is very close to the westward velocity of the cloud cluster (data from Williams and Gray, 1973).

Once a closed circulation has been formed in the 200-500 mb levels, the direct flow of air or ventilation through the cluster is stopped. The enthalpy increase within the upper levels can be contained and concentrated. Cyclone intensification should, and in most cases does follow.

Table 3 compares the vorticity, central pressure decrease for gradient wind balance, and the central 200-500 mb mean temperature increases of four cluster systems of different intensity. Note the very much higher vorticity, central pressure drop, and 200-500 mb core warming of the weak cyclone in comparison with the typical cloud cluster and how little upper tropospheric central warming (i.e. $1^{o}C$) is required for initial cyclone genesis. The typical cloud cluster possesses almost no upper tropospheric warming or surface pressure decrease.

Summary. The forming of tropical cyclones whose circulation extends through most of the troposphere is a most difficult task for the tropical atmosphere to perform. It is seldom accomplished. The crucial problem in understanding cyclone genesis processes is that of

Table 3

Comparison of Inner 200 km Radius Parameter Averages of Cluster Systems of Various Intensity

	Average Vorticity in Lower Troposphere $10^{-6} sec^{-1}$	Minimum Pressure Decrease at Cluster Center to Satisfy Gradient Wind Balance mb	200-500 mb Relative Warming at Cluster Center ^oC
Average 4^o Wide Cloud Cluster	10	0.2	0.1
Pre-Cyclone Cluster at Beginning of Genesis	15	0.3	0.1
Weak Tropical Cyclone Typical of Initial Condition Assumed by Hurricane Genesis Modelers (∿ Maximum Winds of 10 m/sec at 200 km Radius)	100	2.5	1.0
Usual Developed Hurricane (Winds of 30 m/sec at 200 km Radius)	300	50.0	∿15.0

understanding how the 200-500 mb levels can increase their enthalpy. It appears that this can be accomplished only if the upper tropospheric environmental winds and the disturbance from which the cyclone forms move with very much the same direction and velocity.

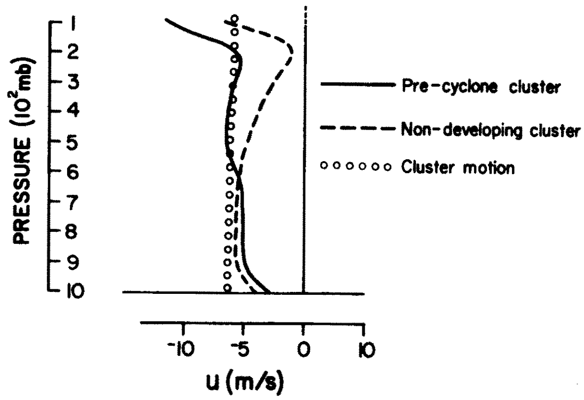

Fig. 18. Vertical variation of the zonal wind velocity in the western North Pacific cloud clusters between 5-20°N latitude and the typical westward propagation of these cloud clusters. Note that the 200-500 mb zonal velocity of the pre-cyclone cluster is very close to that of the cluster westerly movement.

4. SIX PRIMARY GENESIS PARAMETERS

The author (Gray, 1968) has previously discussed the important role which large magnitude low level relative vorticity and small magnitude vertical shear of the horizontal wind play in determining regions of high tropical cyclone genesis frequency. Genesis also requires other favorable conditions to be present. A number of authors (Riehl, 1954, and much personal communication, 1957-1962; Fisher, 1958; Malkus and Riehl, 1960; Miller, 1964; Leipper, 1967; Perlroth, 1967, 1969; Leipper and Volgenau, 1972) have previously discussed the very important role which sea surface temperature and high magnitude ocean thermal energy play in tropical cyclone existence. The necessary role of thermal buoyancy from the surface to middle levels for Cb convection has been discussed by Palmén (1948, 1957) and a number of other researchers. Other authors such as Dunn (1940, 1951) have observed the lack of tropical cyclone development near the equator and have hypothesized the importance of the earth's rotation in the genesis process.

In addition to these important genesis requirements the author has also observed the high frequency of cyclone genesis in regions where the seasonal values of middle level humidity are high (to be discussed).

The author believes that seasonal tropical cyclone frequency can be directly related to a combination of six physical parameters which will henceforth be referred to as primary genesis parameters. These parameters are:

1. Low level relative vorticity (ζ_r)
2. Coriolis Parameter (f)
3. The inverse of the vertical shear (S_z) of the horizontal wind between the lower and upper troposphere or $1/S_z$.

4. Ocean thermal energy or sea temperature above 26^{o}C to a depth of 60 m (E).
5. Vertical gradient of Θ_e between the surface and 500 mb $(\partial\Theta_e/\partial p)$.
6. Middle troposphere relative humidity $(\overline{RH})$.

It will be shown that seasonal cyclone genesis frequency is well related to the adjusted seasonal magnitude of the product of these six parameters, or

$$\begin{pmatrix}\text{Seasonal}\\ \text{Genesis}\\ \text{Frequency}\end{pmatrix} \propto (\zeta_r) \times (f) \times (1/S_z) \times (E) \times \left(\frac{\partial\Theta_e}{\partial p}\right) \times (\overline{RH})$$

Previous authors have emphasized the importance for genesis of one or a few of these parameters. The author believes cyclone genesis is dependent on the magnitude of all of these parameters. The physical role which each of these parameters plays in the genesis process will now be discussed.

4.1 Role of Low Level Relative Vorticity

Tropical cyclones require a continuous low level import of mass, momentum, and water vapor. The magnitude of the import of these quantities in the Boundary (B) Layer (L), or surface to $\sim$ 1 km height, appears to be related in a significant way to the strength of the Ekman-type of frictional wind veering which is occurring. Over the tropical oceans it is observed (Gray, 1972) that this frictional veering of the wind averages between 10-15^{o}. It has been further observed that the top of the layer of frictional wind veering does not increase near the equator as has been previously implied from Ekman theory, but rather is independent of latitude. The top of this layer appears to be largely determined by the degree to which mechanically and thermally driven air parcels in the mixed layer can penetrate into the stable layer just above. Over the tropical oceans the top of the veering level averages about 1-1.5 km while the top of the mixed layer is about 0.5 km.

Figures 19 and 20 portray vertical differences of observed oceanic wind veering and ageostrophic wind component vs. latitude from 5 km height to the surface. Note that most of the change in wind direction and component of the wind relative to the 5 km level occurs in the lowest km. The wind component perpendicular to the 5 km level wind is assumed to be the ageostrophic wind component or V_a. In a very large average like this

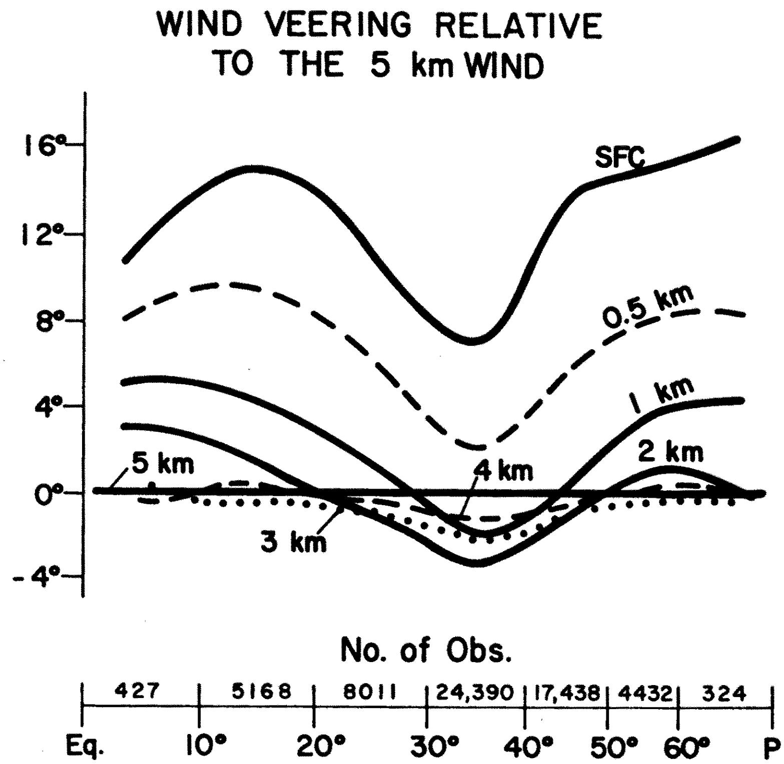

Fig. 19. Latitudinal distribution of the average of upper level oceanic wind direction veering at various levels relative to the 5 km average wind direction. The number of rawin and pibal observations in each latitude belt is shown at the bottom.

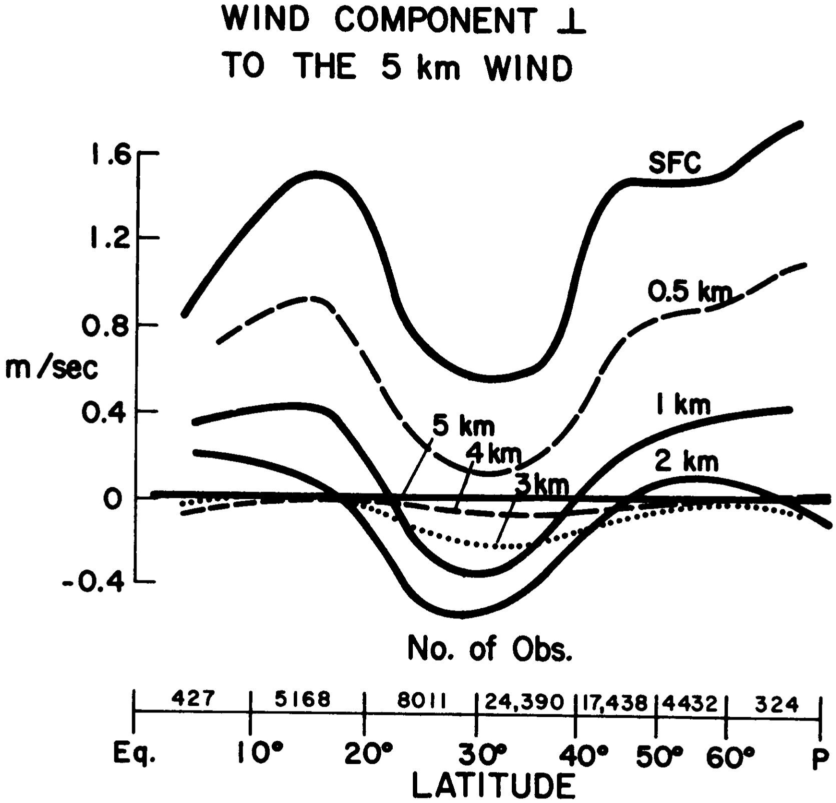

Fig. 20. Latitudinal distribution of the average of upper level oceanic wind components perpendicular to the average 5 km wind.

the thermal wind component is negligible (see Gray, op.cit. for more discussion) and there should then be no appreciable vertical variation in pressure gradient with height. The height of the top of this wind veering (∿ 1-1½ km) does not change with latitude.

Figure 21 is a vertical profile of average wind direction changes and average wind components relative to the 5 km level for all ship upper wind data between the equator and 17^{o} latitude. First km frictional veering is about 10-12^{o}. The Boundary Layer (B.L.) over the tropical oceans will thus be taken to be ∿ 1-1½ km thick. Although local 1-5 hour variations in the height of the B.L. with individual rain shower systems is very large and much beyond the range shown here, the cloud

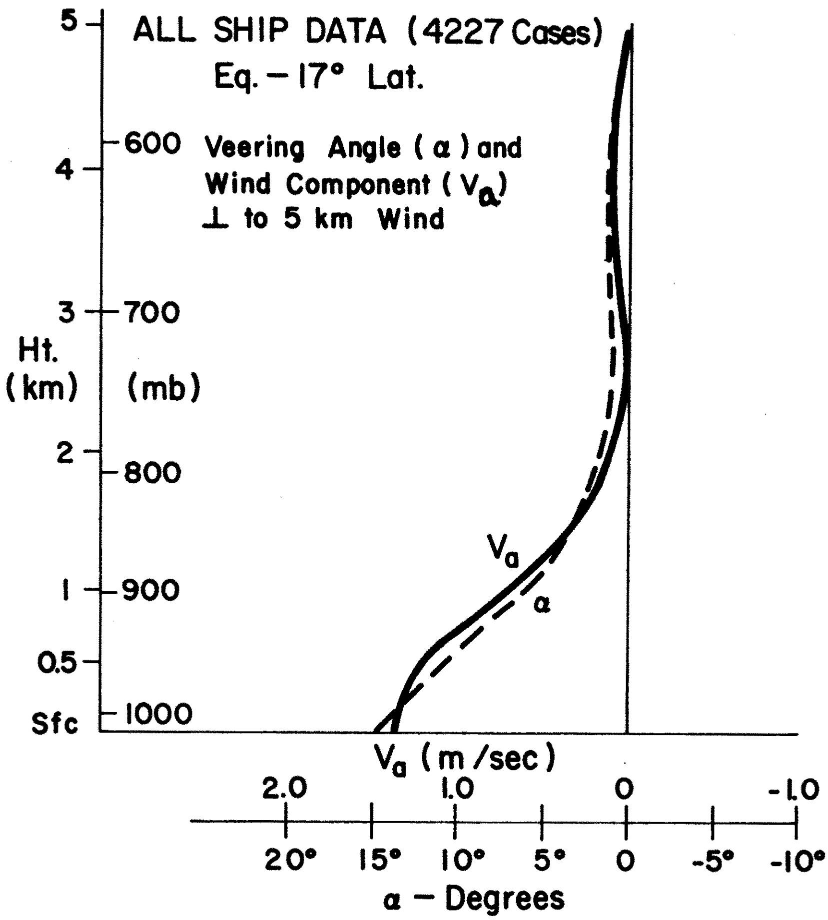

Fig. 21. Vertical profile of the changes of ship rawin and pibal determined upper level wind veering and wind components perpendicular to the 5 km level wind.

cluster scale average veerings and ageostrophic frictional wind components are believed to be characteristic of those shown in these figures.

The average of the first km cross-isobaric or ageostrophic wind velocity ($\overline{V}_a$) is about 15 percent of the average B.L. total wind or ($\overline{V}_t$). Thus, $\overline{V}_a \approx 1/7\ \overline{V}_t$, or in terms of the zonal ($\overline{u}$) and meridional ($\overline{v}$) wind components

$$\begin{aligned} \overline{u}_a &= -\ 1/7\ \overline{v} \\ \overline{v}_a &= 1/7\ \overline{u} \end{aligned} \tag{1}$$

Thus, the B.L. frictional convergence can be directly related to the B.L. average relative vorticity (ζ_r) as

$$\begin{pmatrix}\text{B.L. Frictional}\\ \text{Convergence}\end{pmatrix} = -\left(\frac{\partial \bar{u}_a}{\partial x} + \frac{\partial \bar{v}_a}{\partial y}\right) = 1/7\left(\frac{\partial \bar{v}}{\partial x} - \frac{\partial \bar{u}}{\partial y}\right) = 1/7\,\bar{\zeta}_r \qquad (2)$$

This type of frictionally driven convergence has been discussed by Charney and Eliassen (1949, 1964) and has been employed by many of the numerical modelers in simulating tropical cyclone growth. The association of surrounding low level vorticity with tropical cyclone frequency and cyclone dissipation over tropical water has also been discussed in project reports by Sartor (1968) and Wachtmann (1968).

Significance of Frictional Convergence. It is observed that the actual B.L. convergence in the pre-cyclone cloud cluster is not 15 percent of the cluster's relative vorticity but rather 40-50 percent (see Williams and Gray, 1973). Thus, the direct frictionally induced convergence contributes only a quarter to a third of the net B.L. cluster convergence. Of what importance, then, is this frictional convergence?

The author believes that the frictional convergence acts as the required 'pump primer' for extra non-frictional cumulus and Cb induced convergence. The frictional convergence insures that a continual supply of mass, momentum, and water vapor be provided at low levels to bring about and maintain cumulus convection which feeds back and adds more to the B.L. and upper level convergence. Were the B.L. frictional convergence not present, the extra convergence from the cumulus probably could not be maintained. The B.L. frictional convergence is thus viewed as a necessary ingredient for extra cumulus induced convergence.

Vorticity and the CISK[4] Genesis Hypothesis. It is obvious from the above discussion and the previous discussion on the 4^{o} wide cluster vertical mass recycling that the boundary layer induced convergence from frictional wind veering plays only a small direct role in maintenance of the tropical cluster's lower tropospheric mass profile. The mass recycling profile of Fig. 13 shows how much extra mass is going into and leaving the boundary layer beyond what can be specified by the mean convergence profile of Fig. 15. The convergence above cloud base feeds mainly into cumulus downdrafts which penetrate into the B.L. and produce the extra B.L. mass convergence necessary to force updrafts of 1-3 m/sec over 1-3 percent of the cluster area. The mean B.L. mass convergence is far too weak to produce updrafts of this number and magnitude by itself. Nevertheless, this does not negate the fundamental role of the B.L. frictional convergence mechanism. The B.L. frictional mechanism should be viewed not as a direct cumulus-producing process, for in this it is obviously too weak, but instead as a required ingredient for extra cumulus feedback response.

It is well observed that tropical cyclones form only in regions of large positive low level vorticity. The larger this low level vorticity, the greater appears the potential for cyclone genesis.

Conclusion. Other conditions being favorable and remaining constant, tropical cyclone genesis should be directly related to the magnitude of low level tropospheric relative vorticity.

---

[4] Conditional Instability of the Second Kind as defined by Charney and Eliassen (1964).

4.2 Role of Earth's Rotation (i.e. Coriolis Parameter)

Cyclones do not form within 4-5^{o} of the equator. The influence of the earth's rotation would thus appear to be of primary importance. A number of previous researchers have stressed this relationship. Except for places where strong meridional flow and import of momentum from higher latitudes is occurring, winds on the equator are very weak. Geostrophic considerations dictate that pressure gradients near the equator be very weak.

Near the equator it is impossible to sustain a balance between cross-isobaric momentum acceleration and the planetary Boundary Layer (B.L.) frictional momentum loss when winds are higher than 3-5 m/sec. Assuming geostrophic conditions above the B.L., the ratio of the magnitude of B.L. kinetic energy generation ($f\,\overline{V}_g\,\overline{V}_a$) to frictional dissipation ($V_g \frac{\partial \tau_{xz}}{\rho \partial z}$) can be written as

$$\frac{f\,\overline{V}_g\overline{V}_a}{\overline{V}_g \frac{\partial \tau_{xz}}{\rho \partial z}} \tag{3}$$

where $\overline{V}_g$ is the geostrophic wind velocity in the B.L.

$\overline{V}_a$ is the average ageostrophic or cross-isobaric wind velocity through the B.L.

f is the Coriolis parameter

ρ is density, assumed constant through the B.L.

τ_{xz} is the usual stress representation in the B.L.

To keep the above ratio equal to one at low latitudes, only very small B.L. wind speeds are permitted. This is because dissipation is independent of f. B.L. momentum generation, on the other hand, is directly related to the pressure gradient which, except in highly curved flow, is a function of the Coriolis parameter.

Assuming the surface stress, τ_{xz_o}, is given by the usual formula $C_D \rho V_s^2$ (where C_D is a drag coefficient of the magnitude 1.3×10^{-3}, ρ is density, and V_s is the wind at 10 m height or ship deck level) and that this stress approaches zero at 1 km height (i.e., $\Delta Z = 1$ km - consistent with previous discussion), we can obtain an expression for the ratio of the momentum generation to the momentum dissipation, thus

$$\frac{f \, \overline{V}_g \overline{V}_a}{\overline{V}_g \cdot \frac{\partial \tau_{xz}}{\rho \partial z}} = \frac{f \, \overline{V}_a}{\frac{C_D V_s^2}{\Delta Z}}$$

Assuming that $\overline{V}_a$ through the boundary layer averages 1/7 V_s (see previous section) we obtain the final ratio

$$\frac{1/7 \; f \; \Delta Z}{C_D V_s} = K \frac{f}{V_s} \qquad (4)$$

where K is a constant.

For this expression to be constant V_s must be very small near the equator. The bottom curve of Fig. 22 shows the latitude variation of maximum V_s or V which is possible for B.L. momentum maintenance when no momentum importation from higher levels or horizontal advection is allowed. These winds are very weak indeed. Even when the pressure gradient acceleration ($-\alpha \nabla P$) due to flow curvature is allowed for, maintenance of high wind speeds near the equator is not possible without importation of momentum. Figure 22 also shows curves of maximum B.L. wind speeds vs. latitude which can be sustained for pressure gradients equivalent to various ratios of gradient wind to geostrophic wind. Even when pressure gradients equivalent to curvature acceleration of 5 to 10 times that of geostrophic acceleration

(fV_g) are allowed for, acceleration balance in the B.L. near the equator is possible only for conditions of very weak wind speeds.

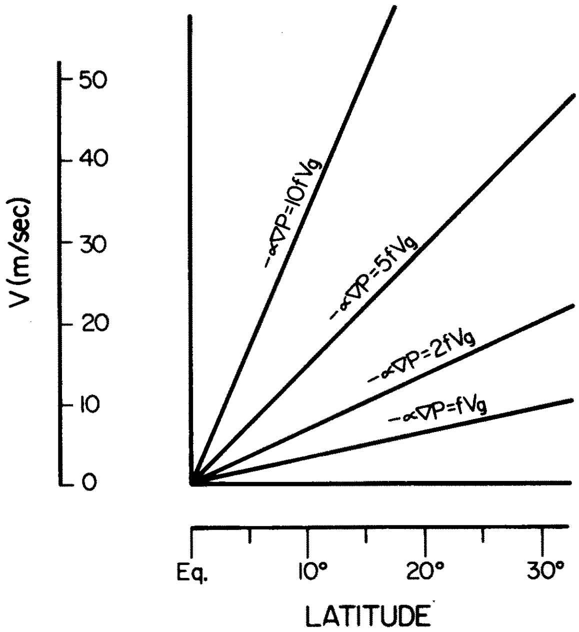

Fig. 22. Latitude variation of equilibrium B.L. wind velocities (V) for pressure gradients ($-\alpha\nabla P$) equal to various factors of geostrophic acceleration (fV_g)

This severe restriction on wind velocities near the equator should likewise restrict tropical cyclone formation. In the very early stages of cyclone formation the ratio of curvature to geostrophic acceleration is not overly large. It is assumed that cyclone genesis cannot proceed if B.L. velocities cannot be maintained.

Besides these difficulties of sustaining B.L. winds near the equator, other special latitudinal factors affect cyclone genesis. A 5^{o} to 10^{o} wide cyclone straddling the equator would have a severe lop-sided balance of acceleration due to reversal of geostrophic relationship at the equator. Even if the near equator cyclone was restricted to one side of the equator, the latitude variation of geostrophic winds would, in the early stages of cyclone growth, create a large latitudinal imbalance of accelerations.

Conclusion. Boundary Layer dissipation is independent of latitude. Momentum generation, on the other hand, is latitude related. Cyclone intensification cannot occur if B.L. winds cannot be maintained. Other conditions being favorable and remaining constant, tropical cyclone genesis should be directly related to the strength of the Coriolis parameter.

4.3 Role of Tropospheric Vertical Wind Shear and Upper Level Ventilation.

As previously discussed by the author (Gray, 1968) the observational evidence clearly shows that tropical cyclones form under conditions of minimum vertical shear of the horizontal wind between the lower and upper troposphere. Because the primary cloud cluster enthalpy gain for cyclogenesis comes between the 200 and 500 mb levels, it is the horizontal winds at the upper levels which are most important in determining whether a cloud cluster will be able to accumulate enthalpy. As shown in Fig. 17 the individual level cluster winds ($\mathbb{V}$) may be quite different than that of the cluster or disturbance velocity($\mathbb{V}_d$). The magnitude of ($\mathbb{V} - \mathbb{V}_d$) determines the extent to which the cumulus induced upper level warming is advected, or ventilated away from the disturbance. If this cloud cluster relative motion is small as in the third diagram from the left of Fig. 17, an upper level enthalpy increase can occur. This will lead to gradual surface pressure decreases and cyclone formation. Once a cyclone has formed, the environmental motion relative to the system becomes very small and further enthalpy gain can be readily accomplished. If, however, the upper tropospheric flow relative to the motion of the disturbance is large as is shown in the other three profiles of Fig. 17, then 200-500 mb ventilation of enthalpy out of the cluster is too rapid to permit concentration and accumulation. Pressure falls will not occur.

Disturbance Ventilation and Enthalpy Accumulation. Let $|\mathbb{V} - \mathbb{V}_d|_p$ represent the flow of the environmental wind through the cloud cluster at any level p. This is a measure of the non-divergent advection or ventilation of the disturbance. Enthalpy accumulation is a function of $|\mathbb{V} - \mathbb{V}_d|_p$ and the diameter (D) of the cluster heating function. Cluster mean ventilation (Ven.) at any level p may be expressed as

$$(\text{Ven.})_p = |\mathbb{V} - \mathbb{V}_d|/2D \tag{5}$$

and the Heating Retention Factor (H.R.F.) due to ventilation at any level p as

$$(\text{H.R.F.})_p = \left[1 - \left(\frac{|\mathbb{V} - \mathbb{V}_d|_p \,\Delta t}{2D}\right)\right] \tag{6}$$

where Δt represents the interval of time over which the calculation is made. Stability of calculations require that $|\mathbb{V} - \mathbb{V}_d|\Delta t / 2D$ be less than 1/2. This factor varies from 0 to 1.

Let H_p be the rate of sensible temperature accumulation $\frac{\Delta T}{\Delta t}$ at any pressure level p in the cluster due to warming processes or the cluster heating function. The net temperature accumulation with time from t_o to t_x at any level is represented by $T_x - T_o$ and is given by

$$(T_x - T_o)_p = \sum_{t=t_o}^{t=t_x} (H)_p \; (H.R.F.)_p \; \Delta t \qquad \text{or} \qquad (7)$$

$$(T_x - T_o)_p = \sum_{t=t_o}^{t=t_x} \left(\frac{\Delta T}{\Delta t}\right)_p \left[1 - \left(\frac{|\mathbb{V} - \mathbb{V}_d|_p \; \Delta t}{2D} \right) \right] \Delta t$$

where T_x = the final temperature at time t_x

T_o = the initial temperature at time t_o.

By assuming various values H, D, and $|\mathbb{V} - \mathbb{V}_d|$ one can calculate typical rates of enthalpy accumulation and see how these are related to D and $|\mathbb{V} - \mathbb{V}_d|$. Table 4 portrays how various values of $|\mathbb{V} - \mathbb{V}_d|$ and D influence the accumulation of enthalpy at an individual level over a period of three days if the heating function $(H)_p$ is assumed to be 1^oC/day over the whole period. Note the large influence which ventilation has on reducing the disturbance enthalpy accumulation. If the heating occurs over a large area, the inhibiting influence of $|\mathbb{V} - \mathbb{V}_d|$ is much reduced. Compare the temperature increase in Table 4 for heating widths of 100 and 250 km with the temperature increase shown in Fig. 23 for an assumed width of 400 km. Thus, a cloud cluster with a very narrow heating area (or small value of D) is much less able to accumulate enthalpy.

If the assumed vertical enthalpy increase or heating rate of Fig. 10 is applied to clusters with various intensities of ventilation, the vertical distributions of temperature accumulation for a heating function of 250 km width are as portrayed in Fig. 24. The left diagram shows the temperature accumulation which would result if ventilation at all levels were zero. The center diagram shows the temperature accumulation which results with only weak ventilation and the diagram on the

Table 4

Accumulated Temperature Increase (^{o}C) vs. Time for Different Values of Disturbance $|\mathbb{V} - \mathbb{V}_d|$ and D and for a Heating Rate of $1^{o}C$/day. Warming Values Were Calculated From Eq. 7.

For Disturbance Warming of 100 km Diameter

$\|V - V_d\|$ in m/sec	Time (t) t_o	12 Hours	1 Day	2 Days	3 Days
0	0	0.5	1.0	2.0	3.0
5	0	0.3	0.4	0.4	0.4
10	0	0.1	0.2	0.2	0.2
15	0	0.1	0.1	0.1	0.1

For Disturbance Warming of 250 km Diameter

$\|V - V_d\|$ in m/sec	Time (t) t_o	12 Hours	1 Day	2 Days	3 Days
0	0	0.5	1.0	2.0	3.0
5	0	0.3	0.6	0.8	0.8
10	0	0.2	0.4	0.5	0.5
15	0	0.2	0.3	0.4	0.4
20	0	0.1	0.2	0.2	0.2

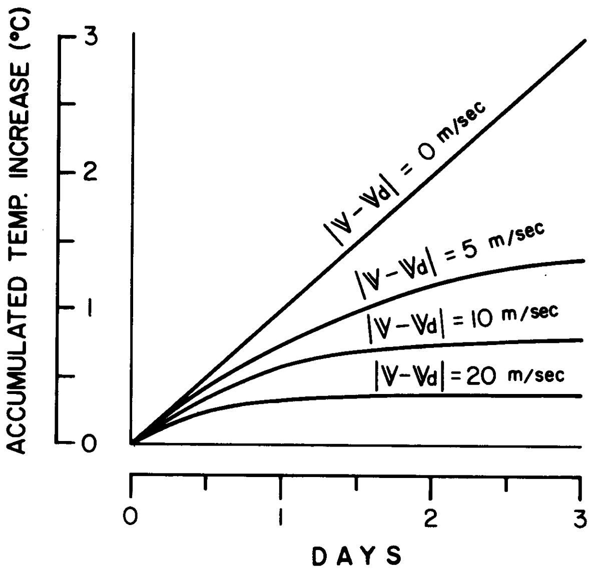

Fig. 23. Individual level rate of temperature accumulation in a cloud cluster with a 400 km wide (or D) 1°C/day heating function for various magnitudes of $|\mathbb{V} - \mathbb{V}_d|$.

right the enthalpy accumulation which results with the usual cloud cluster. In the first case surface pressure falls of 4-5 mb would occur in three days. In the second case pressure falls of 1-2 mb occur after three days. In the third case the surface pressure decrease after three days is only $\sim$ 0.1 mb. In the first case a cyclone rapidly forms. In the second case a cyclone slowly forms. This is typical of the usual genesis situation. No cyclone formation is possible in the third case. Lopez (1968) has previously analyzed two cloud cluster cases of cyclone growth and non-growth and indicated differences in heating rates approximately equivalent to the two cases on the right of this figure.

Figure 25 portrays the author's idea of the realized heating differences between the developing and non-developing cloud cluster. The differences in realized net warming between the two systems are due primarily to upper level ventilation differences and not to heating function differences. Thus, the pre-cyclone cloud cluster and the

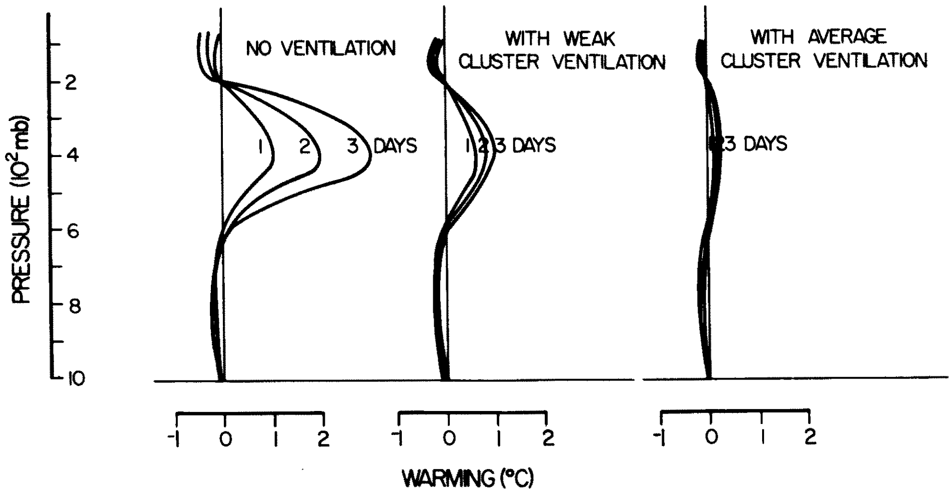

Fig. 24. Rate of temperature accumulation and resulting surface pressure decreases for 250 km wide cloud clusters with identical heating function of Fig. 10. but with different magnitudes of ventilation.

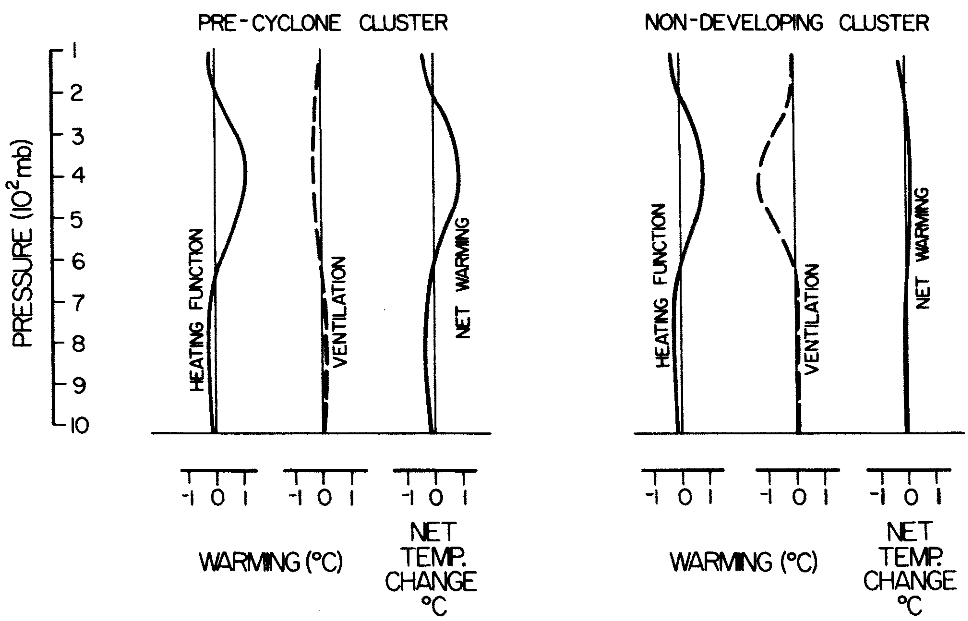

Fig. 25. Portrayal of how ventilation differences between cloud clusters can determine the magnitude of upper level warming and whether the cluster will grow into a cyclone or not.

usual cloud cluster can have very similar mean divergence profiles (as in Fig. 15) and similar rainfall rates, but, due to ventilation differences, their intensification potentials can be very different. Riehl (personal communications - 1957-1962) has often remarked on the lack of direct association of disturbance rainfall and disturbance intensification potential.

These ventilation differences can, in general, be well represented by the vertical shear of horizontal wind between the lower and upper troposphere. The tropical forecast offices in Miami (Simpson, 1971) and Guam (Atkinson, 1973) are presently using tropospheric vertical wind shear as a primary factor in forecasting cyclone genesis. Cyclones do not form when the 950 to 200 mb vertical wind shears are greater than about 10 m/sec or when the 200-500 mb wind velocities relative to the cloud cluster motion are larger than about 5 m/sec. Simpson and Riehl (1958) have earlier commented on the possible importance of middle tropospheric ventilation as a constraint on hurricane development and maintenance. Holton (1971) has also indicated a large influence of vertical shear on the heating pattern of tropical wave disturbances.

Conclusion. Other conditions being favorable and remaining constant cyclone genesis potential should be inversely related to the magnitude of the cloud cluster ventilation between 500 and 200 mb. This ventilation can be rather accurately expressed in terms of the vertical shear of the horizontal wind between 950 and 200 mb.

4.4 Role of Ocean Thermal Energy

As previously discussed by Jordan (1964), Landis and Leipper (1968), Leipper (1967), Leipper and Jensen (1971), Leipper and Volgenau (1972), Heffernan (1972), and Perlroth (1967, 1969), tropical cyclones can have a profound influence on the temperature of the ocean over which they travel. The altered ocean temperature, in turn, can feed back and alter the character of the cyclone.

Leipper and his research group have indicated that the inner region of the average hurricane consumes about 4000 cal/cm^2 per day of ocean sensible and latent heat energy. In their study of the hurricane boundary layer Malkus and Riehl (1960) put this value at $\sim$ 3100 cal/cm^2 per day over the inner 90 km radius of the storm. Whitaker's (1967) calculations for Hurricane Betsy indicate a value of about 3700 cal/cm^2 per day. This large surface energy requirement of the hurricane precludes its existence over land or over the ocean if these transfers should somehow be suppressed. Brand (1971) has discussed how typhoons can weaken when they cross the track of a previous typhoon which has produced a cooler sea surface temperature due to upwelling. Garstang (1967) has presented observational evidence on the way in which the sea transfers sensible and latent heat to the air above it.

The tropical cyclone not only gains energy from the ocean but its cyclonic wind circulation causes oceanic upwelling near the storm's center. The wind circulation produces a cyclonic ocean circulation which is not balanced by an equivalent upward and outward slope of water surface. The reduced air pressure at the storm's center may even cause a slight rising of the inner core ocean surface. Oceanic divergence is developed as a consequence. Upwelling occurs within and around the cyclone center (Black and Mallinger, 1971) as a result of this oceanic divergence. If the ocean has only shallow warm water, then a cold water upwelling will occur and the ocean will not be able to transfer its required energy to the air. Surface air temperature will decrease. The potential moist instability of the inner cyclone area will also be much reduced. O'Brien and Reid (1967) and O'Brien (1967) have provided numerical confirmation of these central hurricane upwelling physical arguments. Leipper and his research colleagues have provided observational arguments.

Figure 26 shows the influence of reduced surface air temperature on surface values of Θ_e for a constant relative humidity of 85 percent. A very substantial decrease in the Θ_e gradient between the surface and 600 mb is noted for surface temperature decreases of only 2-3°C. Surface temperatures less than 26°C do not permit sufficient thermal buoyancy to sustain Cb convection. Palmén (1948, 1957) has earlier demonstrated a well defined cut-off of tropical cyclone activity with the 26½$^\circ$C ocean isotherm. Middle tropospheric values of Θ_e undergo much less daily, seasonal, and geographic variation than do surface values. Thus, potential moist buoyancy $(\frac{\partial \Theta_e}{\partial p})$ between the surface and middle layers is primarily influenced by the change of sea surface temperature.

Ocean Thermal Potential. Leipper and Perlroth have indicated that the influence of hurricanes on the ocean underneath them can extend down to about 60 meters. Given the well established criteria of surface air temperature being above 26°C, then following Leipper and Jensen (1971) and Leipper and Volgenau (1972), an ocean thermal energy potential (E) in units of calories/cm^2 can be defined to be the sum of the ocean thermal energy above 26°C down to a depth of 60 meters, or

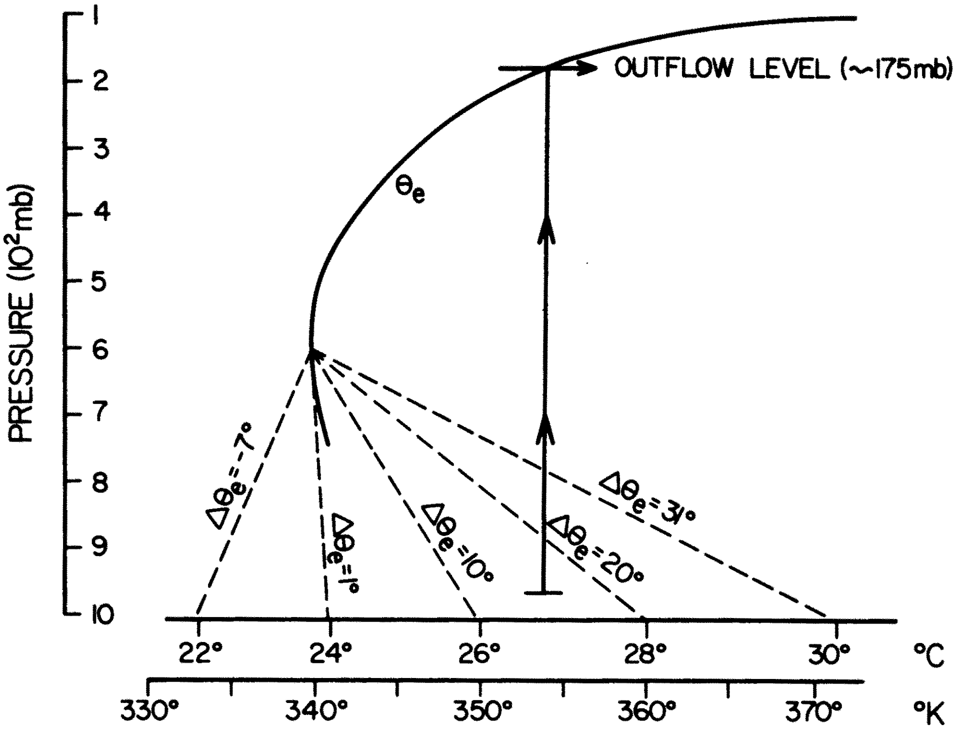

Fig. 26. Portrayal of how oceanic surface temperature changes can influence the Θ_e gradient between the surface and 600 mb under assumed constant surface humidity of 85 percent. Solid arrow portrays the path of undiluted moist ascent from a boundary layer Θ_e value of 354°K to the level of maximum typhoon outflow.

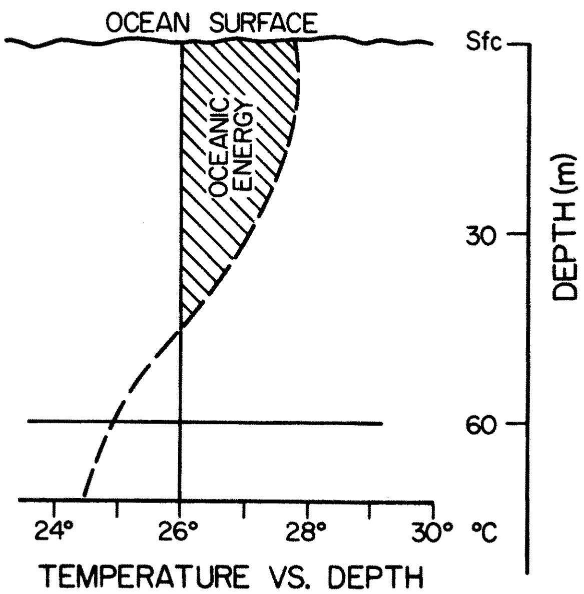

Fig. 27. Cross section view of the typical ocean temperature decrease with depth and how the ocean thermal energy (E) is defined (hatched) following Leipper and Volgenau (1972) as the area to the right of the 26°C isotherm to a depth of 60 meters.

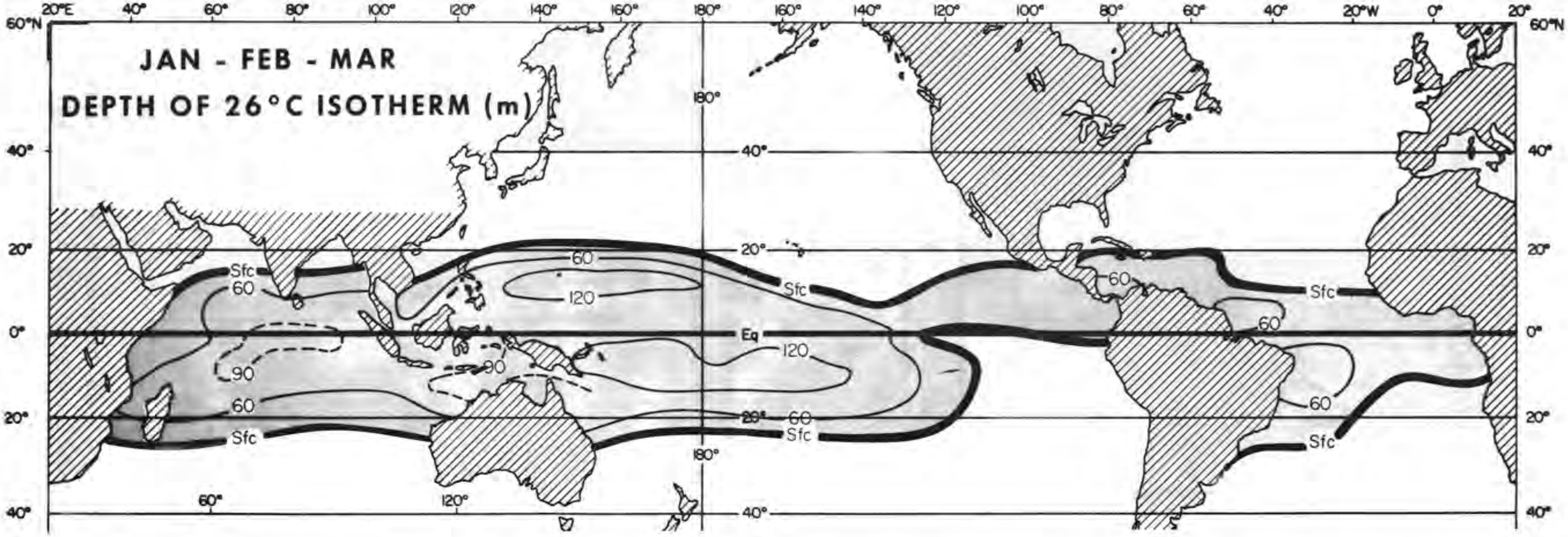
JAN - FEB - MAR
DEPTH OF 26°C ISOTHERM (m)
Sfc
60
120
90
Eq
20°E
40°
60°
80°
100°
120°
140°
160°
180°
140°
120°
100°
80°
60°
40°
20°W
0°
20°
60°N
40°
20°
0°
20°
40°

Fig. 28

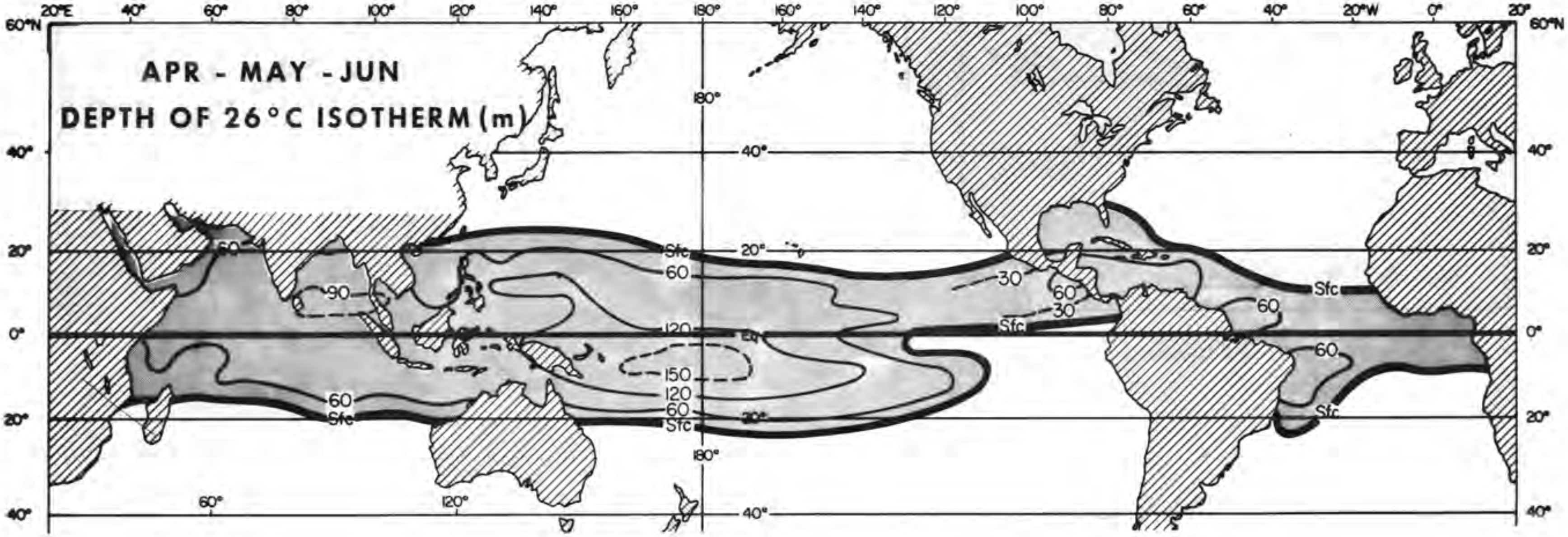
APR - MAY - JUN
DEPTH OF 26°C ISOTHERM (m)
Sfc
30
60
90
120
150
Eq
20°E
40°
60°
80°
100°
120°
140°
160°
180°
140°
120°
100°
80°
60°
40°
20°W
0°
20°
60°N
40°
20°
0°
20°
40°

Fig. 29

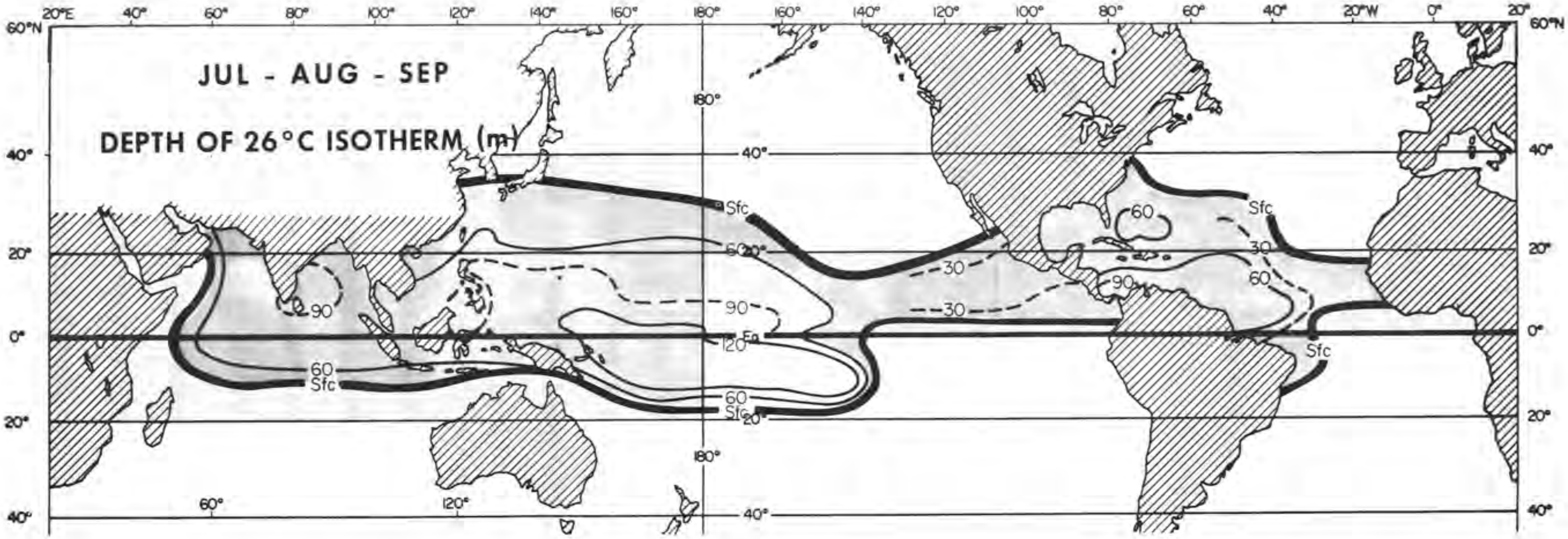
JUL - AUG - SEP
DEPTH OF 26°C ISOTHERM (m)
Sfc
30
60
90
120
Eq
20°E
40°
60°
80°
100°
120°
140°
160°
180°
20°W
0°
20°
60°N
40°
20°
0°
20°
40°

Fig. 30

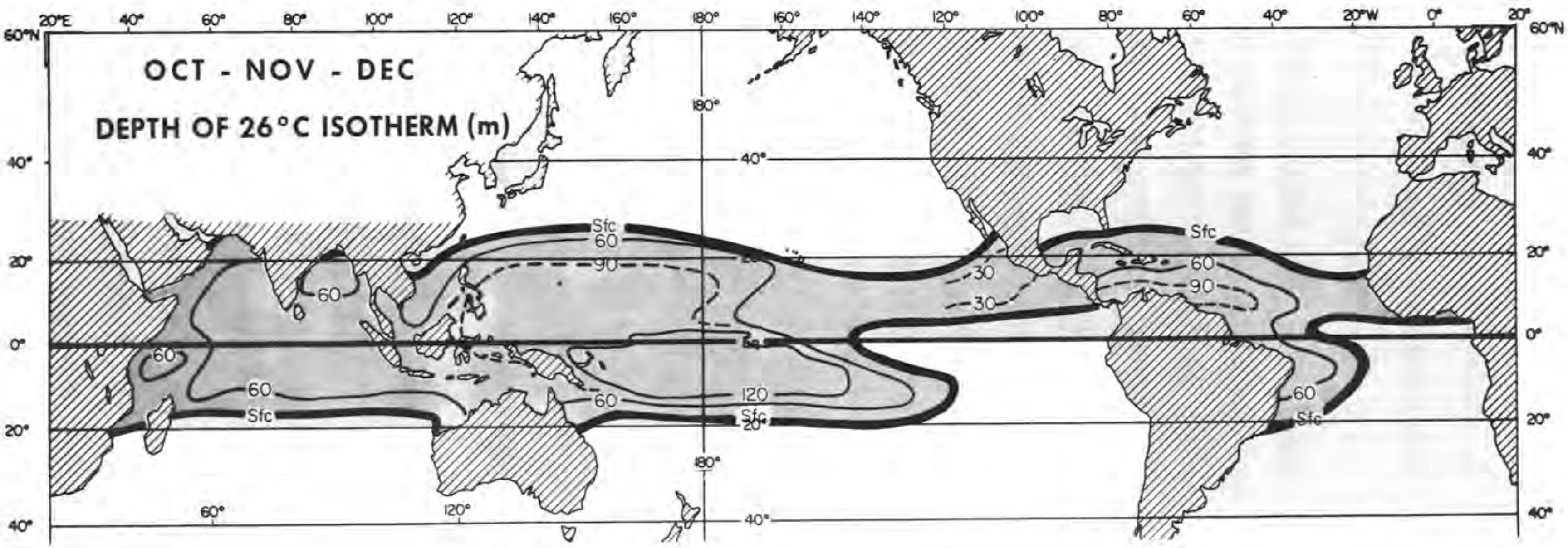
OCT - NOV - DEC
DEPTH OF 26°C ISOTHERM (m)
Sfc
30
60
90
120
Eq
20°E
40°
60°
80°
100°
120°
140°
160°
180°
20°W
0°
20°
60°N
40°
20°
0°
20°
40°

Fig. 31

$$E = \int_{sfc}^{\substack{60 \text{ m or} \\ \text{where } T = 26^{o}C}} \rho_w c_w \,(T - 26)\, dZ \tag{8}$$

where ρ_w is ocean density (1 gm/cm^3)

c_w is the specific heat of water (1 cal/gm ^oC)

T is ocean temperature in ^oC.

This energy is portrayed in Fig. 27.

Figures 28-31 show the depth of the 26^{o}C ocean isotherm in meters (m) for each season (see the appendix for the data sources of this information). Note the general shallowness of the 26^{o}C isotherm in the eastern oceans. The energy contained in the Eastern Hemisphere is much greater than in the Western Hemisphere.

Figures 40, 55, 70, and 85 (section 5) portray seasonal values of ocean thermal energy (E) as here defined in units of 10^3 cal/cm^2. Note the very high energy levels in the Western Pacific.

Conclusion. Other conditions being favorable and remaining constant, tropical cyclone genesis should be directly related to the magnitude of ocean thermal energy (as here defined).

4.5 Role of Surface to Middle Troposphere Θ_e Gradient

Except when there is deep cumulus convection to produce vertical coupling, the flow features of the tropical upper and lower troposphere appear to operate independently (Riehl, 1954). Tropical cyclone circulations, however, extend through the entire troposphere. Cyclones do not occur unless there is a well established vertical coupling of the lower and upper tropospheric flow patterns. Cumulonimbus convection acts as the primary mechanism for this vertical coupling.

Cb convection requires substantial ($10^{o}K$ or more) decrease of Θ_e between the boundary layer and the middle troposphere (lowest values of Θ_e are typically at 600 mb, see Fig. 26). A number of other researchers such as Aspliden (1971) have discussed the characteristics of the ($\Theta_{e_{sfc}} - \Theta_{e_{600mb}}$) differences over the tropical oceans with different types of convection. For convenience and following the author's previous paper (Gray, 1968) Θ_e gradients are taken between the surface and 500 mb These values typically range between 15-20^{o}K. Figures 41, 56, 71, and 86 give seasonal values of this parameter plus 5 units over all the oceans. Except in sub-tropical latitudes in winter, the values of this parameter are usually adequate for cyclone development. Daily parameter deviations are small and typically not well related to cyclone genesis potential.

Conclusion. Other conditions being favorable and remaining constant, cyclone genesis should be directly related to the moist buoyancy potential or the magnitude of the boundary layer to middle troposphere difference of Θ_e. This buoyancy is well specified by the Θ_e difference between the surface and the 500 mb level.

4.6 Role of Middle Troposphere Humidity

It is observed that tropical cyclones form only in regions where the seasonally averaged values of middle level humidity are high. Cyclones do not form where seasonal values of middle level humidity are low.

Other factors being equal, an environment of high middle level humidity is more conducive to deep cumulus convection and greater vertical coupling of the troposphere than is a dry middle level environment. High middle level humidity is also conducive to high cloud precipitation efficiency.

It must be remembered that in cyclone genesis situations the oceanic boundary layer does not experience a diurnal warming cycle as is present over land and that tropospheric vertical wind shears are small. These conditions preclude squall line development and intense buoyant up-and-downdraft activity that is possible where large diurnal heating cycles and strong tropospheric wind shears are present. Although deep and intense Cb convection occurs over middle latitude land areas in conditions of low middle level relative humidity, Cb convection does not typically occur over ocean regions when middle level humidity is less than 50-60 percent. Over tropical oceans high middle level vapor content appears to be a strong enhancer rather than an inhibitor of deep cumulus convection.

To better understand the influence of middle level humidity on Cb parcel buoyancy, Table 5 has been prepared. This table compares the temperature of a parcel lifted moist adiabatically from 850 to 250 mb under assumed entrainment rates of 0, 10, and 20 percent per 100 mb in two environments whose humidity above 850 mb is different by 25 percent. An initial parcel buoyancy of 1.7^{o} at 850 mb is assumed for both environments. Parcels entrain air with the humidity values of the environment listed at the left of this table. The large influence of middle level humidity differences of only 25 percent in reducing updraft parcel buoyancy when entrainment is occurring is evident.

High middle level humidity also leads to increased precipitation efficiency and the greater likelihood of enthalpy increase. Lopez's (1973b) model of the cumulus life cycle indicates a direct relationship between cumulus induced precipitation at the ground and upper level relative humidity. When upper level humidity is low, much of the cumulus induced condensation does not fall to the ground, but is

Table 5

Influence of Middle Troposphere Humidity on Parcel Buoyancy for Different Values of Entrainment from 850 mb.

Pressure Level (mb)	Relative Humidity (percent)		Cumulus Parcel Temperature Minus Environment Temperature (^oC): No Entrainment		For Environment Entrainment of 10% per 100 mb		For Environment Entrainment of 20% per 100 mb	
	Typical Cluster Humidity	Typical Cluster Humidity less 25%	Higher Humidity	Lower Humidity	Higher Humidity	Lower Humidity	Higher Humidity	Lower Humidity
850	80	55	1.7	1.7	1.7	1.7	1.7	1.7
750	78	53	2.2	2.2	1.5	0.8	0.6	-1.1
650	76	51	3.0	3.0	1.7	0.4	0.2	-2.7
550	74	49	3.8	3.8	2.0	0.2	0.1	-3.7
450	72	47	4.2	4.2	2.0	-0.1	0	-4.6
350	70	45	4.0	4.0	1.6	-0.5	-0.7	-5.6
250	65	40	4.0	4.0	1.5	-0.7	-0.9	-6.0

re-evaporated. This produces upper level cooling which can act to suppress rather than enhance the increase of enthalpy.

It will thus be assumed that cyclone genesis is directly related to the average of 500 and 700 mb relative humidity. Figure 32 shows how seasonal values of middle level humidity are related to a humidity parameter which is assumed to be associated with cyclone genesis. This humidity parameter varies from 0 to 1. Cyclone development is not possible if seasonal 500-700 mb humidity is less than 40 percent. This factor increases linearly to 1 for seasonal 700-500 mb humidity equal to or greater than 70 percent or

$$\text{Humidity Parameter} = \frac{\overline{RH} - 40}{30} \quad \text{if } \overline{RH} \text{ is between 40 and 70\% .}$$

This parameter is one for seasonal humidity above 70 percent and zero for seasonal humidities less than 40 percent. Figures 42, 57, 72, and 87 show the average seasonal values of 500-700 mb humidity.

<u>Conclusion</u>. Other conditions being favorable and remaining constant, tropical cyclone genesis frequency should be directly related to seasonal values of middle tropospheric humidity. The relationship between middle level moisture and cyclone genesis is expressed by the above humidity parameter.

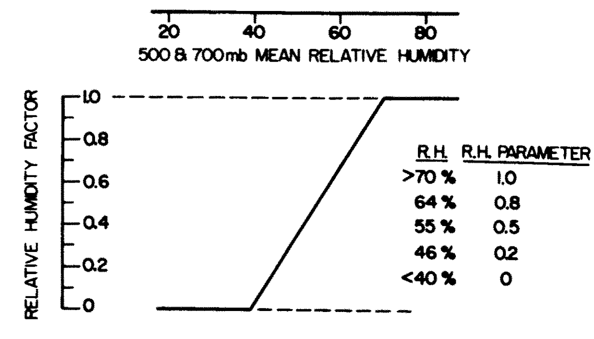

Fig. 32. Relationship between average 500 to 700 mb seasonal relative humidity and the Humidity Parameter.

5. SPECIFICATION OF SEASONAL GENESIS FREQUENCY

It is hypothesized that tropical cyclone formation will be most frequent in the regions and in the seasons when the product of the six primary genesis parameters just discussed are a maximum. Seasonal Genesis Frequency should be determined by the product of:

$$(\zeta_r)\ (f)\ (1/S_z) \times (E)\ \left(\frac{\partial \Theta_e}{\partial p}\right)\ (\overline{RH})$$

where ζ_r = Relative vorticity at top of planetary boundary layer or~950 mb

f = Coriolis parameter

$1/S_z$ = $1/\left|\partial \mathbb{V}_h/\partial p\right|$ or the inverse of the absolute value of the vertical shear of the horizontal wind between 950 and 200 mb

E = Ocean thermal energy above 26°C to 60 m depth

$\frac{\partial \Theta_e}{\partial p}$ = Vertical gradient of Θ_e between the surface and 500 mb

$\overline{RH}$ = Mean relative humidity between the levels of 500-700 mb

Zero and negative values of the above parameters indicate no genesis potential.

There is some difficulty with using these seasonal values directly. Seasonal values are not always a close measure of what the daily parameter values can be. Thus, the seasonal relative vorticity in the Western Atlantic is slightly negative. The above seasonally determined genesis potential would not predict cyclone genesis in a region where it obviously occurs. When the seasonal values of $\left|\partial \mathbb{V}_h/\partial p\right|$ are small, unreasonably large values of $1/S_z$ are obtained, which are not representative of the average of the daily values. Similarly the seasonal values of

$\partial\Theta_e/\partial p$ between the surface and 500 mb could be zero or negative, but individual time period values can be positive.

To cover the range of possible daily deviations of three of these parameters arbitrary units were added to the seasonal values to simulate in an approximate sense what the average of the positive daily deviations of these values could be. Thus, five units of 10^{-6}sec^{-1} vorticity were added to all the seasonally measured values of this parameter and 5°K was added to all the seasonal values of $\partial\Theta_e/\partial p$. To prevent unreasonably large values of the genesis frequency when $|\partial \mathbb{V}_h/\partial p|$ approaches zero, and also to assure that the seasonal average of $|\partial \mathbb{V}_h/\partial p|$ is more representative of the seasonal average of the daily values, 3 m/sec was arbitrarily added to all the seasonal vertical shear values. The minimum value of the vertical shear parameter is thus 3 units.

A Seasonal Genesis Parameter is now defined as

$$\begin{pmatrix}\text{Seasonal}\\\text{Genesis}\\\text{Parameter}\end{pmatrix} \propto \left[\begin{pmatrix}\text{Vorticity}\\\text{Parameter}\end{pmatrix}\begin{pmatrix}\text{Coriolis}\\\text{Parameter}\end{pmatrix}\begin{pmatrix}\text{Vertical Shear}\\\text{Parameter}\end{pmatrix} \times \begin{pmatrix}\text{Ocean Energy}\\\text{Parameter}\end{pmatrix}\begin{pmatrix}\text{Moist Stability}\\\text{Parameter}\end{pmatrix}\begin{pmatrix}\text{Humidity}\\\text{Parameter}\end{pmatrix}\right] \tag{9}$$

where

$\begin{pmatrix}\text{Vorticity}\\\text{Parameter}\end{pmatrix}$ = $(\zeta_r + 5)$, where ζ_r is determined in units of 10^{-6}sec^{-1}.

$\begin{pmatrix}\text{Coriolis}\\\text{Parameter}\end{pmatrix}$ = f or $2\Omega\sin\varphi$, where Ω is the rotation rate of the earth and φ denotes latitude.

$\begin{pmatrix}\text{Vertical Shear}\\\text{Parameter}\end{pmatrix}$ = $1/(S_z+3)$ where $S_z = |\partial \mathbb{V}_h/\partial p|$ is determined in units of m/sec per 750 mb.

$\begin{pmatrix}\text{Ocean Energy}\\\text{Parameter}\end{pmatrix}$ = E or $\int_{60\text{ m}}^{\text{sfc}} \rho_w c_w\ (T - 26^{\circ})\ \delta z$, where ρ_w and c_w are the density and specific heat capacity of water. T is expressed in ^{o}C. T - 26^{o}=zero if T $\leq$ 26^{o}C. E is expressed in units of 10^{3} cal/cm^{2}.

(Moist Stability) = $\partial\Theta_e/\partial p + 5$, where $\partial\Theta_e/\partial p$ is in units of ^{o}K per 500 mb.

(Humidity Parameter) = $\frac{\overline{RH} - 40}{30}$ or $(\overline{RH} - 40)/30$ where $\overline{RH}$ is the mean relative humidity between 500 and 700 mb. Parameter is zero for $\overline{RH} < 40$, and 1 for $\overline{RH} \geq 70$.

Table 6 summarizes these parameters and their role in cyclone genesis. This Seasonal Genesis Parameter (SGP) may also be thought of in the form of

$$\begin{pmatrix}\text{Seasonal}\\ \text{Genesis}\\ \text{Parameter}\end{pmatrix} = (\text{Dynamic Potential}) \times (\text{Thermal Potential}) \qquad (10)$$

where

$$\text{Dynamic Potential} = (f)\,(\zeta_r + 5)\,[1/(S_z + 3)] \qquad (11)$$

$$\text{Thermal Potential} = (E)\,(\partial\Theta_e/\partial p + 5)\,(\overline{RH}\ \text{Parameter}) \qquad (12)$$

Dynamic Potential is expressed in units of (10^{-11}sec^{-2} per m/sec per 750 mb), and Thermal Potential in units of (10^{5} cal/cm^{2} ^{o}K per 500 mb). Thermal Potential may also be thought of as the potential for Cb convection.

Figures 33 to 92 have been arranged to portray all parameters in sequence by season where January-March is portrayed by Figs. 33-47, April-June by Figs. 48-62, July-September by Figs. 63-77 and October-December by Figs. 78-92.

Relation of Seasonal Wind Fields and Sea Surface Temperature to Cyclone Genesis. To understand cyclone genesis one must have knowledge of how the lower (∿ 950 mb) and upper (∿ 200 mb) tropospheric wind fields and the sea surface temperature (SST) fields are related to

Table 6

Summary of Primary Genesis Parameters

Parameter	Favorable Condition	Genesis Role
1. Vorticity Parameter -- $(\zeta_r + 5)$ at $\sim$950 mb where ζ_r is in units of $10^{-6}sec^{-1}$	Large	Produce necessary low level mass, moisture, and momentum convergence through Ekman-type boundary layer friction
2. Coriolis Parameter -- or f	Large	Allow for pressure gradient and sustaining of boundary layer winds against frictional dissipation
3. Vertical Shear Parameter -- $1/(S_z + 3)$ where $1/S_z$ is in units of $(m/sec)^{-1}$ 750 mb	Large	Allow condensation warming to be concentrated over moving disturbance; i.e. inhibit 200-500 mb ventilation energy
4. Ocean Energy Parameter -- or E	Large	Maintain surface Θ_e values in conditions of strong winds, upwelling, and large sea to air energy transfers
5. Moist Stability Parameter -- $(\frac{\partial \Theta_e}{\partial p})$ from surface to 500 mb	Large	Permit Cb cumulus convection
6. Humidity Parameter -- $\overline{RH}$ between 500 and 700 mb	Large	Allow for deep cumulus convection and high rainfall efficiency

places and frequency of formation. To better acquaint the reader with the seasonal averages of these features, Figs. 33-36, 48-51, 63-66 and 78-81 have been constructed (see the appendix for the data sources). Note that seasonal genesis is most prevalent in association with the Doldrum Equatorial Troughs and where the seasonal 200 mb wind is variable or weakly from the east.

The strong correlation between cyclone genesis and upper tropospheric easterly winds is well established. A study of 10 years of U. S. Navy Fleet Weather Central, Joint Typhoon Warning Center (Guam), Annual Typhoon reports by the author has shown that the Guam analysis of 200 mb winds as best they could be determined over incipient disturbances which later became typhoons were from the NE, E, or SE in 123 out of 158 cases. Cyclones seldom form in regions where the upper tropospheric wind is from the west. Genesis is also inhibited off South India in July-September when the upper tropospheric easterly winds are too strongly from the east.

Genesis is also frequent in latitudes of 5-10^{o} in the Hemisphere opposite the Doldrum Trough such as in the Western North Pacific from January to March and in the South Indian and South Pacific Oceans from April to June. At these latitudes winter and autumn trade wind strengths decrease sharply equatorwards and low level cyclonic shear is present on both sides of the equator. As discussed by Hubert, Kreuger, and Winston (1969), this can give the appearance of a double inter-tropical convergence zone. Thus, winter time tropical cyclone genesis should not be unexpected at some low latitude locations. The 26^{o}C SST isotherm well specifies the poleward limit of cyclone genesis.

Spatial and Seasonal Variations of Genesis Parameters. Figures 37-38, 52-53, 67-68 and 82-83 portray the observationally determined seasonal average values of the vorticity and vertical shear parameters. The places of highest seasonal values of vorticity are usually places where doldrum equatorial troughs or Inter-Tropical Convergence Zones (ITCZ) are located. These are very favorable locations for cyclone genesis. Ramage (1974) has recently given more statistics on the relation of the ITCZ and cyclone genesis. Vorticity is naturally high on the equatorial or cyclonic side of the trade winds at latitudes of 5-15°. In the subtropical high pressure regions the values of ζ_r (in $10^{-6}sec^{-1}$) + 5 units are near zero or negative. The absence of doldrum equatorial troughs in the eastern South Pacific and South Atlantic is one important factor precluding development in those areas. The author has previously presented observational information (Gray, 1968) to show that genesis is favored just to the poleward side of the equatorial trough. Here the low-level cyclonic wind shear and vorticity are at a maximum.

The vertical shear $|\partial \mathbb{V}_h/\partial p|$ in m/sec per 750 mb + 3 units is generally a minimum in the areas just to the poleward side of the doldrum equatorial troughs. Note how the vertical shear is a minimum in the 5-15° latitude belts in the spring and autumn, but is larger near the equator following the summer solstice when genesis occurs at higher latitudes. Vertical shears are always large in the Southern Hemisphere poleward of 20-22°. Cyclone genesis is not possible at latitudes poleward of 22° in this Hemisphere. By contrast, in the western ocean areas of the Northern Hemisphere cyclone genesis can occur in summer at latitudes as high as 34° to 36°. It is no accident that in the eastern

South Pacific and in the South Atlantic where cyclones do not form, tropospheric vertical shears are large.

Dynamic Potential. Seasonal values of the dynamic potential or $[(\zeta_r + 5)\ (f)\ 1/(S_z + 3)]$ in units of $10^{-11}sec^{-2}$ per m/sec per 750 mb are portrayed in Figs. 39, 54, 69 and 84. A rather good general relationship between high values of this potential and the location and frequency of seasonal cyclone genesis is noted. But the direct association of dynamic potential with seasonal cyclone genesis has some important failings:

1) the highest magnitudes of dynamic potential do not always correspond with highest cyclone frequency,

2) genesis is predicted in a number of poleward latitudes where it does not occur,

3) genesis is predicted in summer in the eastern North Atlantic where it does not occur,

4) trade winds are stronger in winter, horizontal shear and vorticity are generally higher. Vertical shear at latitudes of 5-10° is no larger than in summer. One would expect more frequent cyclone genesis in winter than summer, especially in the western North Pacific. This is not the case.

Cyclone frequency is related to more than dynamic influences. Thermal and cumulus buoyancy considerations also play an important role.

Thermal Potential. Figures 40-42, 50-52, 70-72 and 85-87 give seasonal values of the ocean thermal energy (E), moist stability $(\partial\theta_e/\partial p + 5)$, and 500-700 mb relative humidity. The product of these three parameters may be considered as the thermal potential, or the potential for Cb convection.

Observe the large gradients of ocean thermal energy and the very high values in the Western Pacific. Note also that in the eastern North Atlantic the ocean thermal energy is not high in June-September. This is believed to be the primary reason why tropical cyclones do not form in this region despite the relatively high value of vorticity and low values of vertical shear. This was first noted by Perlroth (1969). The sharp cut-off of ocean thermal energy at latitudes of $\sim 20^{o}$ in the Southern Hemisphere and $\sim 25\text{-}35^{o}$ in the Northern Hemisphere precludes genesis at higher latitudes.

The moist stability parameter ($\partial\Theta_e/\partial p + 5$) is generally large at all oceanic locations except in the sub-tropical latitudes in winter. Cyclone genesis will not generally occur when the magnitude of this parameter is less than 10. When above 10, variations of this parameter do not greatly affect spatial and seasonal variations of genesis. The seasonal variation of the 10 line rather well specifies the poleward extent of cyclone genesis.

By contrast with the values of $\partial\Theta_e/\partial p$, the seasonal values of the humidity parameter are very important in specifying the spatial and seasonal frequency of cyclone genesis. Cyclones do not form in regions where the seasonal 500 to 700 mb relative humidity is less than 40 percent. The humidity parameter is a major factor in specifying differences in winter and summer cyclone frequency at low latitudes. Low humidity is also a primary factor in explaining the lack of cyclone genesis in the eastern South Pacific, South Atlantic, and in the South Indian Ocean poleward of 20^{o} latitude.

Seasonal values of the product of ocean energy parameter, moist stability parameter, and humidity parameter are presented in Figs. 43, 58, 73, and 88. Isolines are expressed in units of 10^5 cal/cm^2 ^{o}K per 500 mb. Note the higher values of this thermal or cumulonimbus potential in the western Pacific and in the Eastern Hemisphere in general. It is zero over large areas of the Western Hemisphere oceans. The dynamic potential, on the other hand, does not show such a large Eastern

Hemisphere dominance. Figure 9 shows that Eastern Hemisphere cyclone frequency is more than double that of the Western Hemisphere. Thus, it must be the very high thermal potentials of the Eastern Hemisphere which cause that Hemisphere's higher genesis frequency.

Verification. Figures 44-46, 59-61, 74-76, and 89-91 portray seasonal values of the Dynamic Potential and Thermal Potential, and their product, which is defined as the Seasonal Genesis Parameter. This has units of 1.5×10^{-8} cal $^{o}K\ sec^{-1}cm^{-3}$. When expressed in these units this gives just the right value required to specify seasonal cyclone genesis frequency in number per 5^{o} latitude-longitude square per 20 years. Hereafter the Seasonal Genesis Frequency will be expressed in these latter units. A comparison of Figs. 46 and 47, 61 and 62, 76 and 77 and 91 and 92 shows how closely this seasonal Genesis Parameter specifies the actual number of seasonal cyclone genesis occurrences in number per 5^{o} latitude-longitude per 20 years.

Figures 93-94 show the combined four season average of the genesis parameter and observed genesis frequency, also in number per 5^{o} square per 20 years. Again the correspondence between our defined genesis parameter and the observed genesis frequency is very close.

Conclusion. The very close correspondence between predicted and observed seasonal cyclone frequency lends support to the earlier arguments concerning the relevant physical genesis parameters. It was not expected that the agreement between predicted and observed genesis frequencies would be this close.

Application to Daily Forecasting. It is hoped that these seasonal genesis statistics can be adapted for use on a daily basis at the various government offices responsible for tropical cyclone monitoring.

As the satellite and jet aircraft wind measurements become more frequent and accurate, better daily measurements of low level vorticity and tropospheric vertical shear will be obtained. This should lead to improvement in the daily measurement of the genesis potential and also, hopefully, in the improved forecasting of individual cyclone genesis.

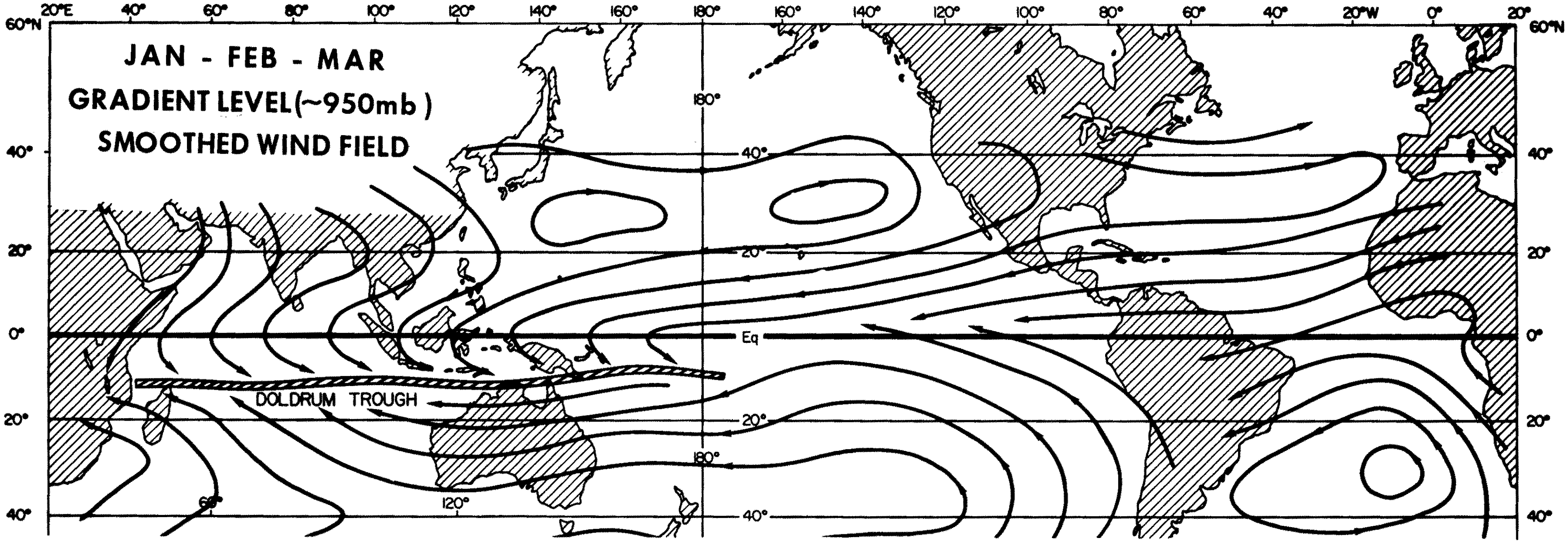
JAN - FEB - MAR
GRADIENT LEVEL(~950mb)
SMOOTHED WIND FIELD
DOLDRUM TROUGH
Eq

Fig. 33

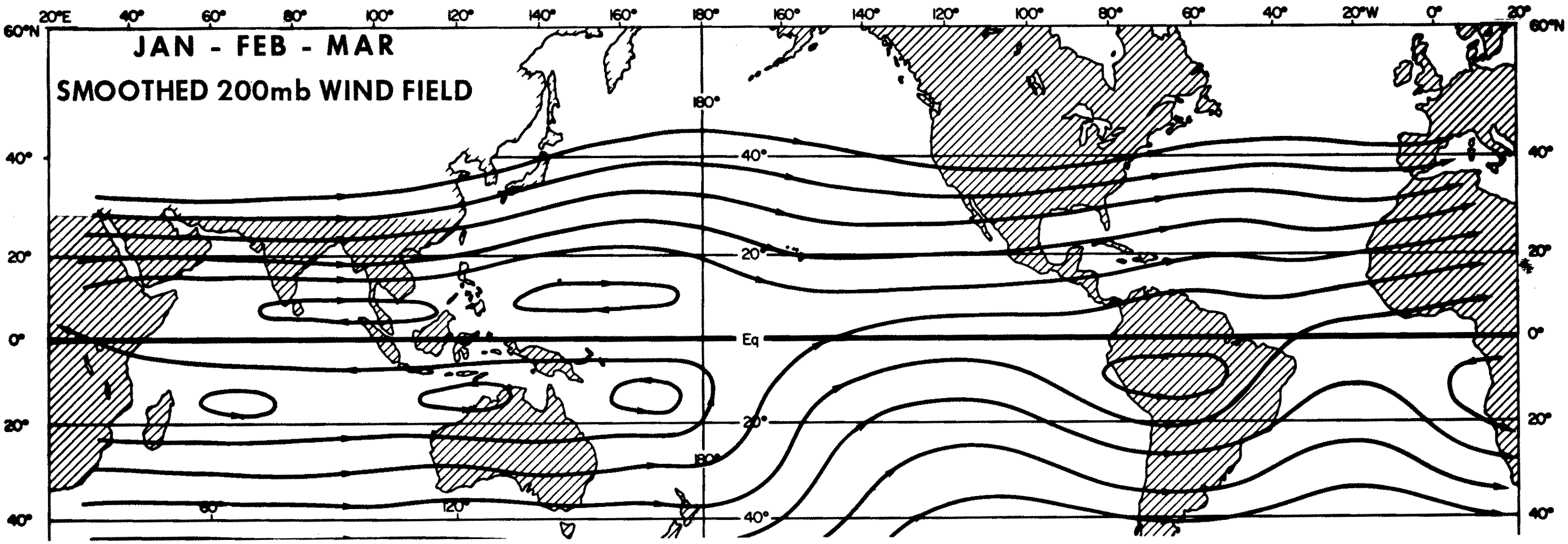
JAN - FEB - MAR
SMOOTHED 200mb WIND FIELD
Eq

Fig. 34

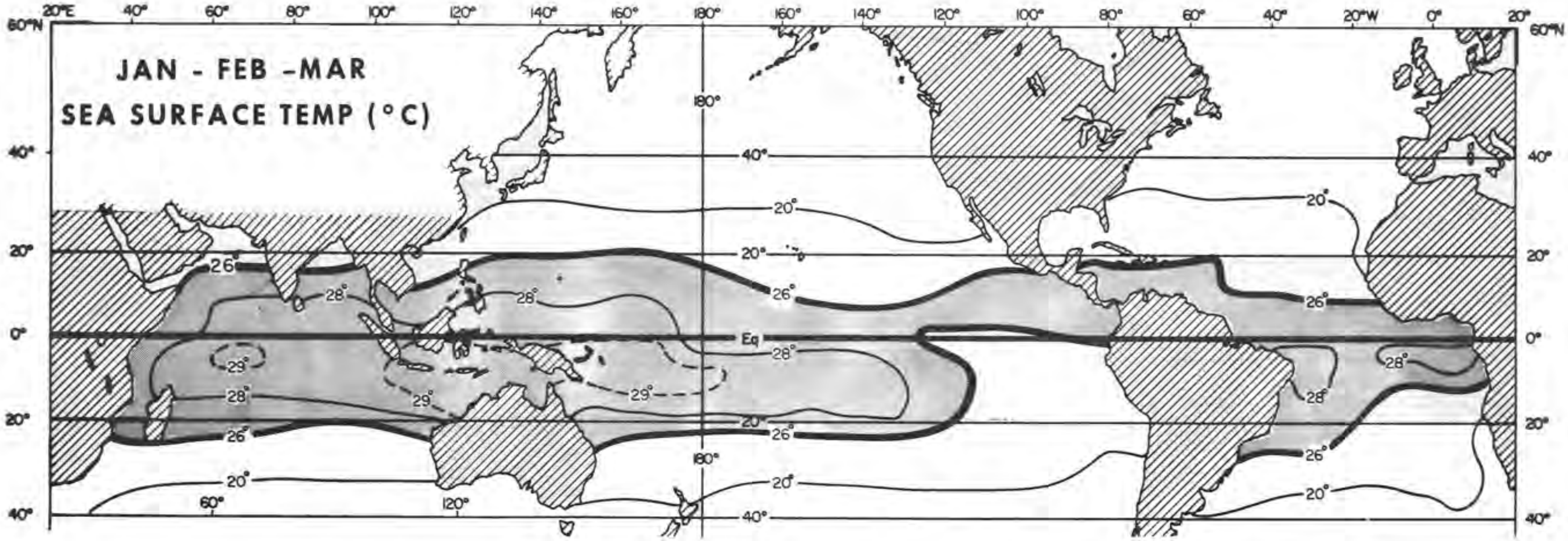
JAN - FEB -MAR
SEA SURFACE TEMP (°C)
20°
26°
28°
29°
Eq

Fig. 35

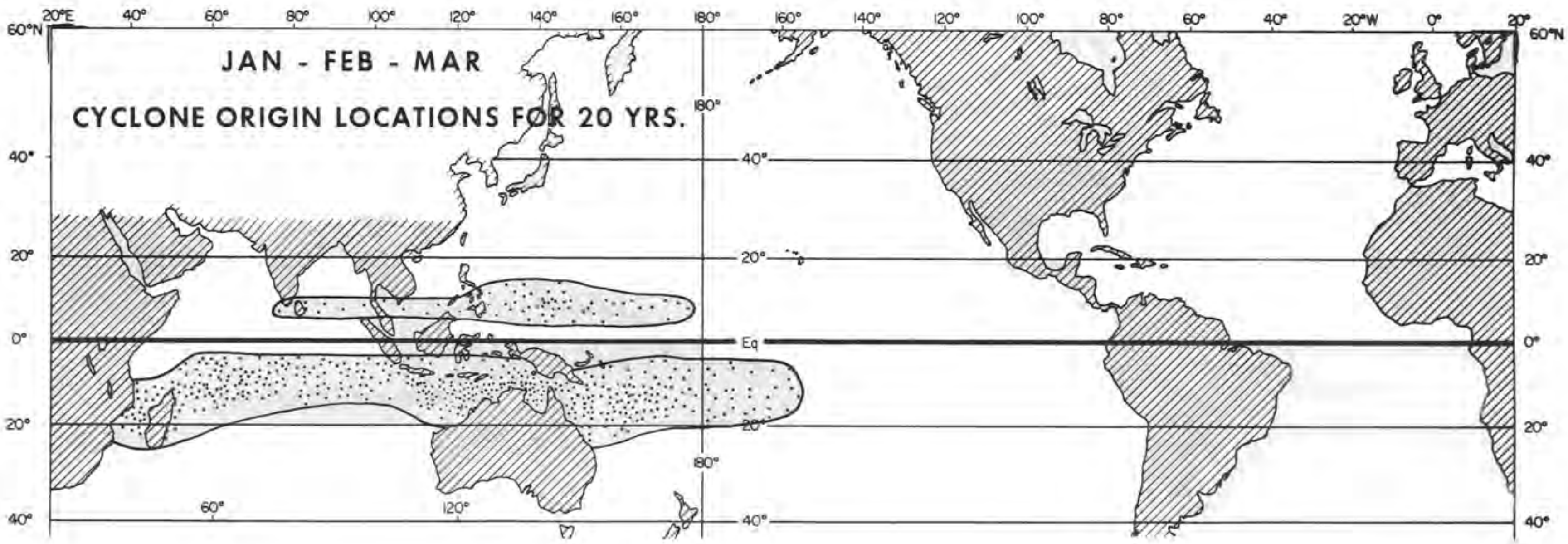
JAN - FEB - MAR
CYCLONE ORIGIN LOCATIONS FOR 20 YRS.
Eq

Fig. 36

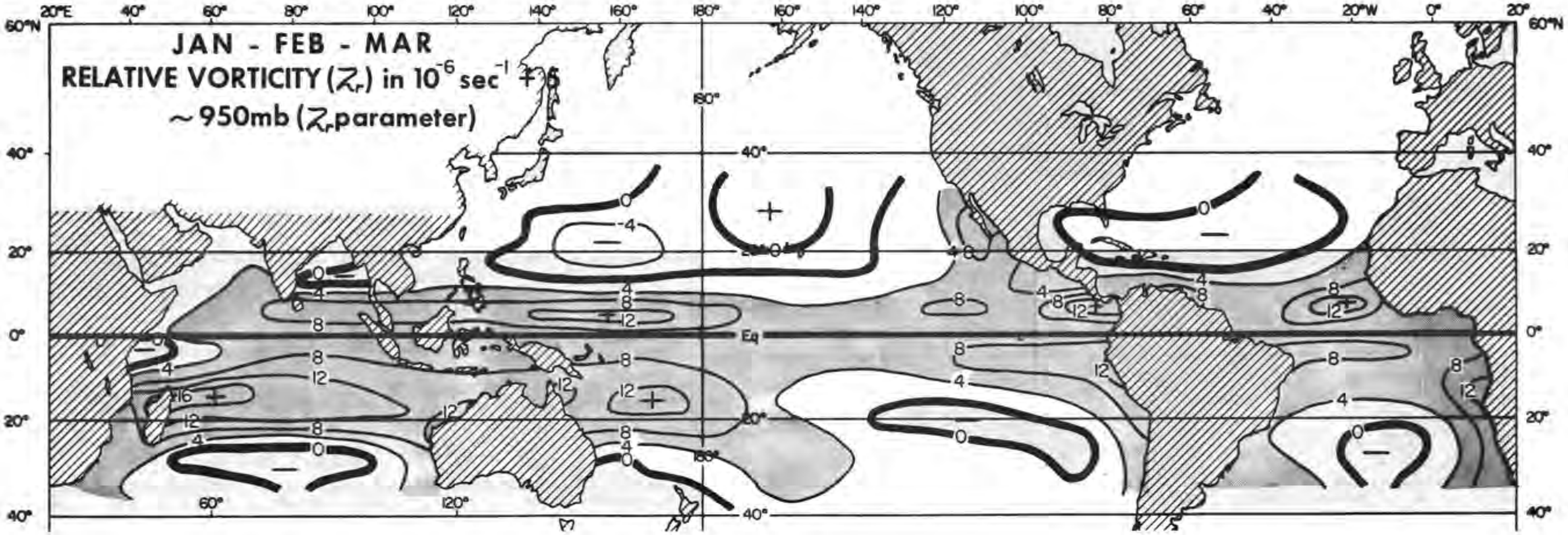
JAN - FEB - MAR
RELATIVE VORTICITY (ζ_r) in 10^{-6} sec^{-1} + 5
~950mb (ζ_r parameter)

Fig. 37

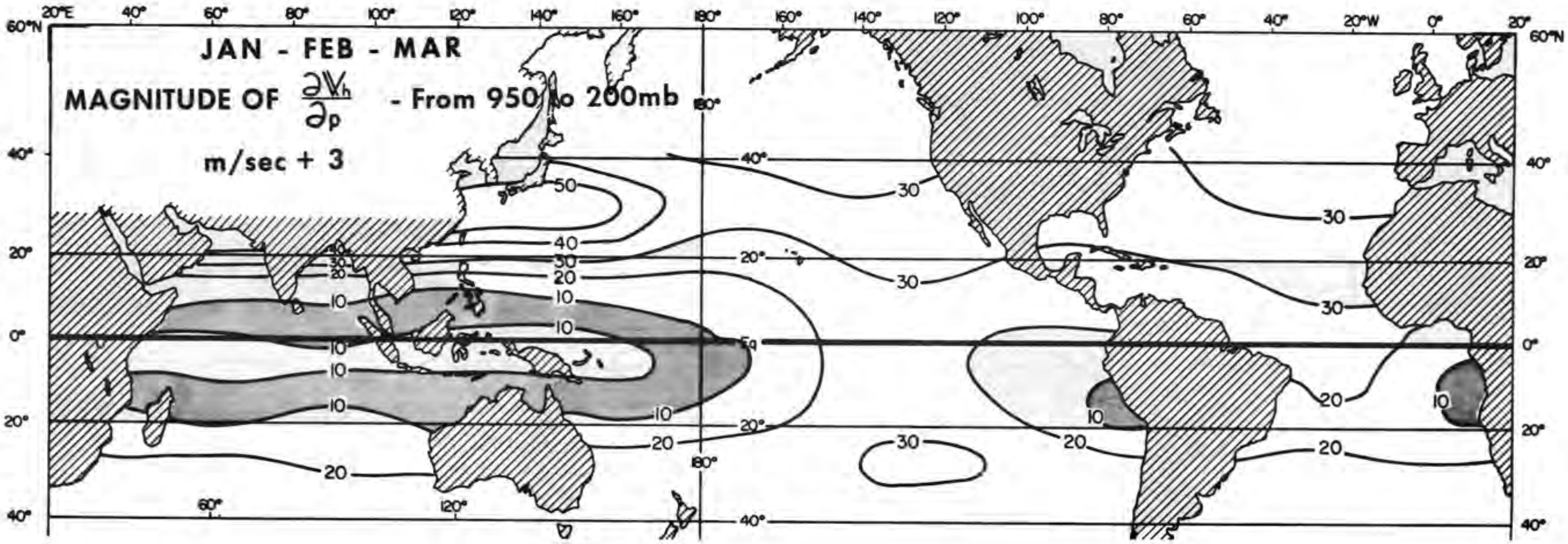
JAN - FEB - MAR
MAGNITUDE OF $\frac{\partial \mathbb{V}_h}{\partial p}$ - From 950 to 200mb
m/sec + 3

Fig. 38

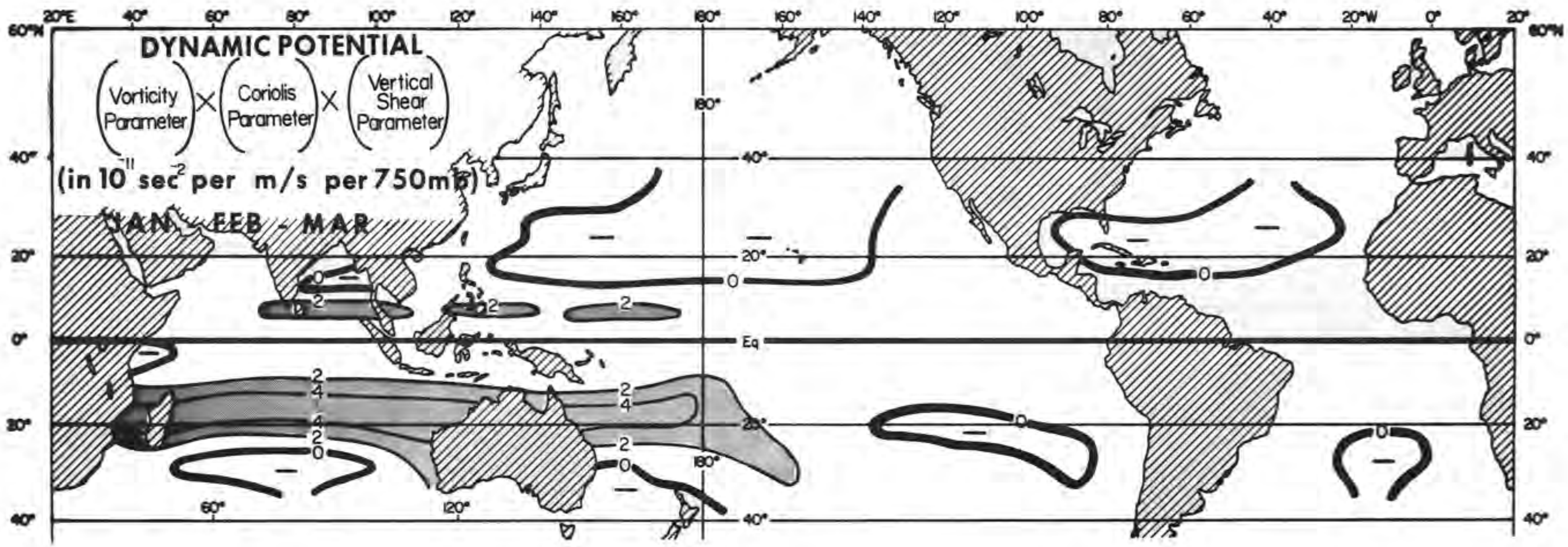
DYNAMIC POTENTIAL
(Vorticity Parameter) X (Coriolis Parameter) X (Vertical Shear Parameter)
(in 10^{-11} sec^{-2} per m/s per 750mb)
JAN - FEB - MAR
20°E 40° 60° 80° 100° 120° 140° 160° 180° 160° 140° 120° 100° 80° 60° 40° 20°W 0° 20°
60°N 40° 20° 0° 20° 40°
Eq
0
2
4

Fig. 39

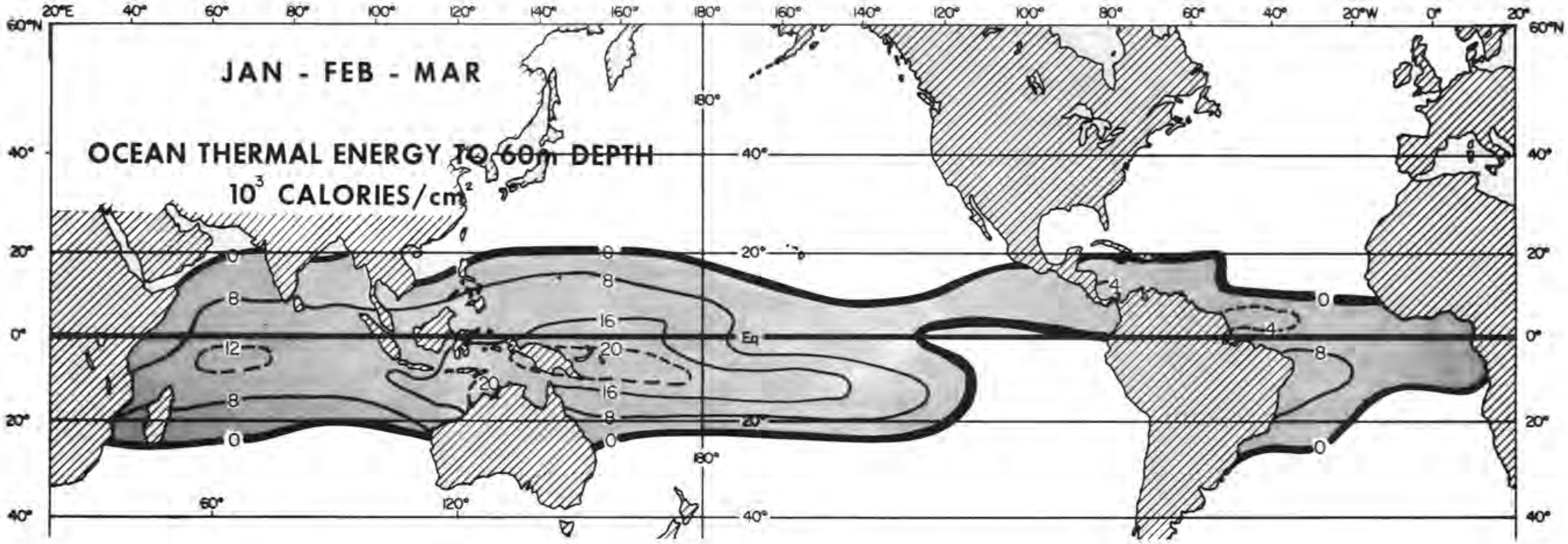
JAN - FEB - MAR
OCEAN THERMAL ENERGY TO 60m DEPTH
10^3 CALORIES/cm^2

Fig. 40

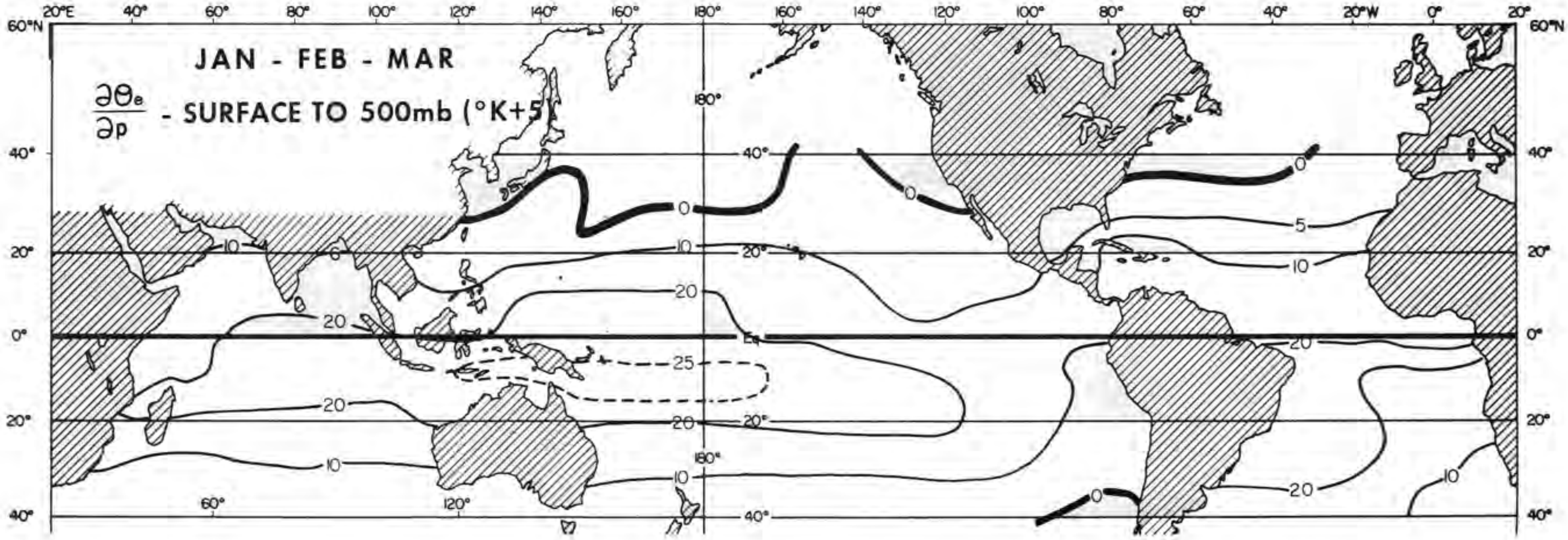
JAN - FEB - MAR
$\frac{\partial \theta_e}{\partial p}$ - SURFACE TO 500mb (°K+5)

Fig. 41

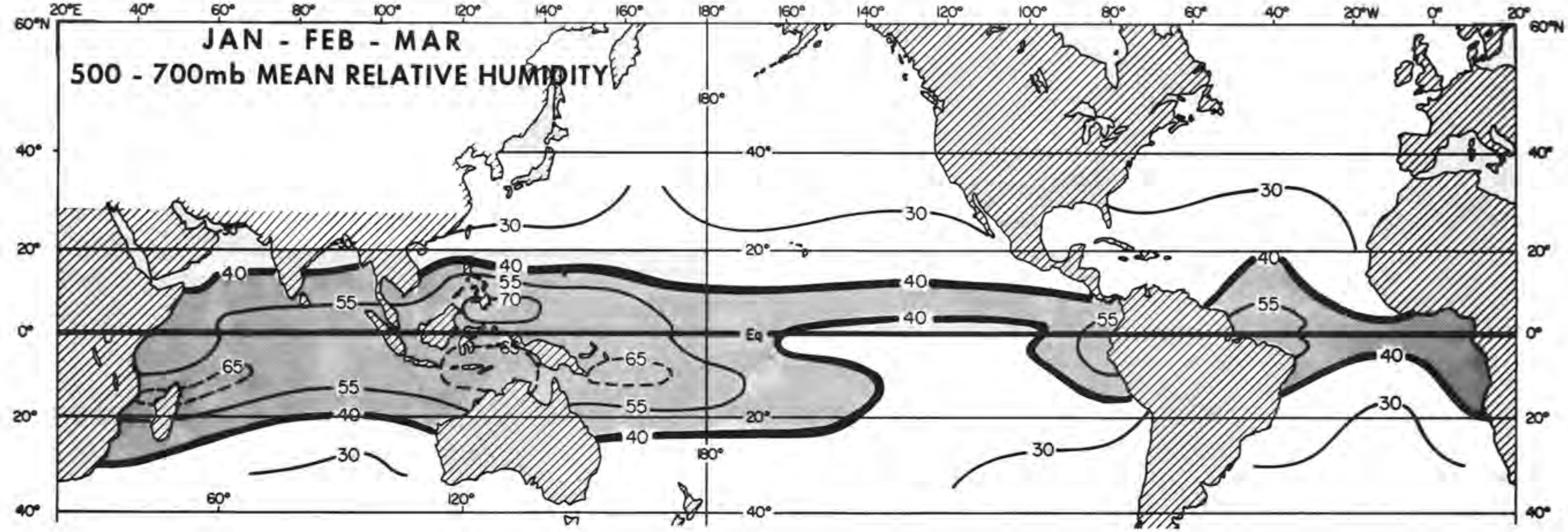
JAN - FEB - MAR
500 - 700mb MEAN RELATIVE HUMIDITY
30
40
55
65
70
Eq
60°N
40°
20°
0°
20°
40°

Fig. 42

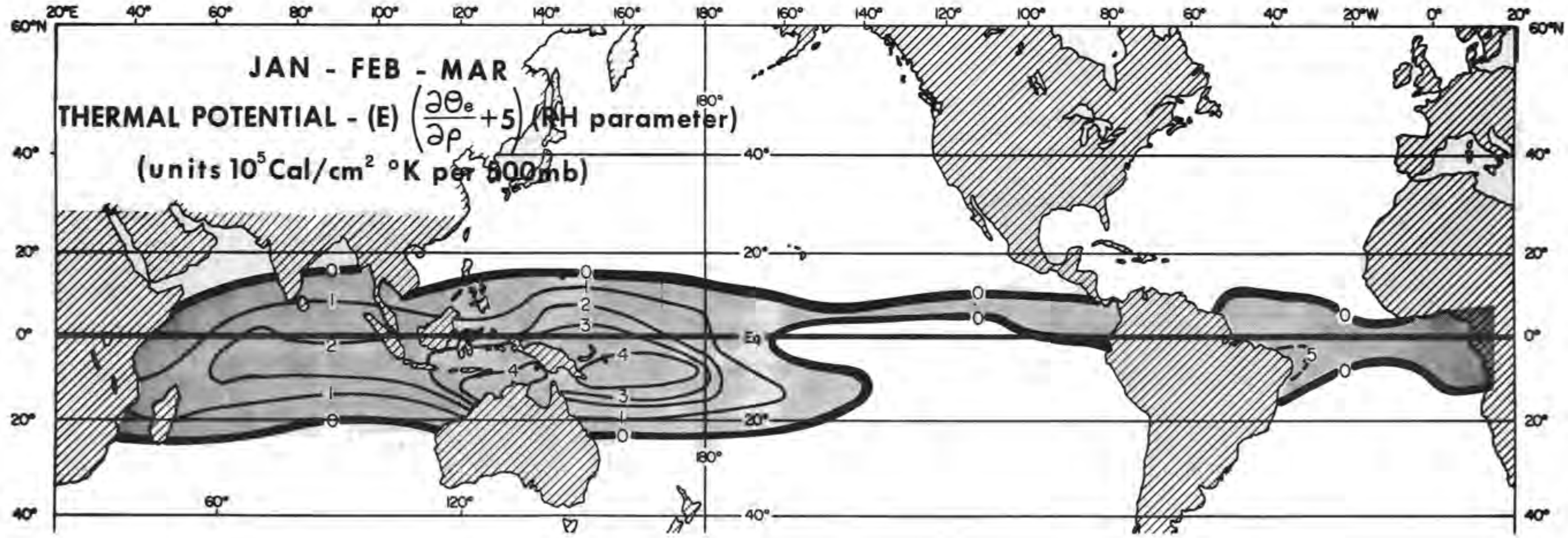
JAN - FEB - MAR
THERMAL POTENTIAL - (E) $\left(\frac{\partial\theta_e}{\partial p}+5\right)$ (RH parameter)
(units 10^5 Cal/cm^2 °K per 100mb)
0
1
2
3
4
5
Eq

Fig. 43

Fig. 44

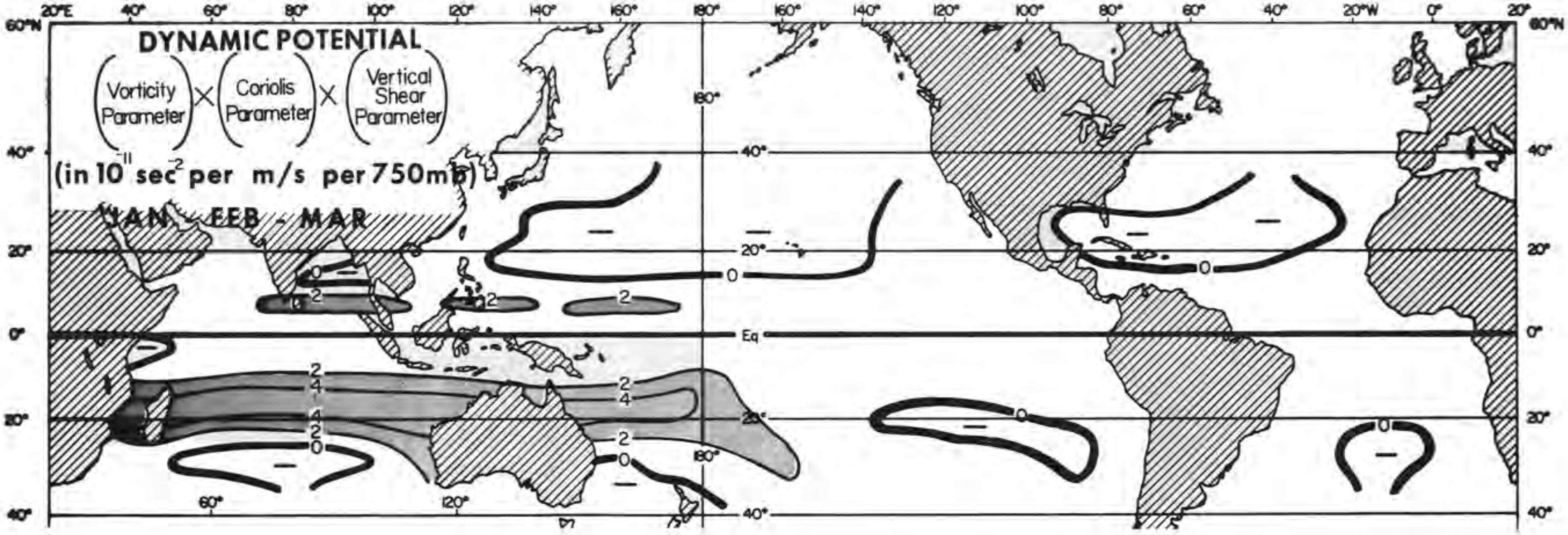

DYNAMIC POTENTIAL
(Vorticity Parameter) × (Coriolis Parameter) × (Vertical Shear Parameter)
(in 10^{-11} sec^{-2} per m/s per 750mb)
JAN - FEB - MAR

Fig. 45

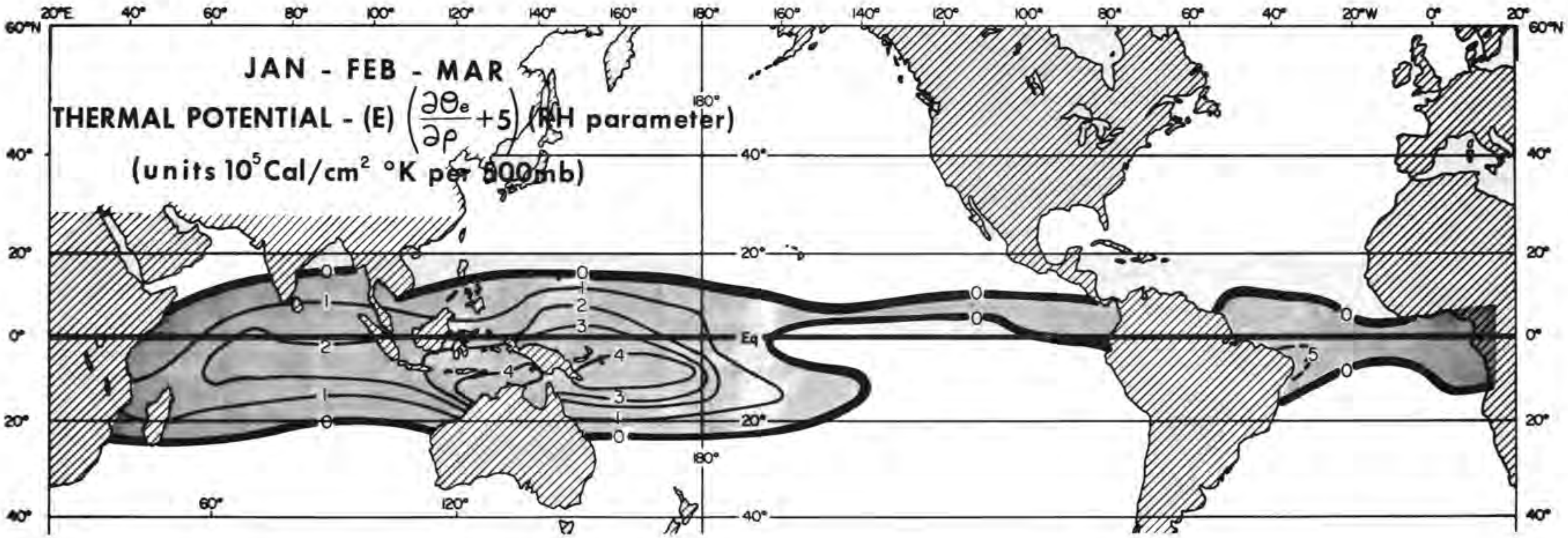

JAN - FEB - MAR
THERMAL POTENTIAL - (E) $\left(\frac{\partial\theta_e}{\partial p}+5\right)$ (RH parameter)
(units 10^5 Cal/cm^2 °K per 500mb)

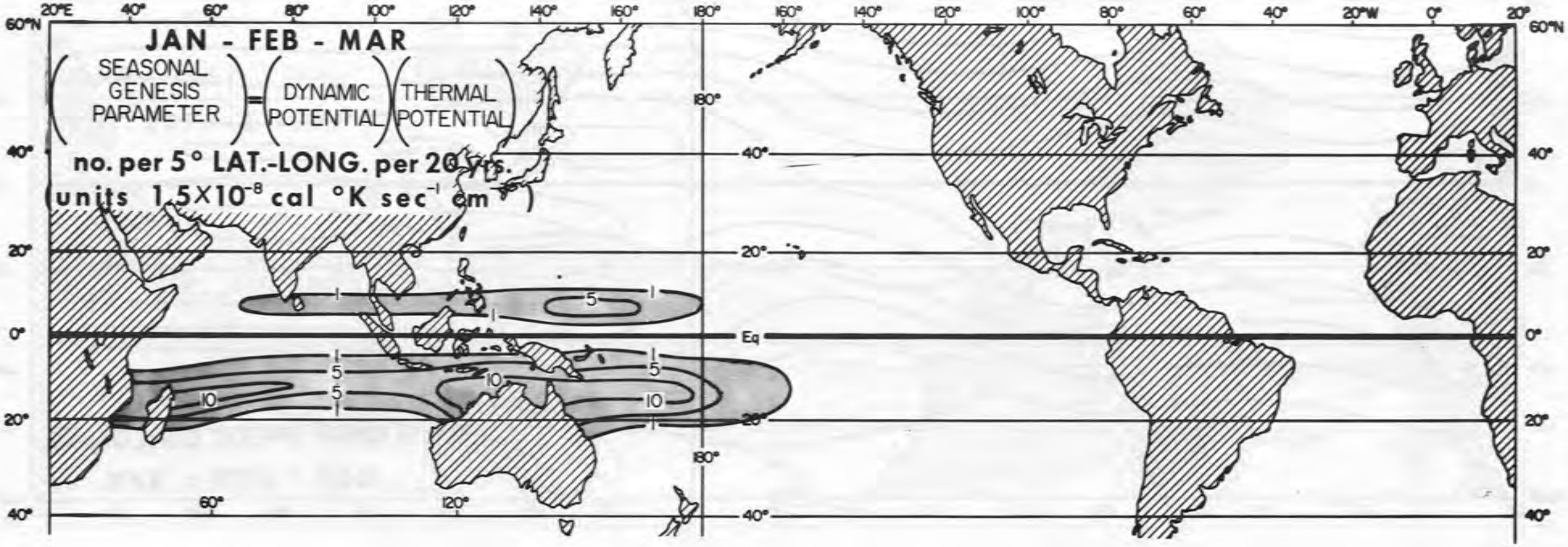
JAN - FEB - MAR
(SEASONAL GENESIS PARAMETER) = (DYNAMIC POTENTIAL)(THERMAL POTENTIAL)
no. per 5° LAT.-LONG. per 20 yrs.
(units 1.5X10^{-8} cal °K sec^{-1} cm^{-1})

Fig. 46

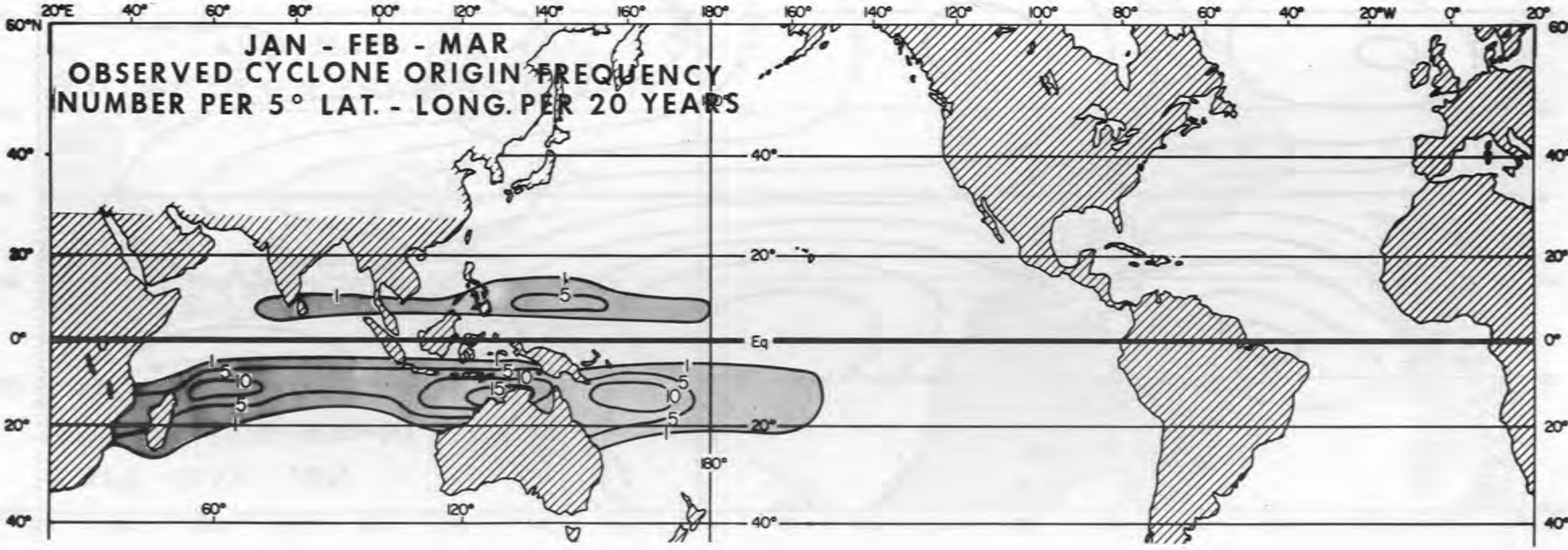
JAN - FEB - MAR
OBSERVED CYCLONE ORIGIN FREQUENCY
NUMBER PER 5° LAT. - LONG. PER 20 YEARS

Fig. 47

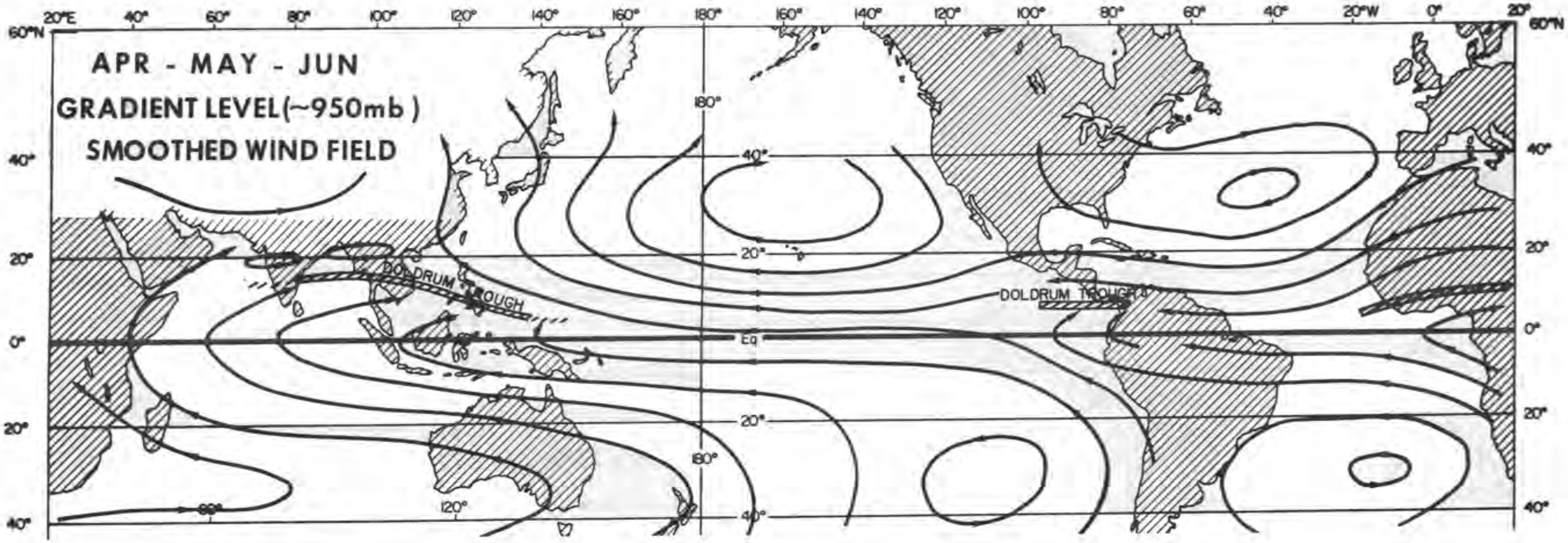
APR - MAY - JUN
GRADIENT LEVEL(~950mb)
SMOOTHED WIND FIELD
DOLDRUM TROUGH
DOLDRUM TROUGH
Eq

Fig. 48

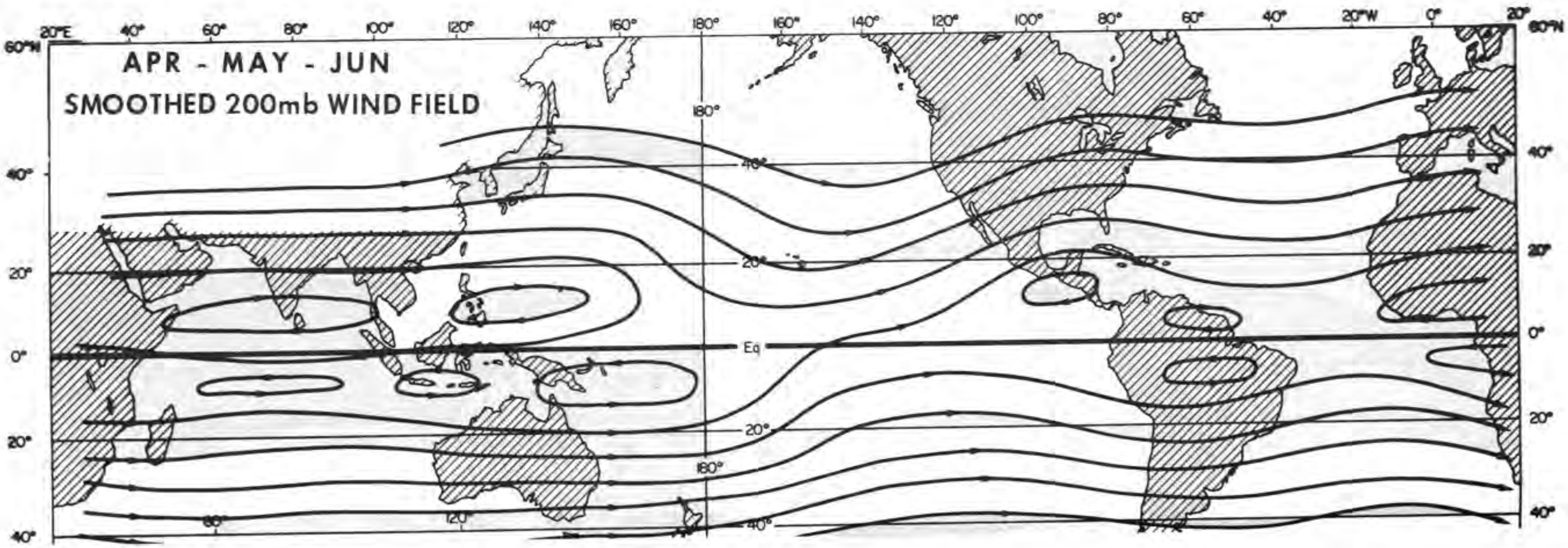
APR - MAY - JUN
SMOOTHED 200mb WIND FIELD
Eq

Fig. 49

Fig. 50

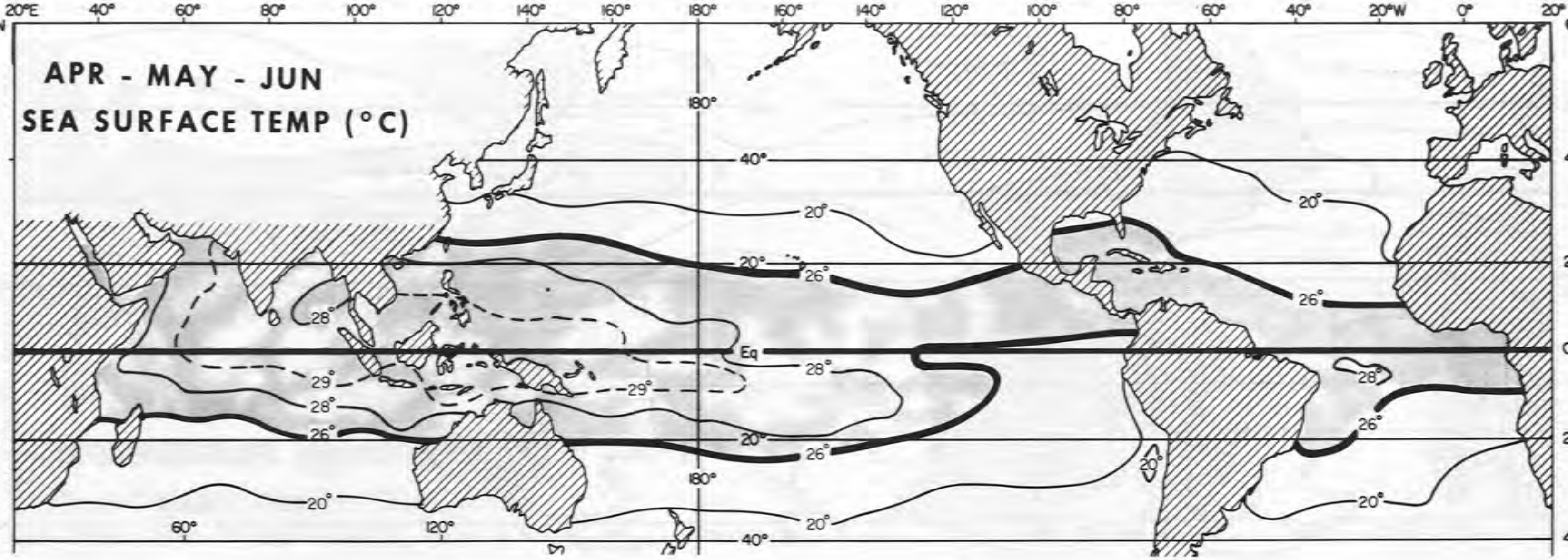

APR - MAY - JUN
SEA SURFACE TEMP (°C)
20°
26°
28°
29°
Eq

Fig. 51

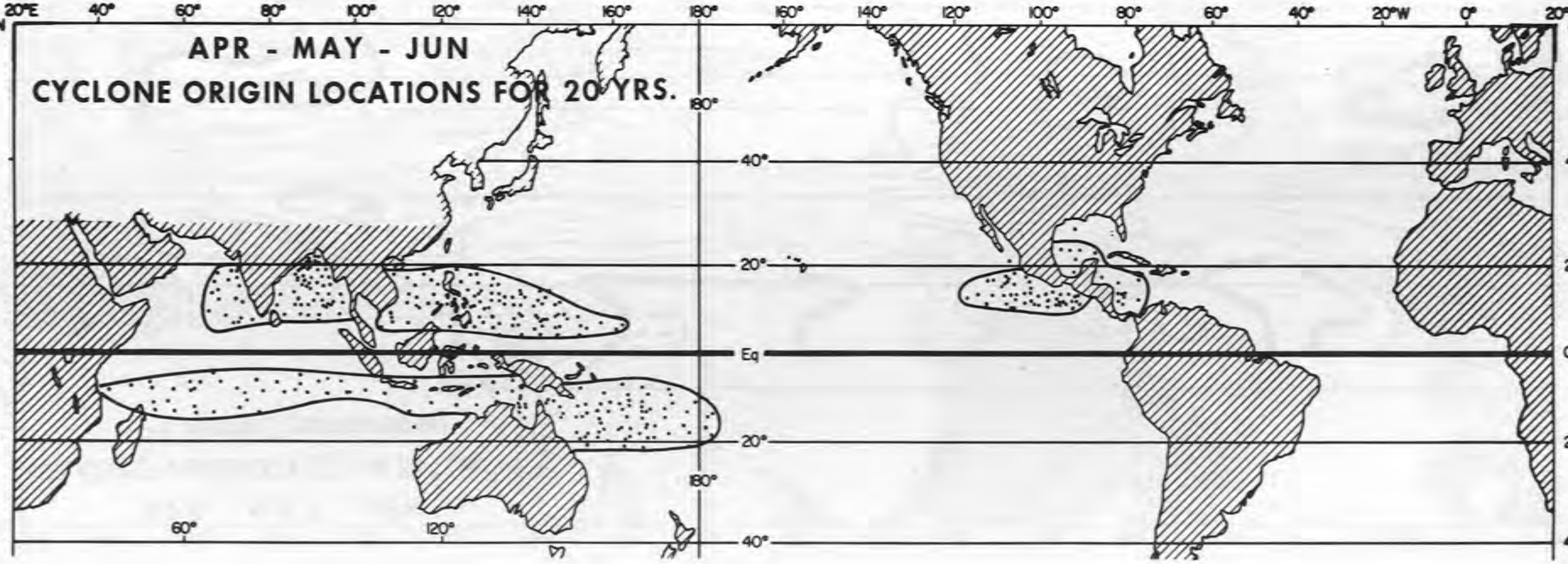

APR - MAY - JUN
CYCLONE ORIGIN LOCATIONS FOR 20 YRS.
Eq

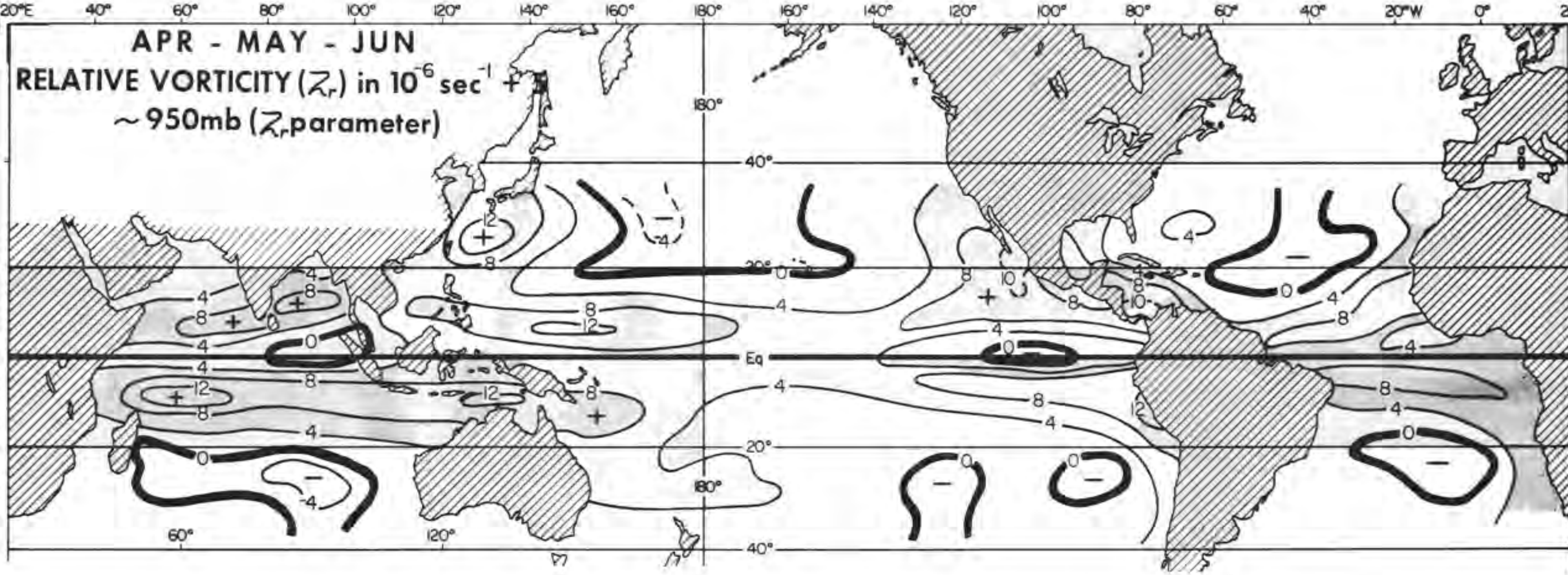
APR - MAY - JUN
RELATIVE VORTICITY (ζ_r) in 10^{-6} sec^{-1} + 5
~950mb (ζ_r parameter)

Fig. 52

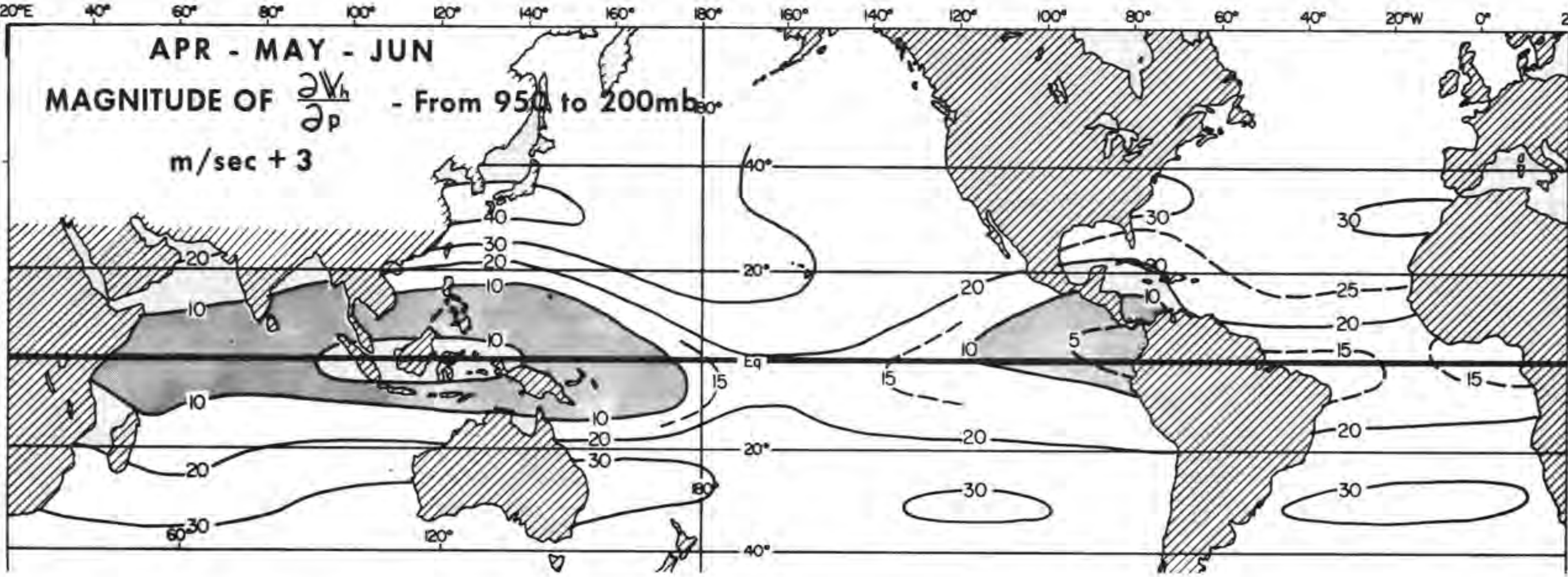
APR - MAY - JUN
MAGNITUDE OF $\frac{\partial V_h}{\partial p}$ - From 950 to 200mb
m/sec + 3

Fig. 53

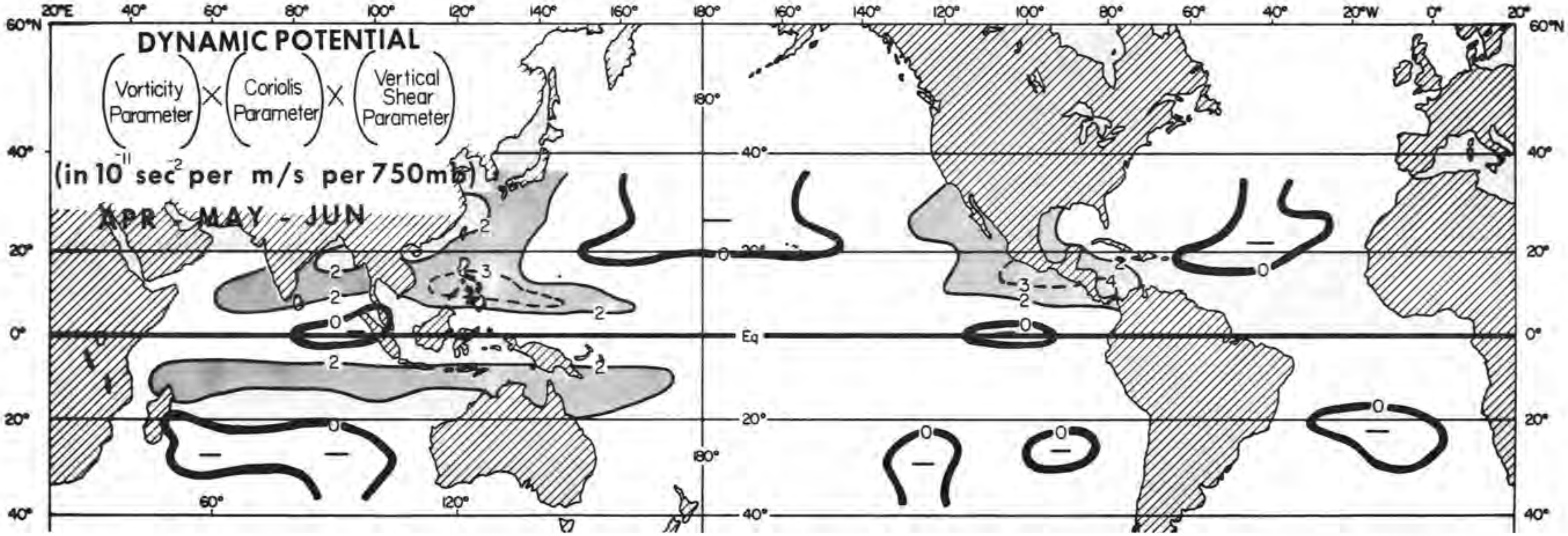
DYNAMIC POTENTIAL
(Vorticity Parameter) × (Coriolis Parameter) × (Vertical Shear Parameter)
(in 10^{-11} sec^{-2} per m/s per 750mb)
APR - MAY - JUN

Fig. 54

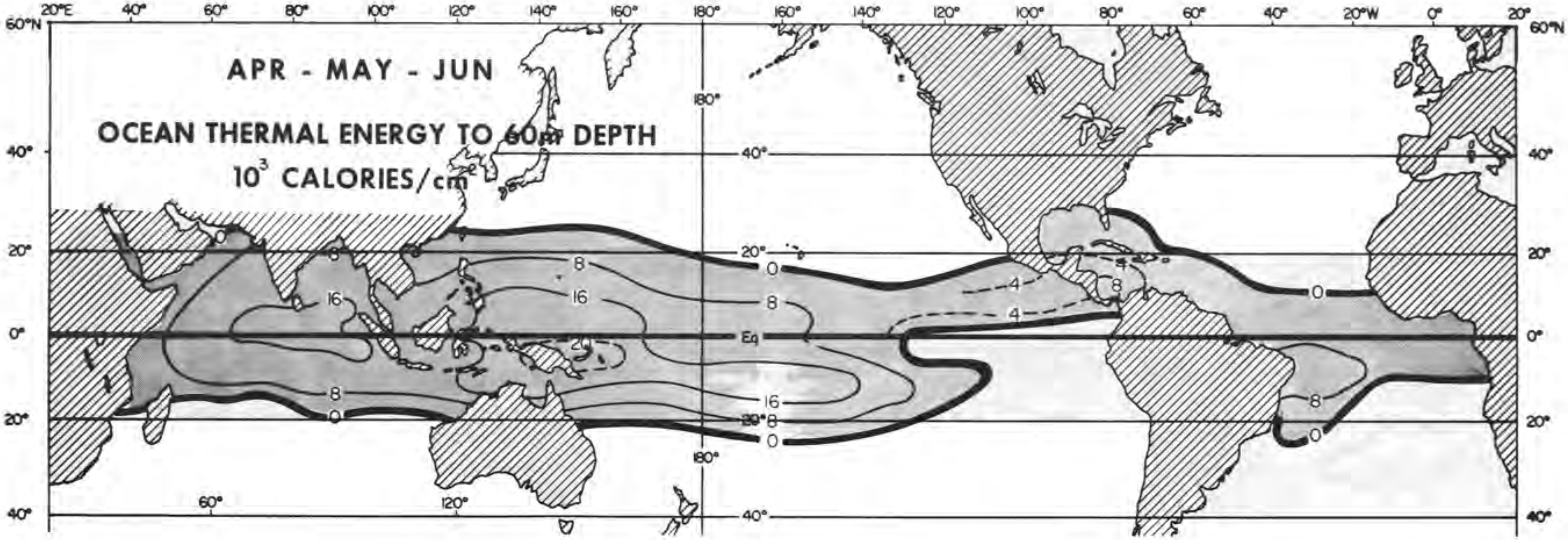
APR - MAY - JUN
OCEAN THERMAL ENERGY TO 60m DEPTH
10^3 CALORIES/cm^2

Fig. 55

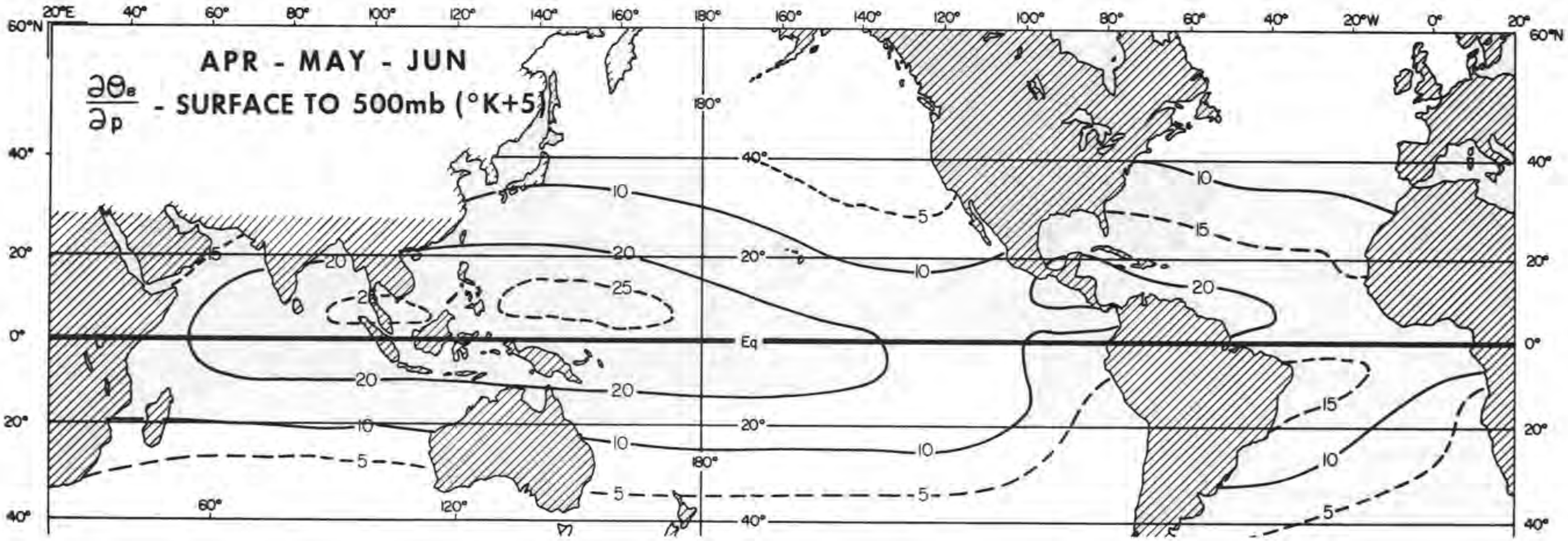
APR - MAY - JUN
$\frac{\partial \Theta_e}{\partial p}$ - SURFACE TO 500mb (°K+5)

Fig. 56

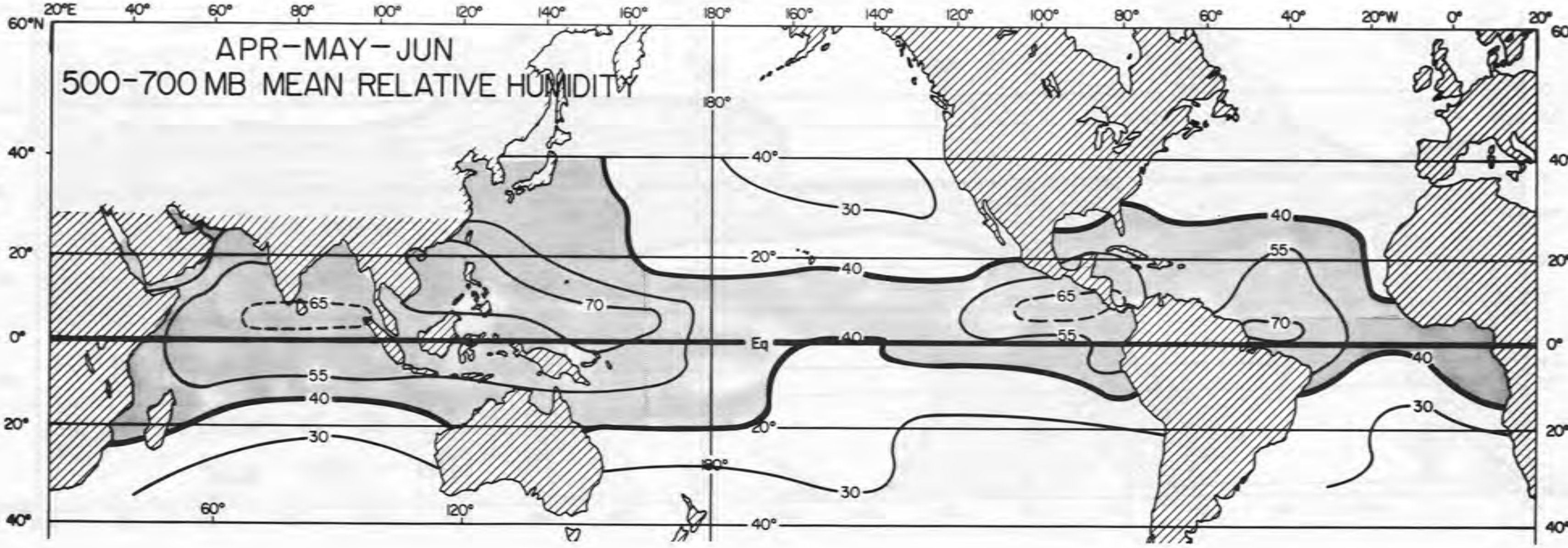
APR-MAY-JUN
500-700 MB MEAN RELATIVE HUMIDITY

Fig. 57

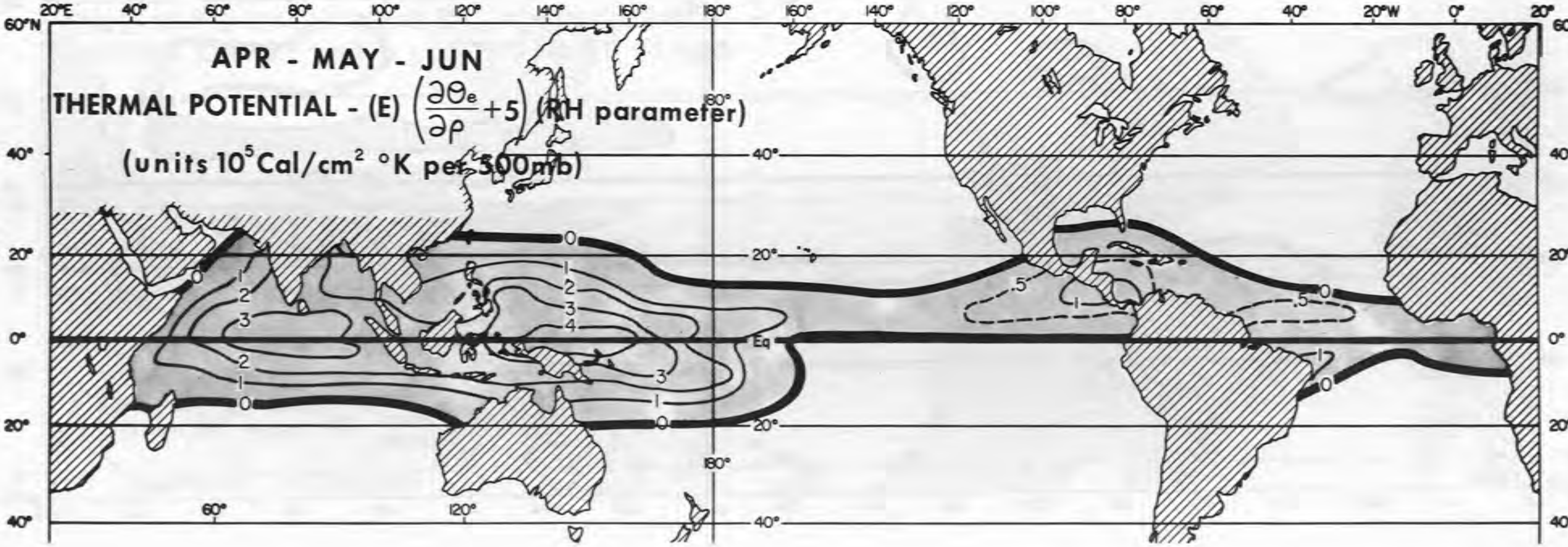
APR - MAY - JUN
THERMAL POTENTIAL - (E) $\left(\frac{\partial\theta_e}{\partial p}+5\right)$ (RH parameter)
(units 10^5 Cal/cm^2 °K per 300mb)

Fig. 58

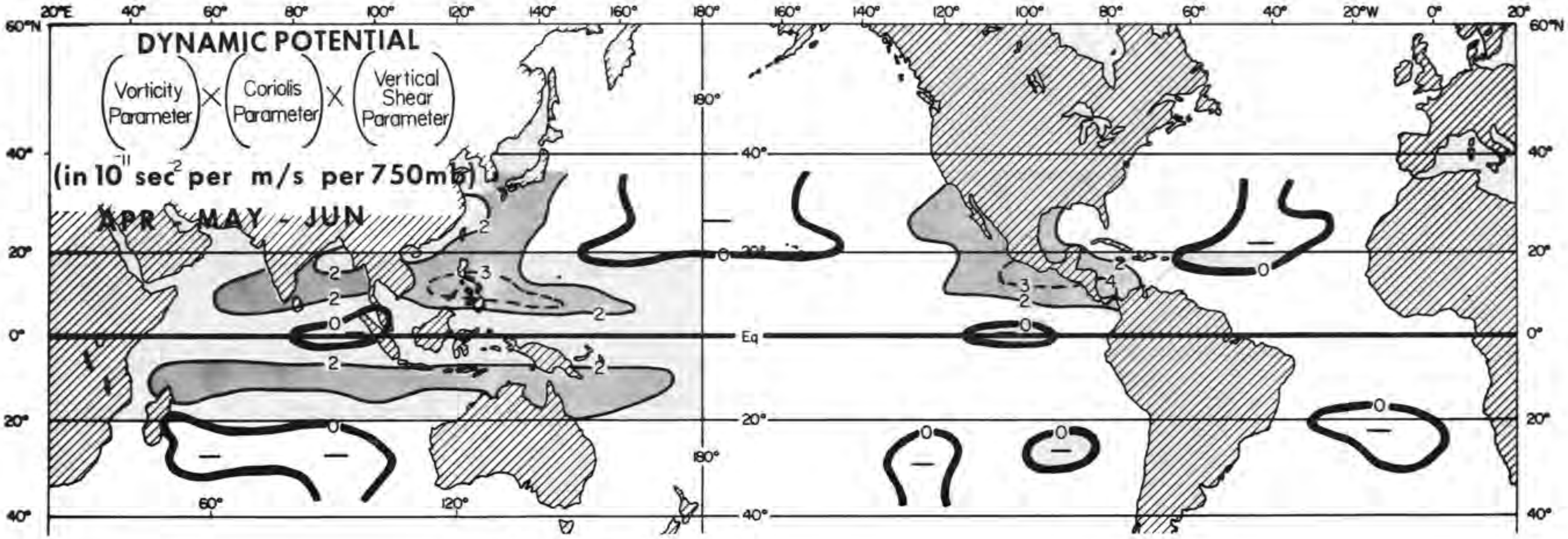
DYNAMIC POTENTIAL
(Vorticity Parameter) X (Coriolis Parameter) X (Vertical Shear Parameter)
(in 10^{-11} sec^{-2} per m/s per 750mb)
APR - MAY - JUN

Fig. 59

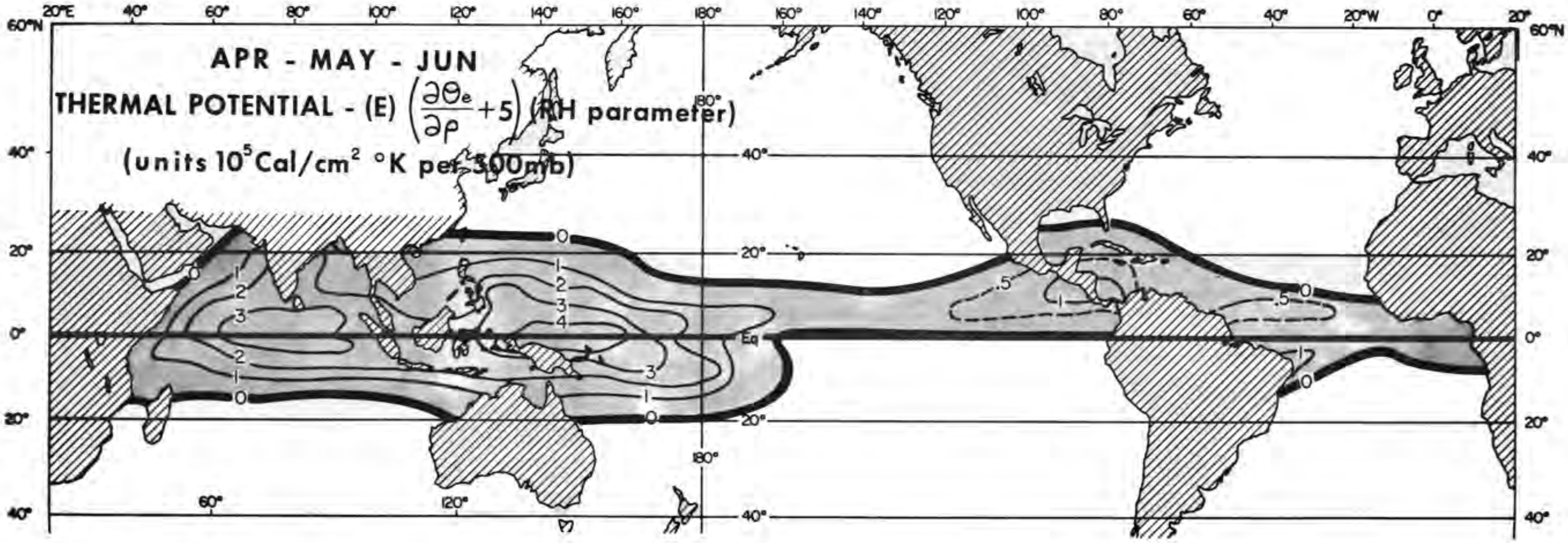
APR - MAY - JUN
THERMAL POTENTIAL - (E) $\left(\frac{\partial \theta_e}{\partial p}+5\right)$ (RH parameter)
(units 10^5 Cal/cm^2 °K per 300mb)

Fig. 60

Fig. 61

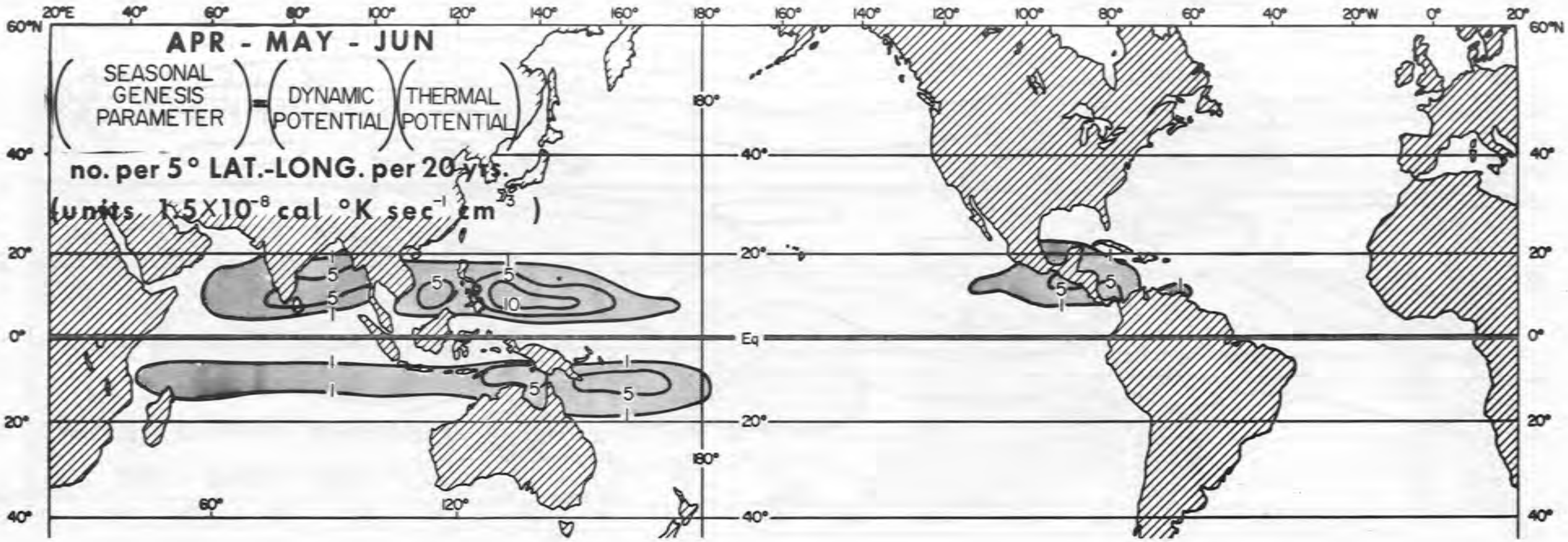
APR - MAY - JUN
(SEASONAL GENESIS PARAMETER) = (DYNAMIC POTENTIAL)(THERMAL POTENTIAL)
no. per 5° LAT.-LONG. per 20 yrs.
(units 1.5X10^{-8} cal °K sec^{-1} cm)

Fig. 62

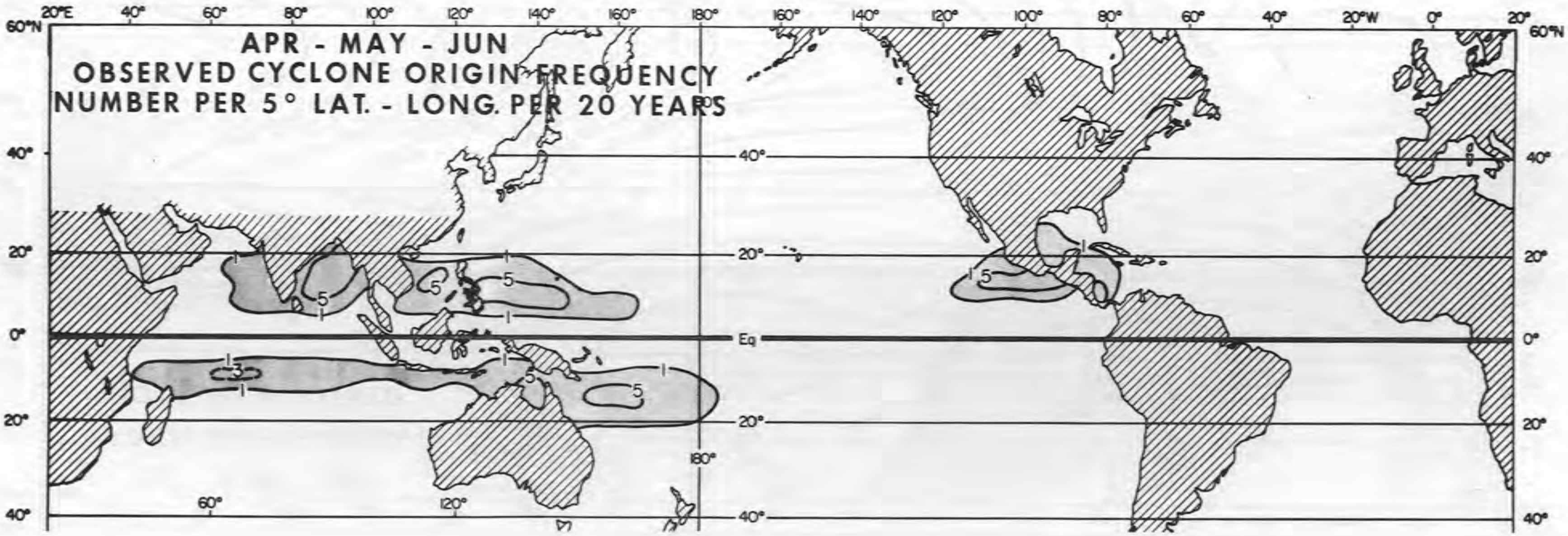
APR - MAY - JUN
OBSERVED CYCLONE ORIGIN FREQUENCY
NUMBER PER 5° LAT. - LONG. PER 20 YEARS

Fig. 63

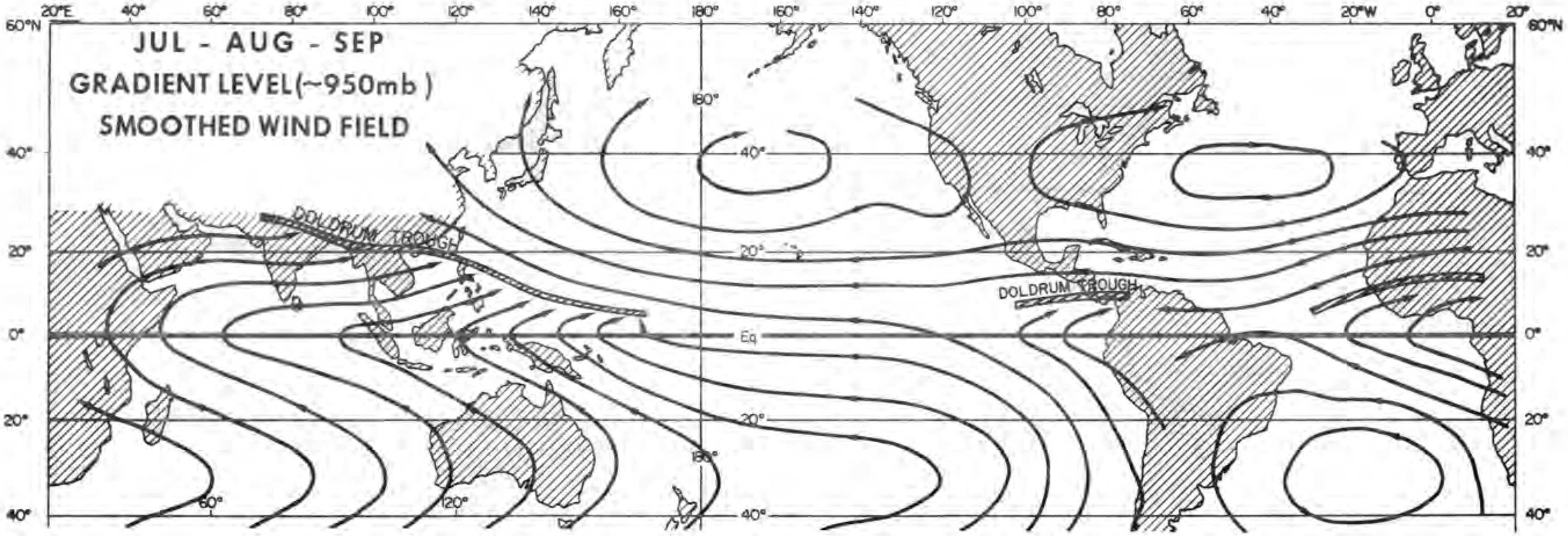
JUL - AUG - SEP
GRADIENT LEVEL(~950mb)
SMOOTHED WIND FIELD
DOLDRUM TROUGH
DOLDRUM TROUGH

Fig. 64

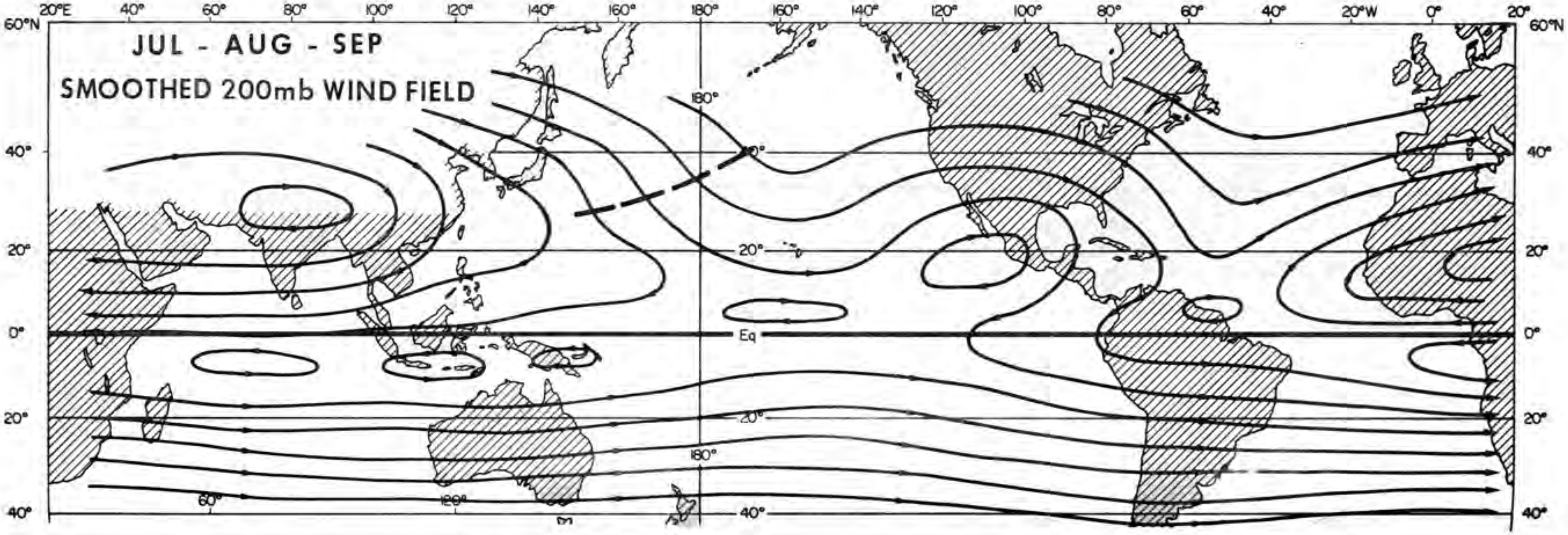
JUL - AUG - SEP
SMOOTHED 200mb WIND FIELD

Fig. 65

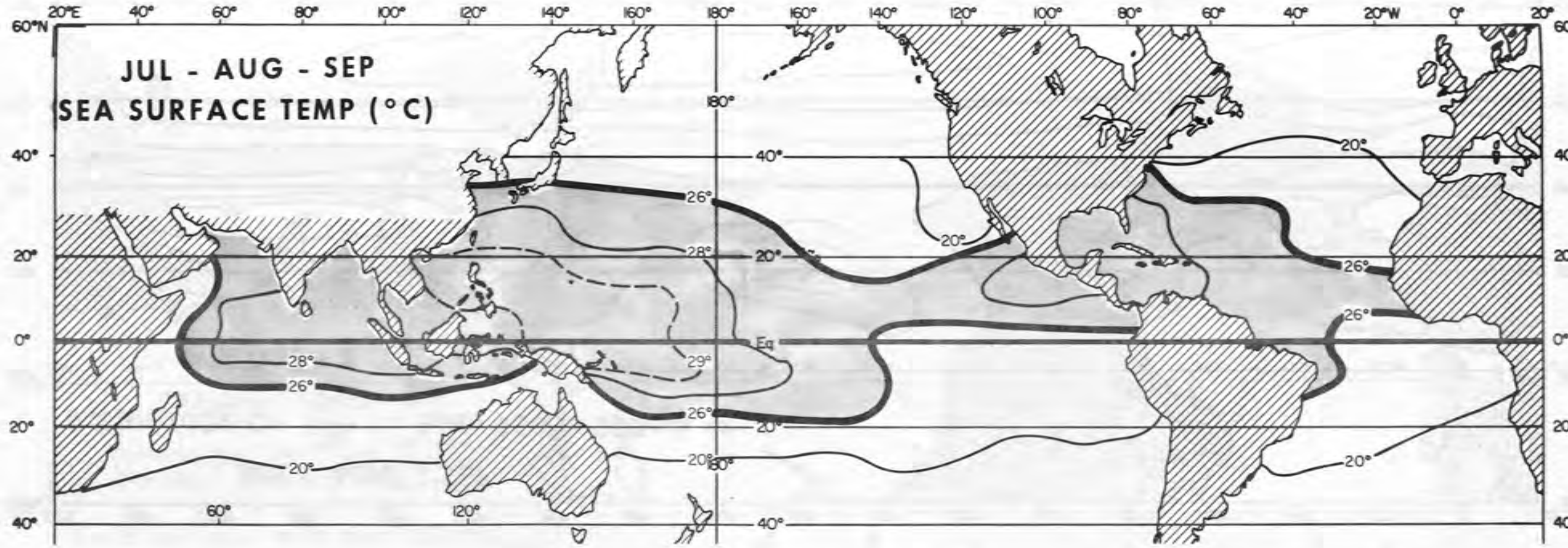
JUL - AUG - SEP
SEA SURFACE TEMP (°C)
26°
28°
29°
20°
Eq

Fig. 66

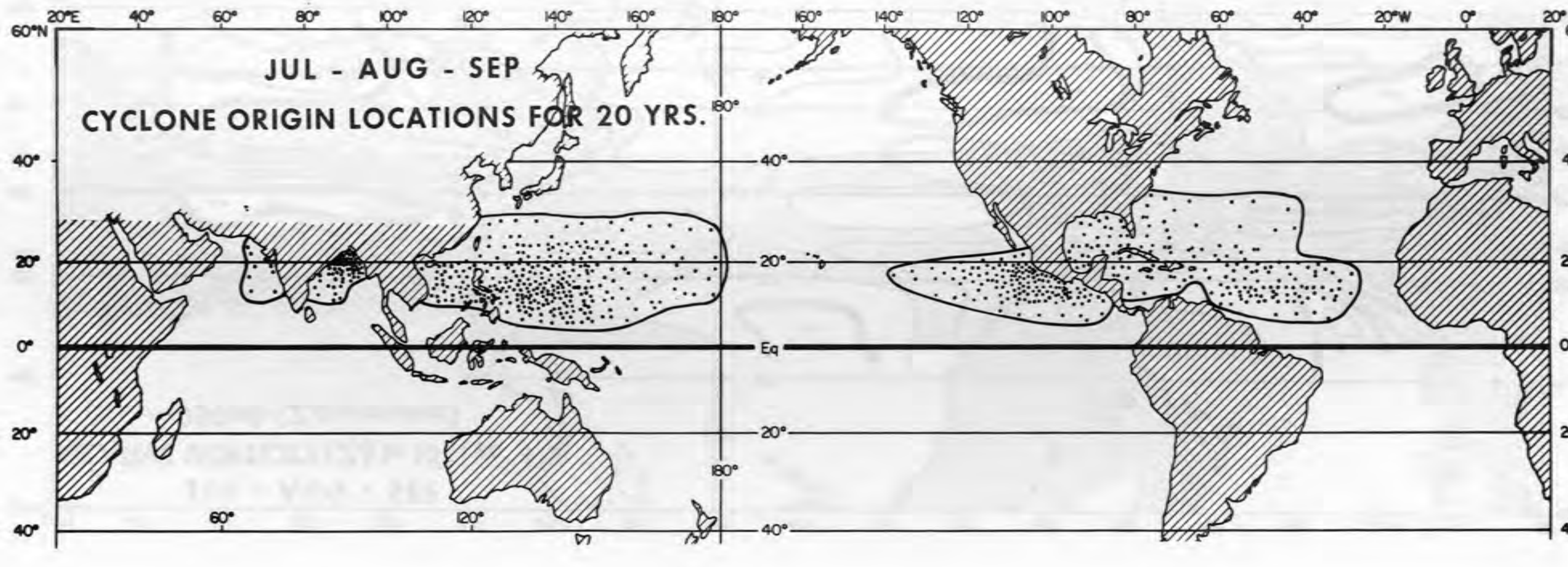
JUL - AUG - SEP
CYCLONE ORIGIN LOCATIONS FOR 20 YRS.
Eq

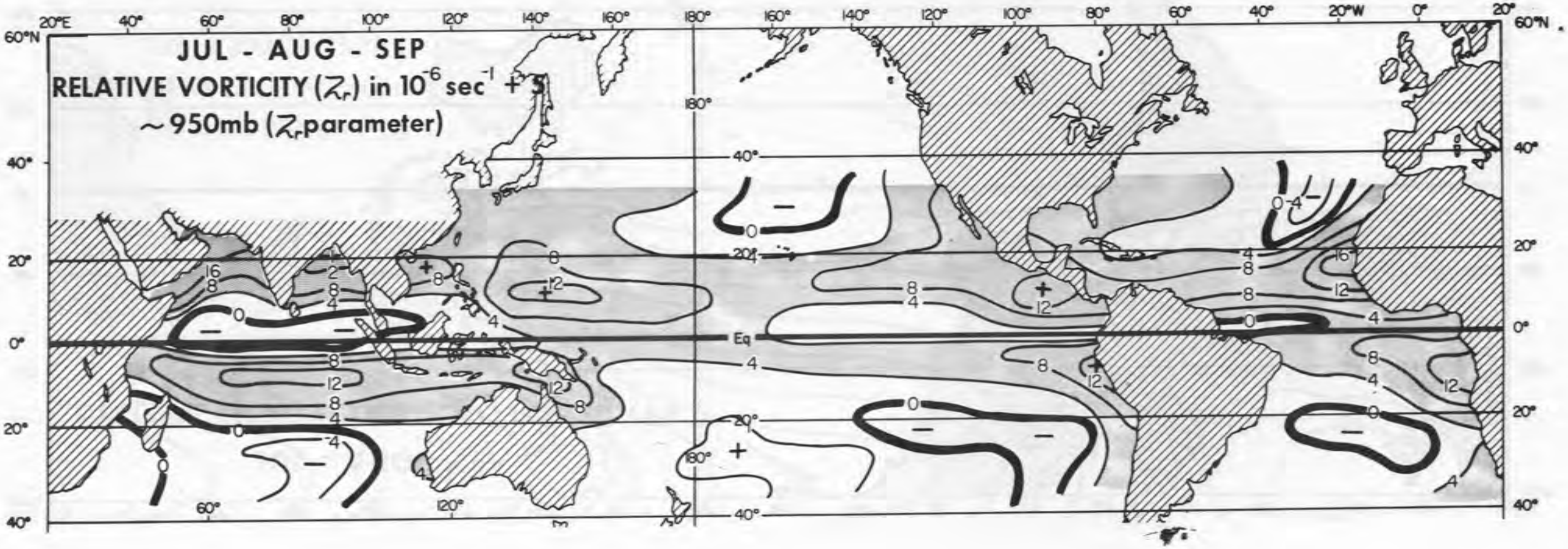
JUL - AUG - SEP
RELATIVE VORTICITY (ζ_r) in 10^{-6} sec^{-1} ± 5
~950mb (ζ_r parameter)

Fig. 67

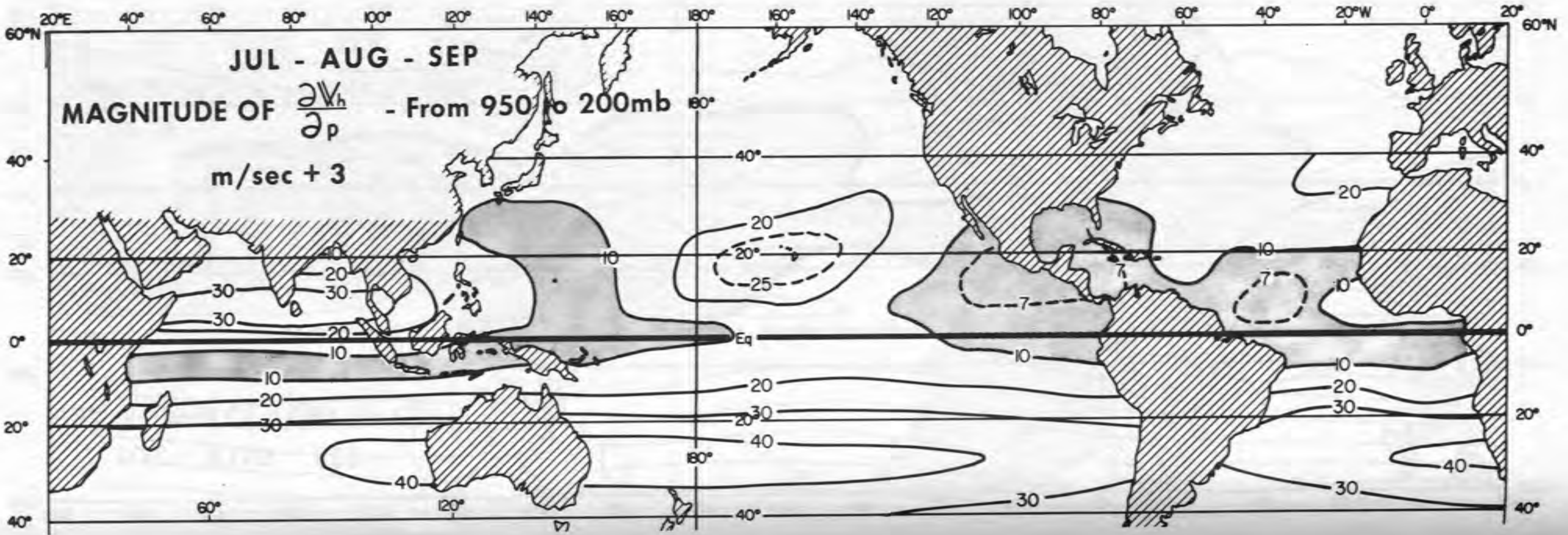
JUL - AUG - SEP
MAGNITUDE OF $\frac{\partial \mathbb{V}_h}{\partial p}$ - From 950 to 200mb
m/sec ± 3

Fig. 68

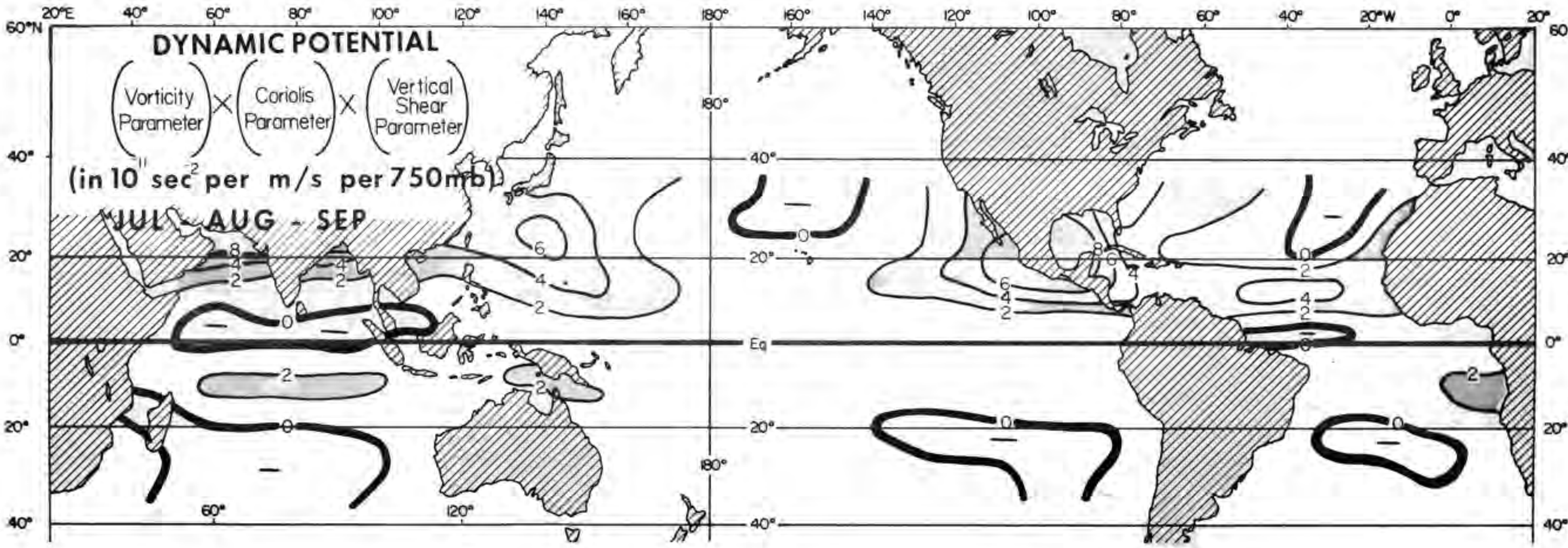
DYNAMIC POTENTIAL
(Vorticity Parameter) × (Coriolis Parameter) × (Vertical Shear Parameter)
(in 10^{-11} sec^{-2} per m/s per 750mb)
JUL - AUG - SEP
Eq

Fig. 69

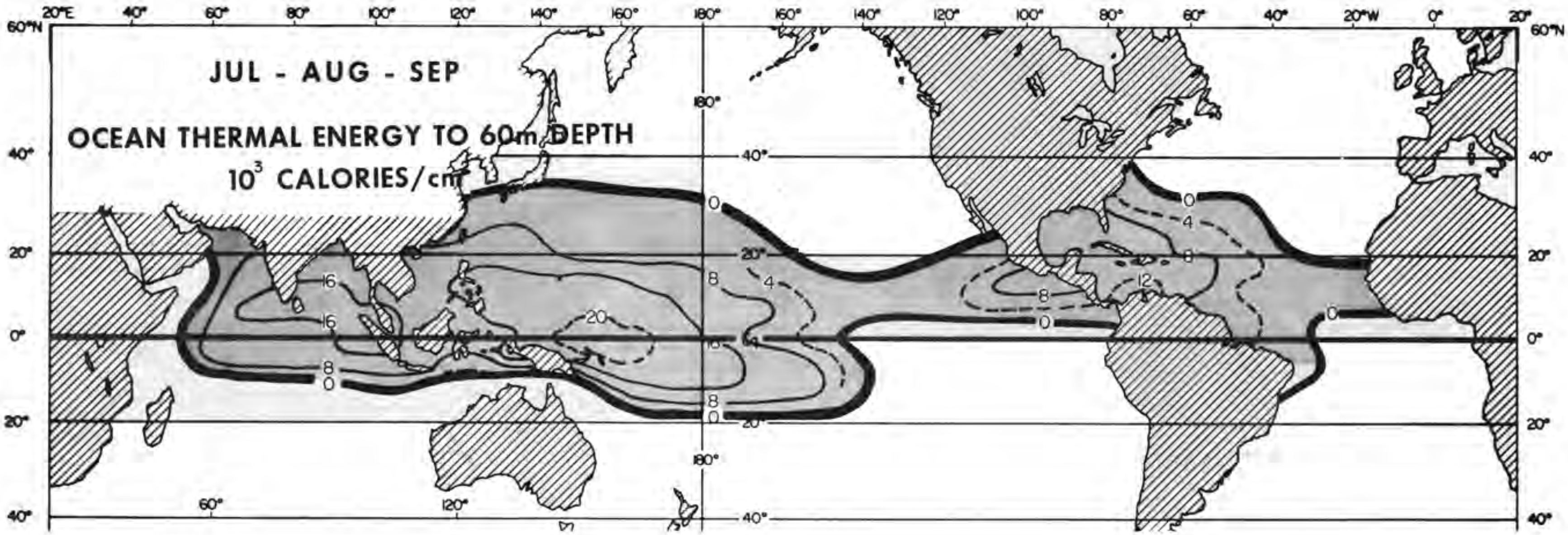
JUL - AUG - SEP
OCEAN THERMAL ENERGY TO 60m DEPTH
10^3 CALORIES/cm²

Fig. 70

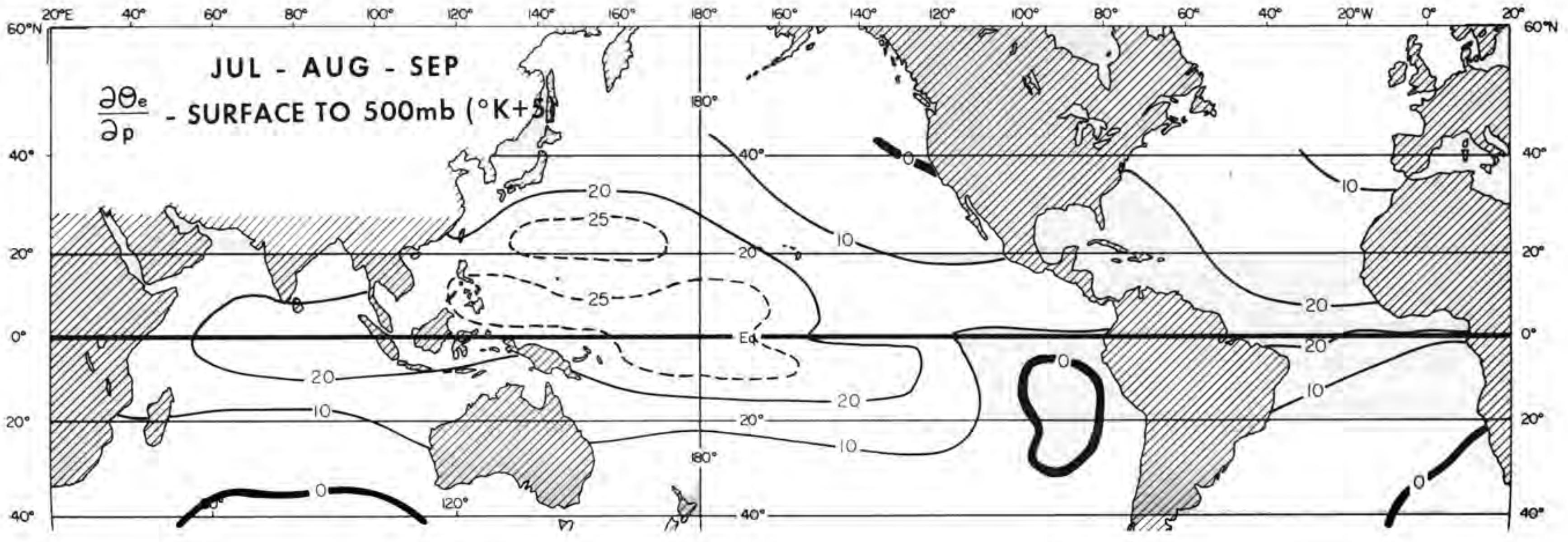
JUL - AUG - SEP
$\frac{\partial\theta_e}{\partial p}$ - SURFACE TO 500mb (°K+5)

Fig. 71

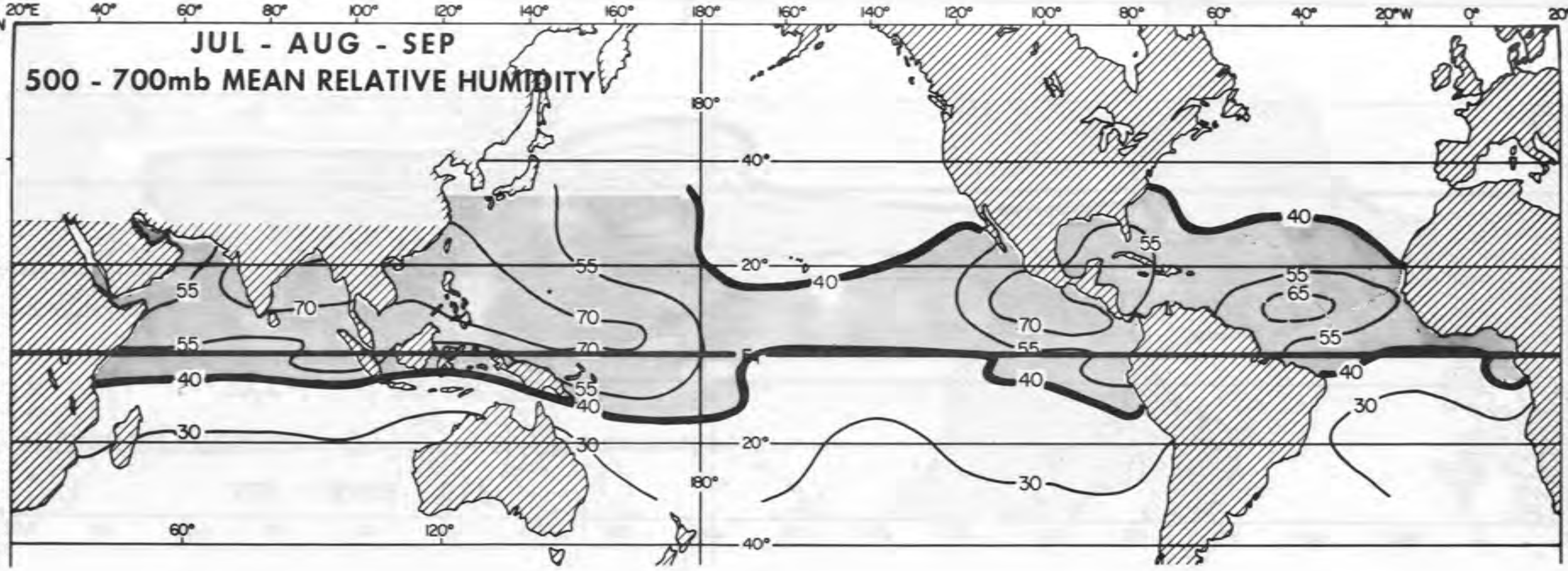
JUL - AUG - SEP
500 - 700mb MEAN RELATIVE HUMIDITY
60°N
40°
20°
0°
20°
40°
20°E
40°
60°
80°
100°
120°
140°
160°
180°
160°
140°
120°
100°
80°
60°
40°
20°W
0°
20°
55
70
40
30
65

Fig. 72

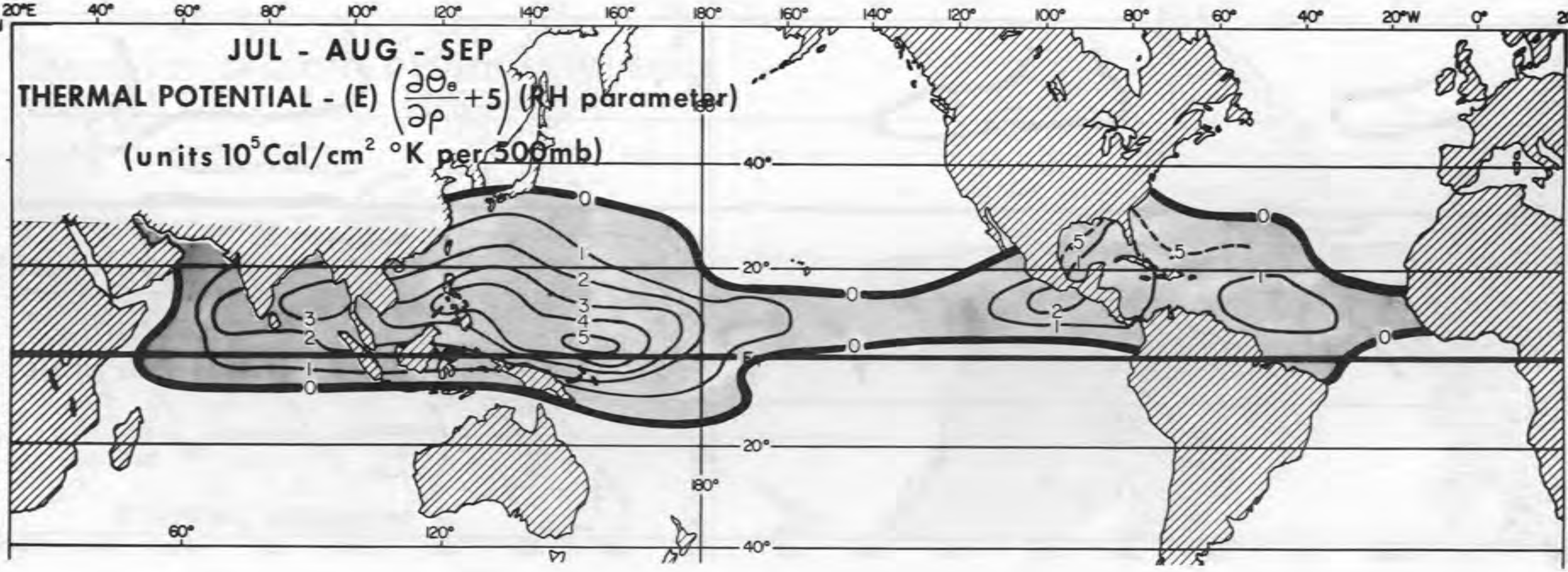
JUL - AUG - SEP
THERMAL POTENTIAL - (E) $\left(\frac{\partial\theta_e}{\partial p}+5\right)$ (RH parameter)
(units 10^5 Cal/cm^2 °K per 500mb)
60°N
40°
20°
0°
20°
40°
20°E
40°
60°
80°
100°
120°
140°
160°
180°
160°
140°
120°
100°
80°
60°
40°
20°W
0°
20°
0
1
2
3
4
5

Fig. 73

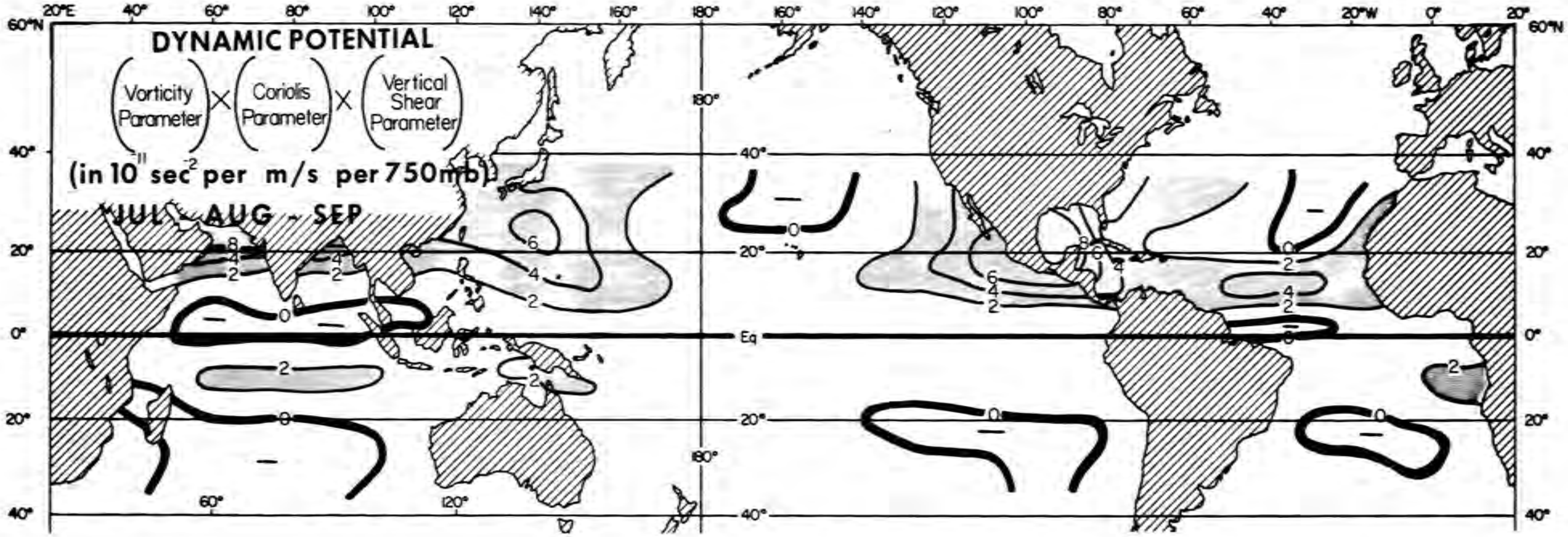
DYNAMIC POTENTIAL
(Vorticity Parameter) × (Coriolis Parameter) × (Vertical Shear Parameter)
(in 10^{-11} sec^{-2} per m/s per 750mb)
JUL - AUG - SEP
Eq

Fig. 74

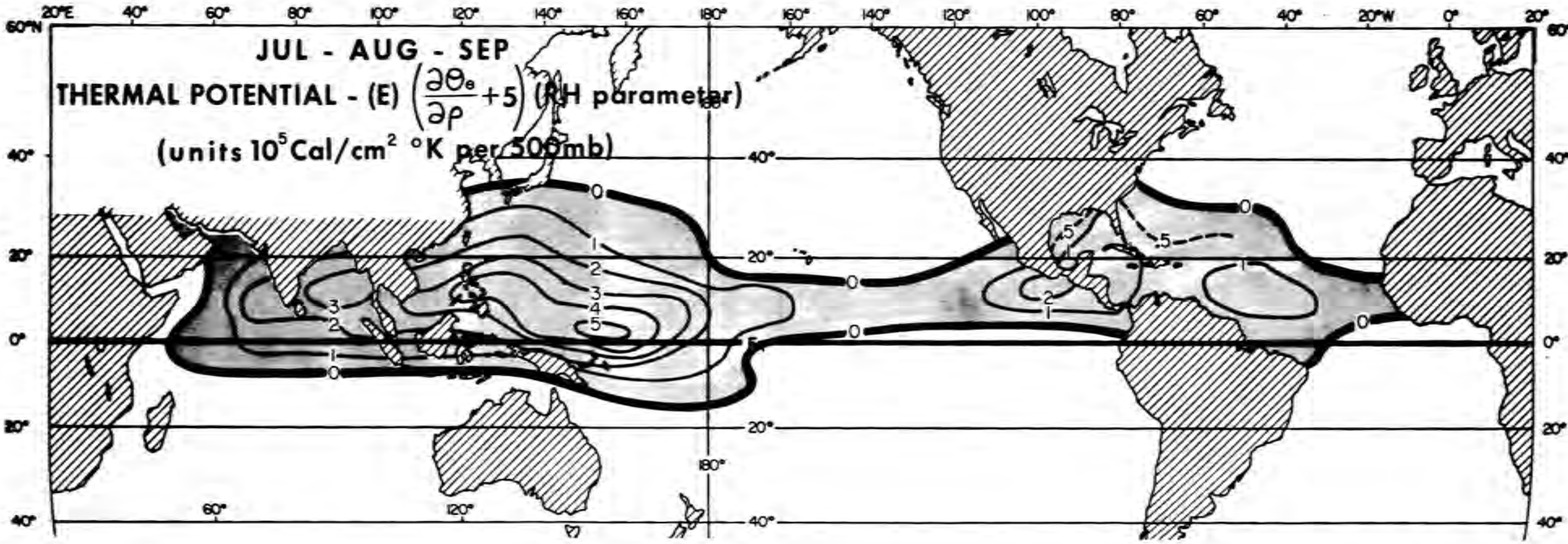
JUL - AUG - SEP
THERMAL POTENTIAL - (E) $\left(\frac{\partial\theta_e}{\partial p}+5\right)$ (RH parameter)
(units 10^5 Cal/cm^2 °K per 500mb)

Fig. 75

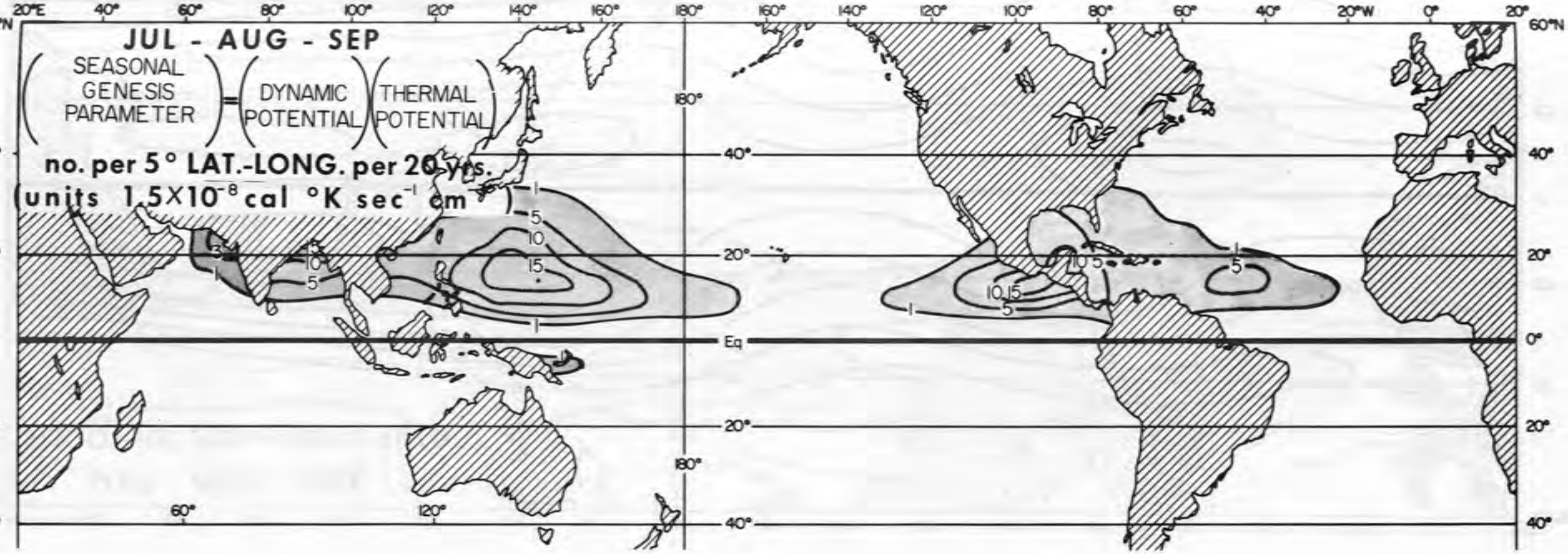
JUL - AUG - SEP
SEASONAL GENESIS PARAMETER = DYNAMIC POTENTIAL THERMAL POTENTIAL
no. per 5° LAT.-LONG. per 20 yrs.
(units 1.5X10^{-8} cal °K sec^{-1} cm^{-1})

Fig. 76

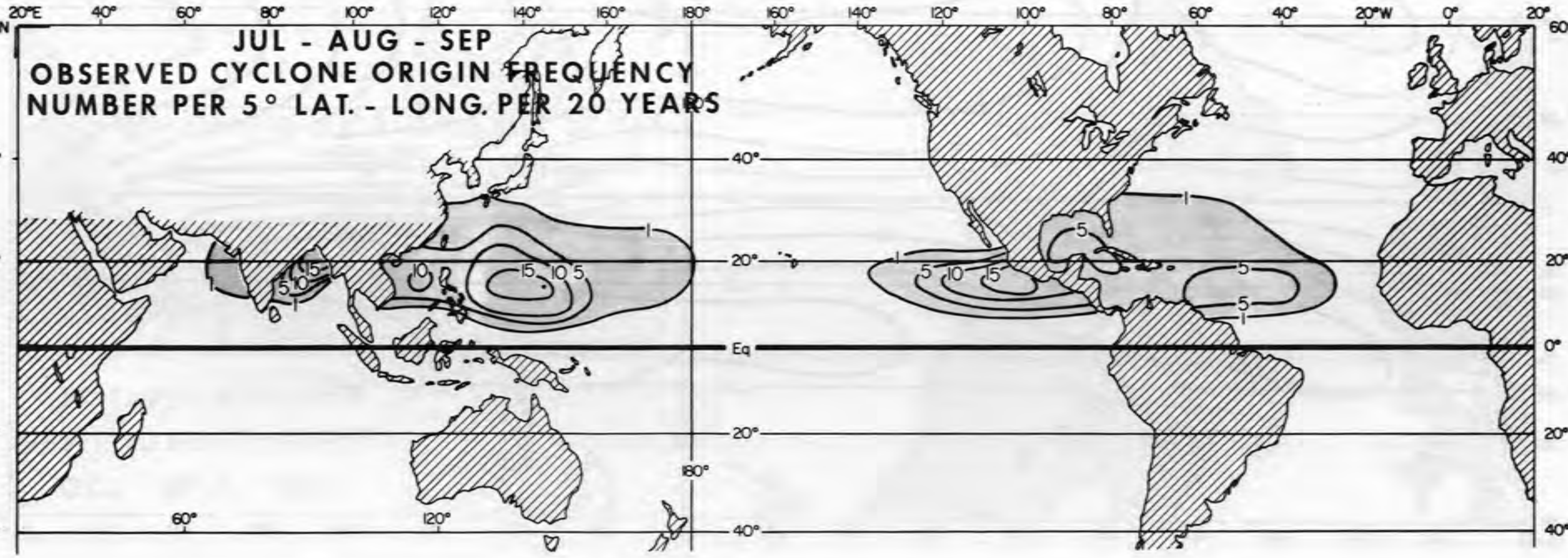
JUL - AUG - SEP
OBSERVED CYCLONE ORIGIN FREQUENCY
NUMBER PER 5° LAT. - LONG. PER 20 YEARS

Fig. 77

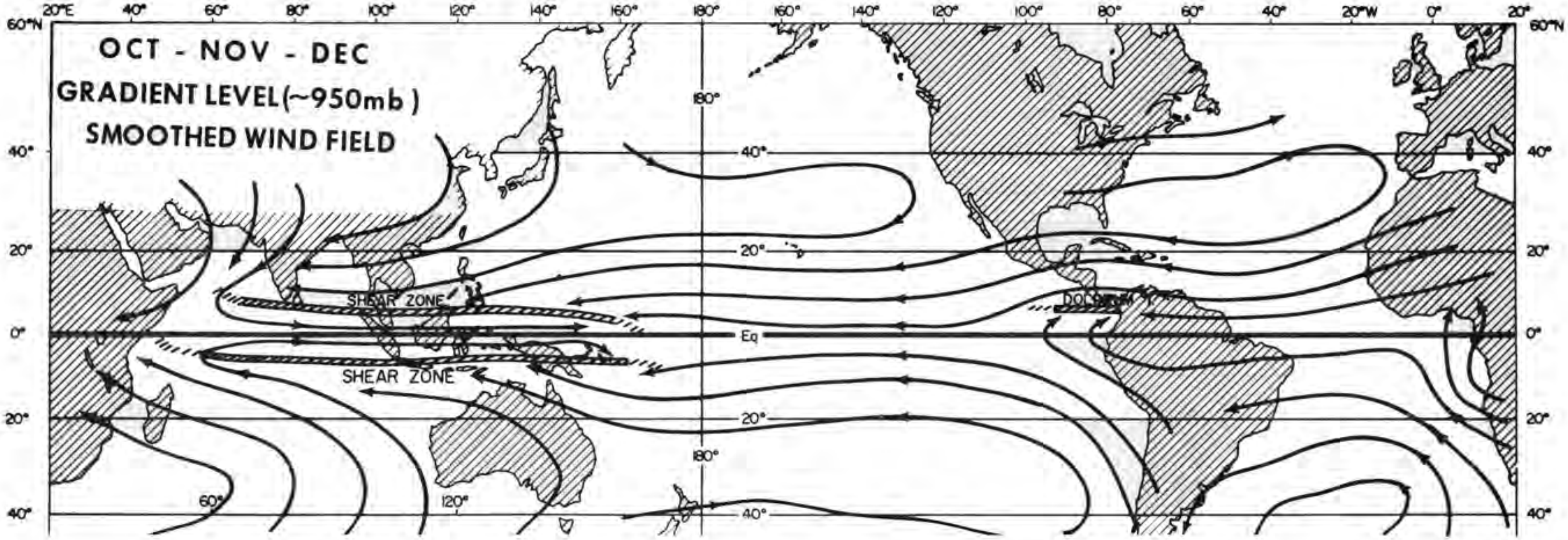
OCT - NOV - DEC
GRADIENT LEVEL(~950mb)
SMOOTHED WIND FIELD
SHEAR ZONE
SHEAR ZONE
DOLDRUM
Eq
20°E
40°
60°
80°
100°
120°
140°
160°
180°
20°W
0°
20°
60°N
40°
20°
0°

Fig. 78

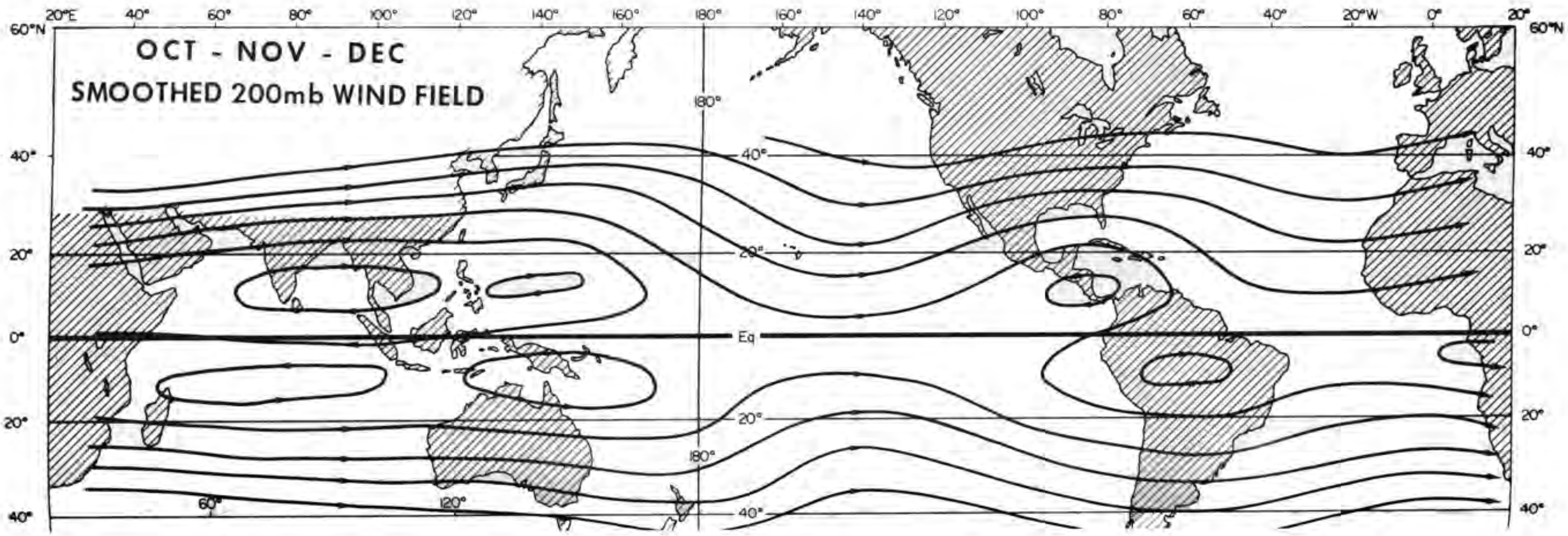
OCT - NOV - DEC
SMOOTHED 200mb WIND FIELD
Eq
20°E
40°
60°
80°
100°
120°
140°
160°
180°
20°W
0°
20°
60°N
40°
20°
0°

Fig. 79

Fig. 80

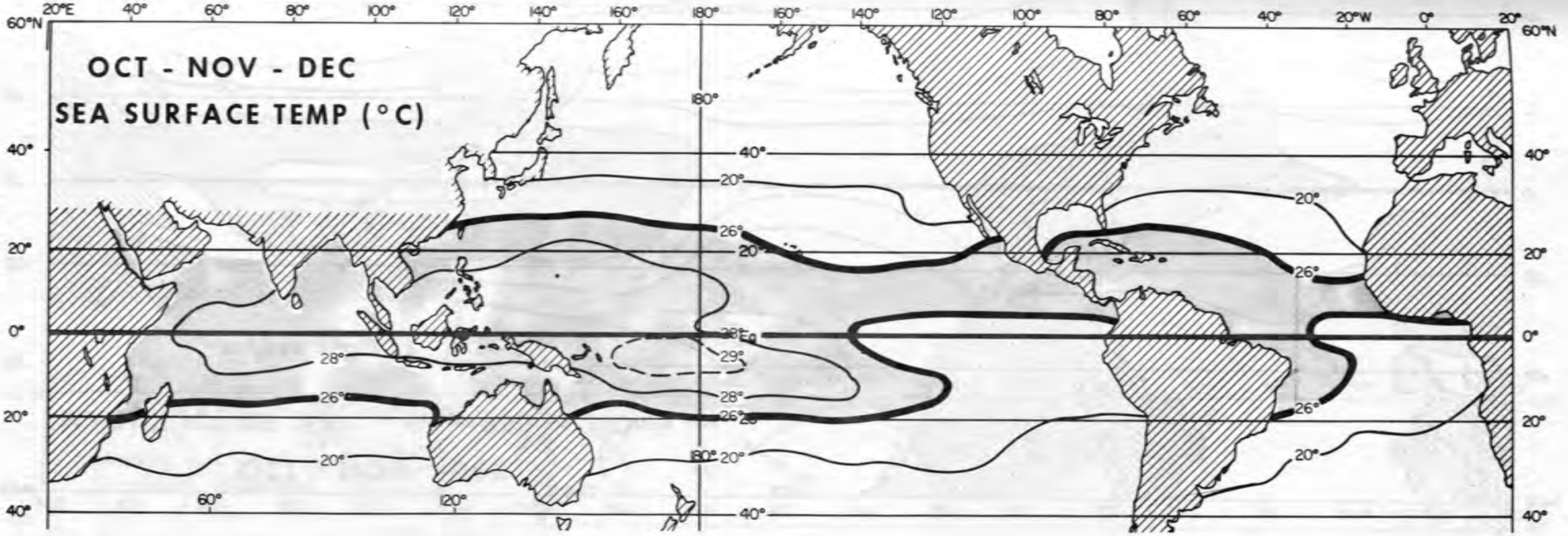
OCT - NOV - DEC
SEA SURFACE TEMP (°C)
20°
26°
28°
29°
Eq
60°N
40°
20°
0°
20°E
40°
60°
80°
100°
120°
140°
160°
180°
20°W

Fig. 81

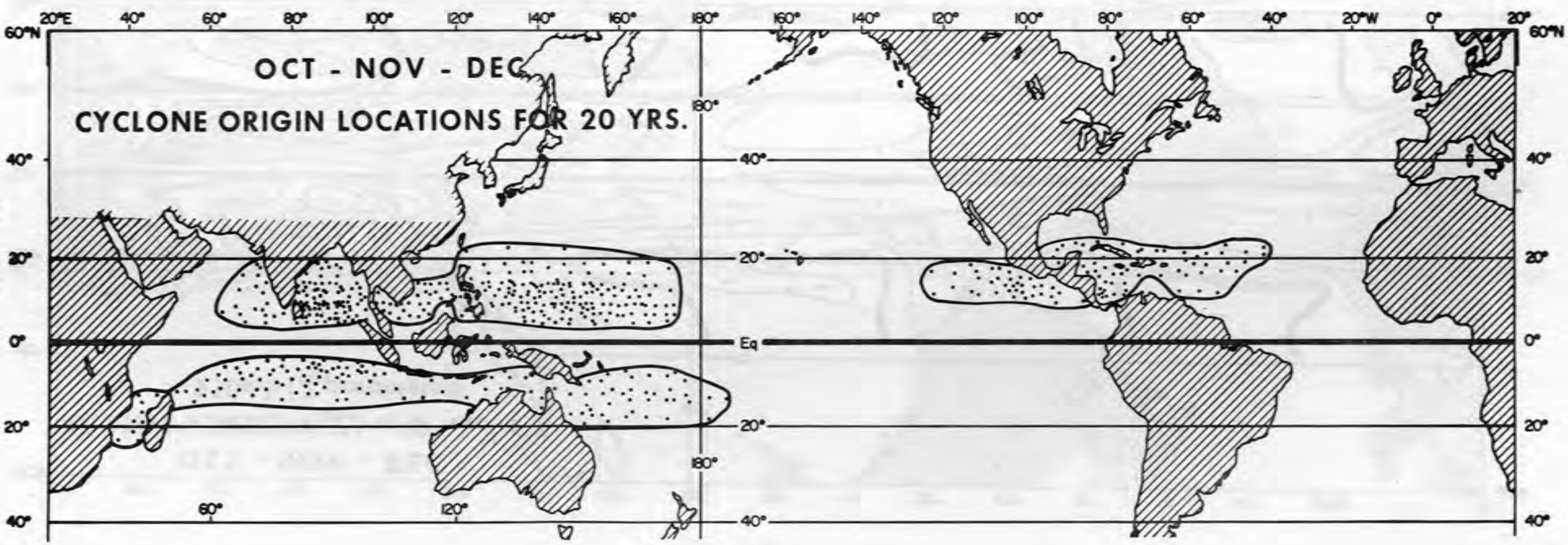
OCT - NOV - DEC
CYCLONE ORIGIN LOCATIONS FOR 20 YRS.
Eq
60°N
40°
20°
0°
20°E
40°
60°
80°
100°
120°
140°
160°
180°
20°W

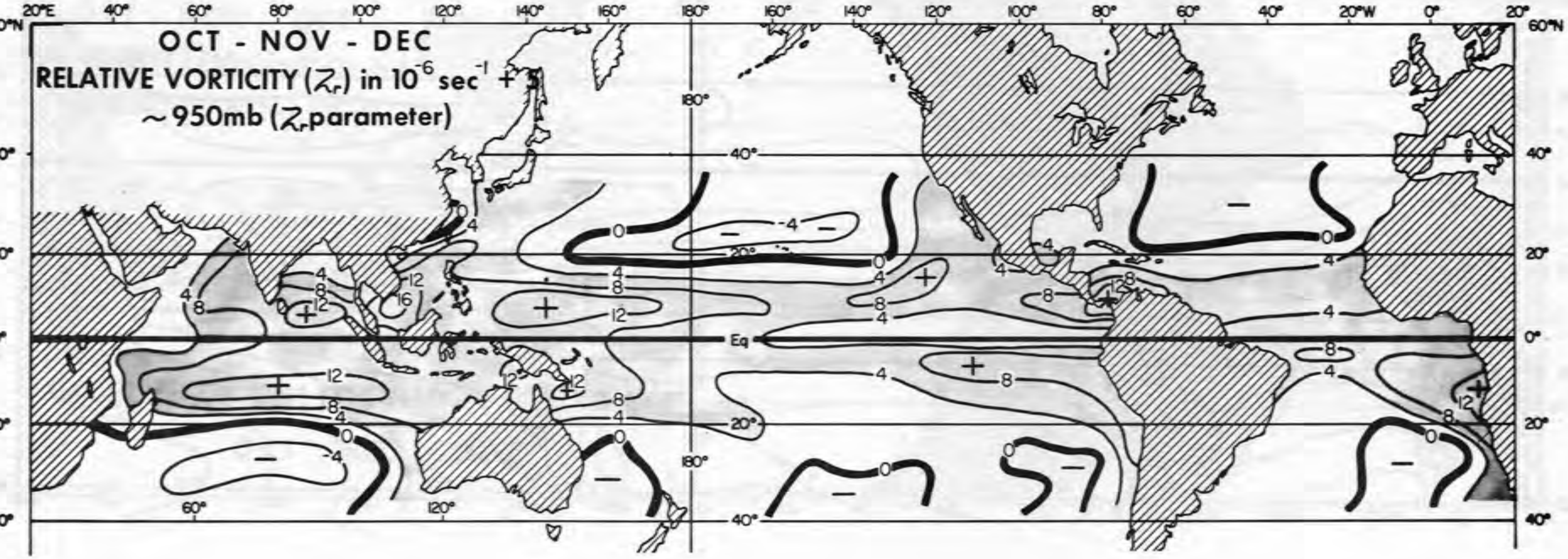
OCT - NOV - DEC
RELATIVE VORTICITY (ζ_r) in 10^{-6} sec^{-1} + 5
~950mb (ζ_r parameter)

Fig. 82

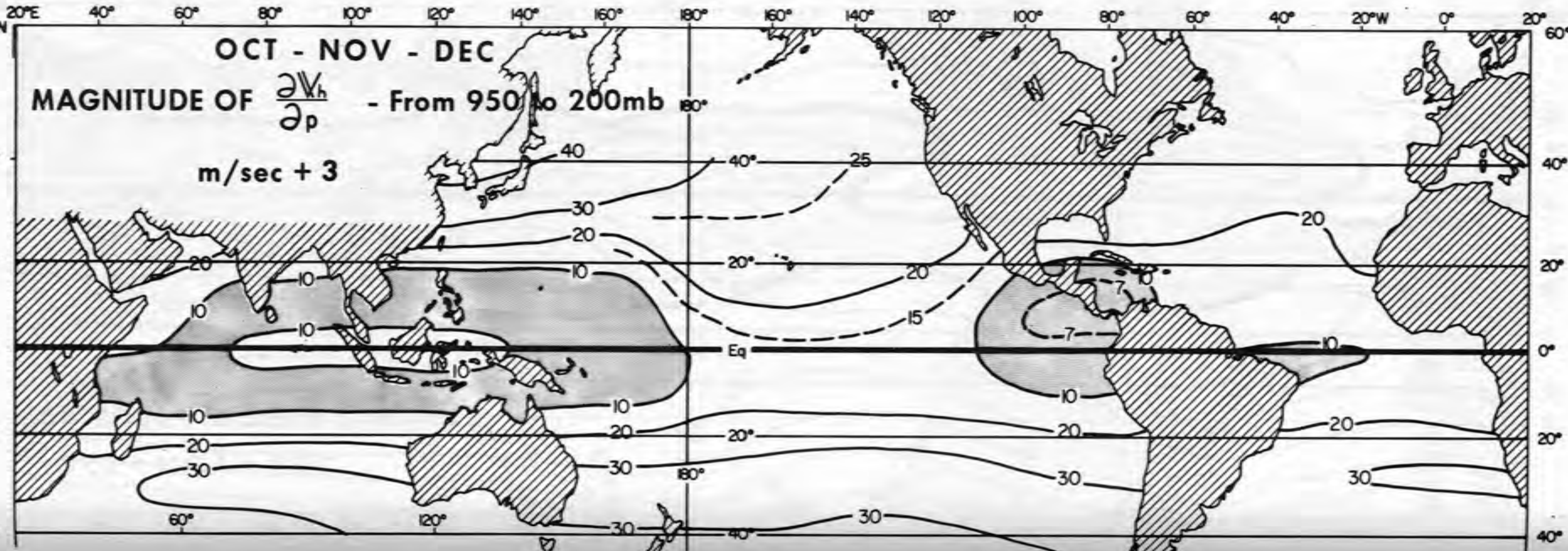
OCT - NOV - DEC
MAGNITUDE OF $\frac{\partial \mathbb{V}_h}{\partial p}$ - From 950 to 200mb
m/sec + 3

Fig. 83

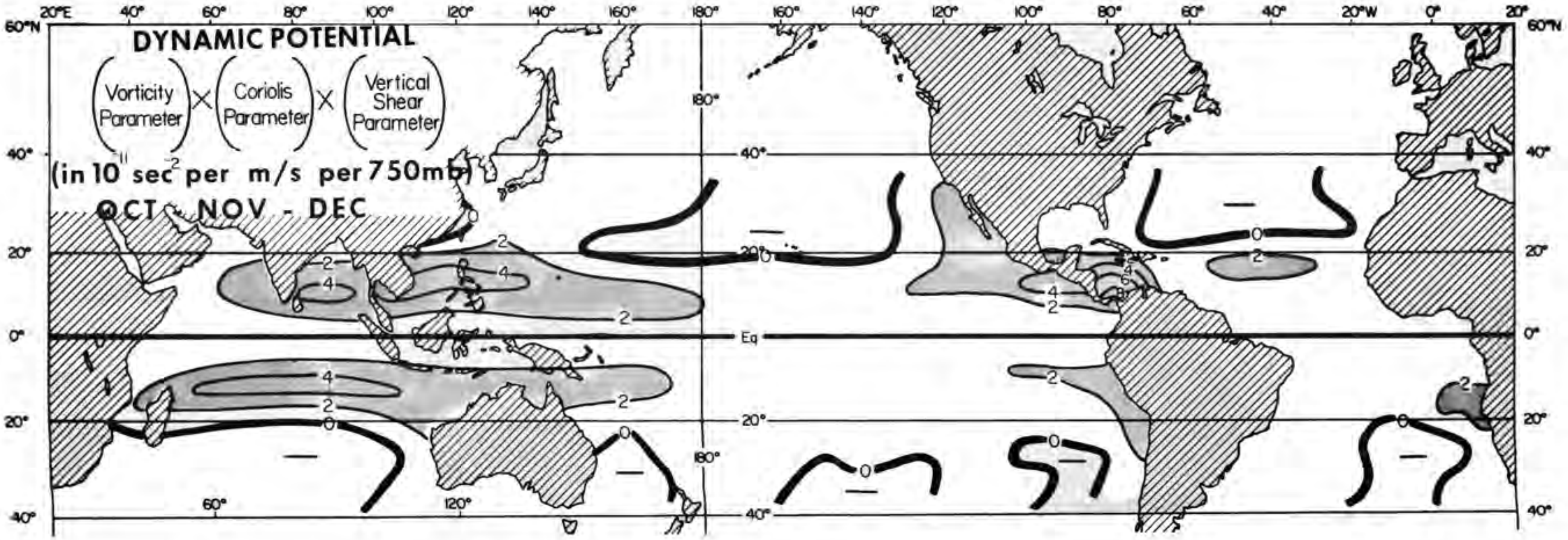
DYNAMIC POTENTIAL
(Vorticity Parameter) × (Coriolis Parameter) × (Vertical Shear Parameter)
(in 10⁻¹¹ sec⁻² per m/s per 750mb)
OCT - NOV - DEC
Eq

Fig. 84

Fig. 85

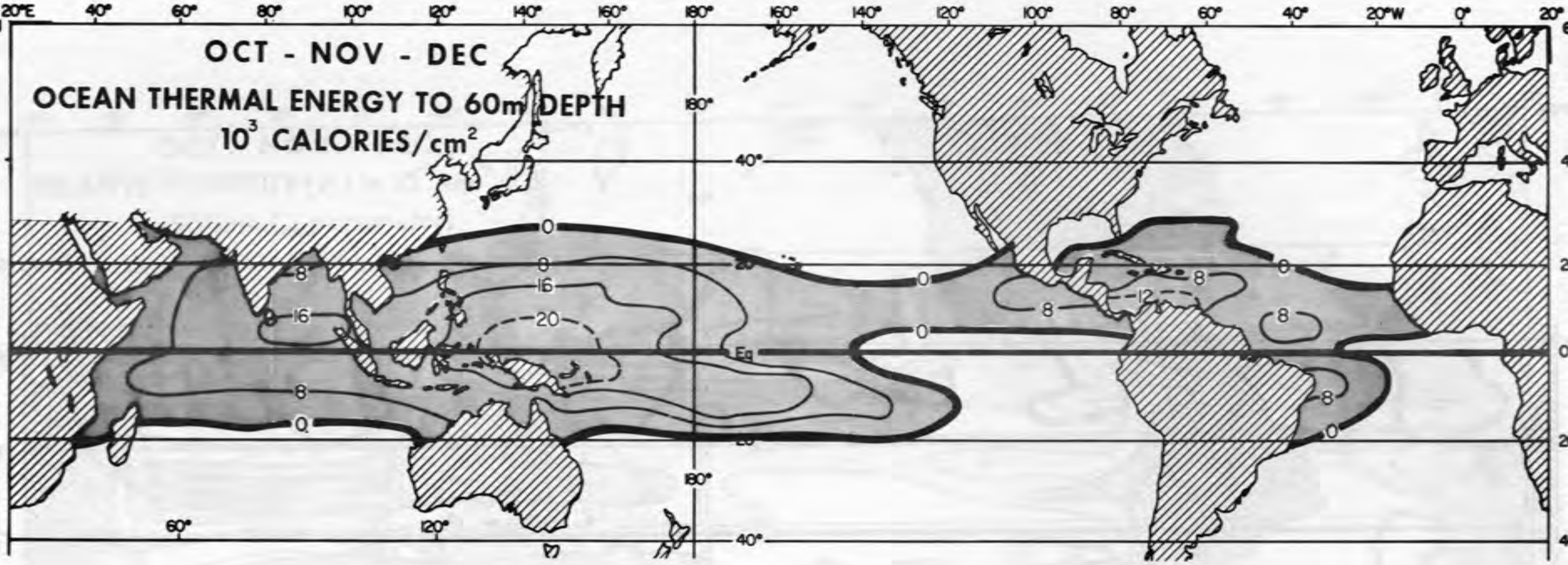
OCT - NOV - DEC
OCEAN THERMAL ENERGY TO 60m DEPTH
10³ CALORIES/cm²

Fig. 86

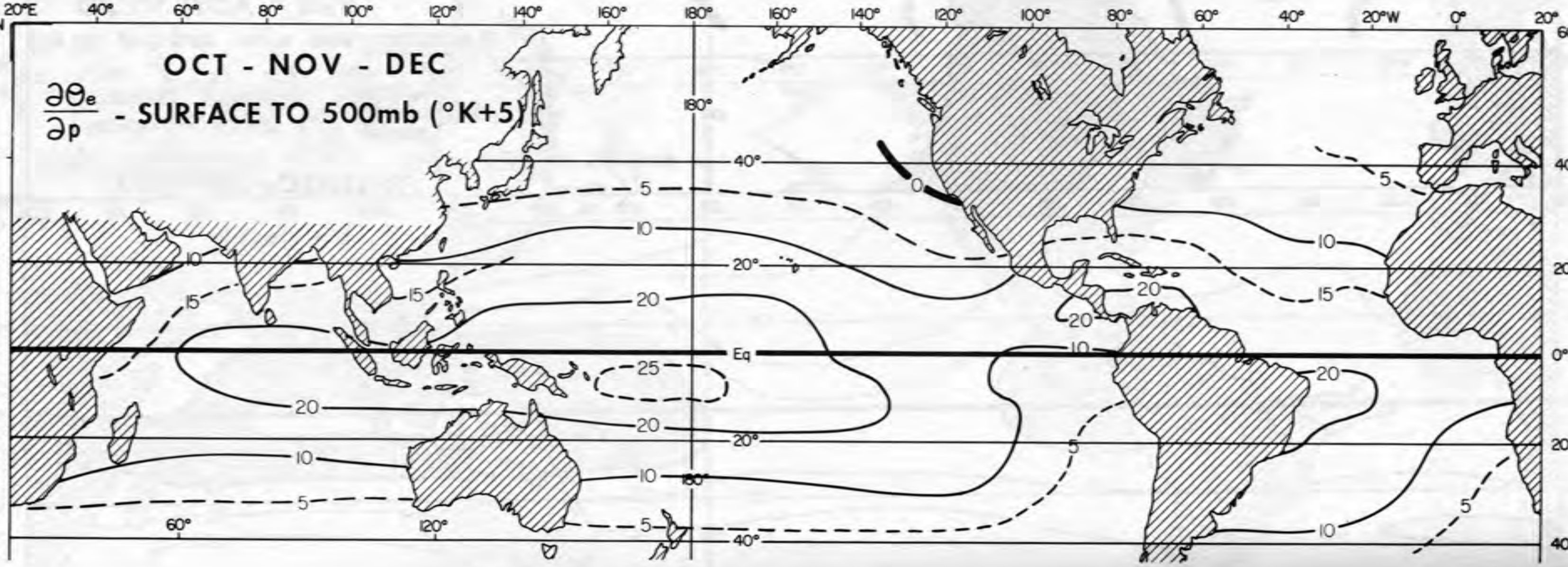
OCT - NOV - DEC
∂θe/∂p - SURFACE TO 500mb (°K+5)

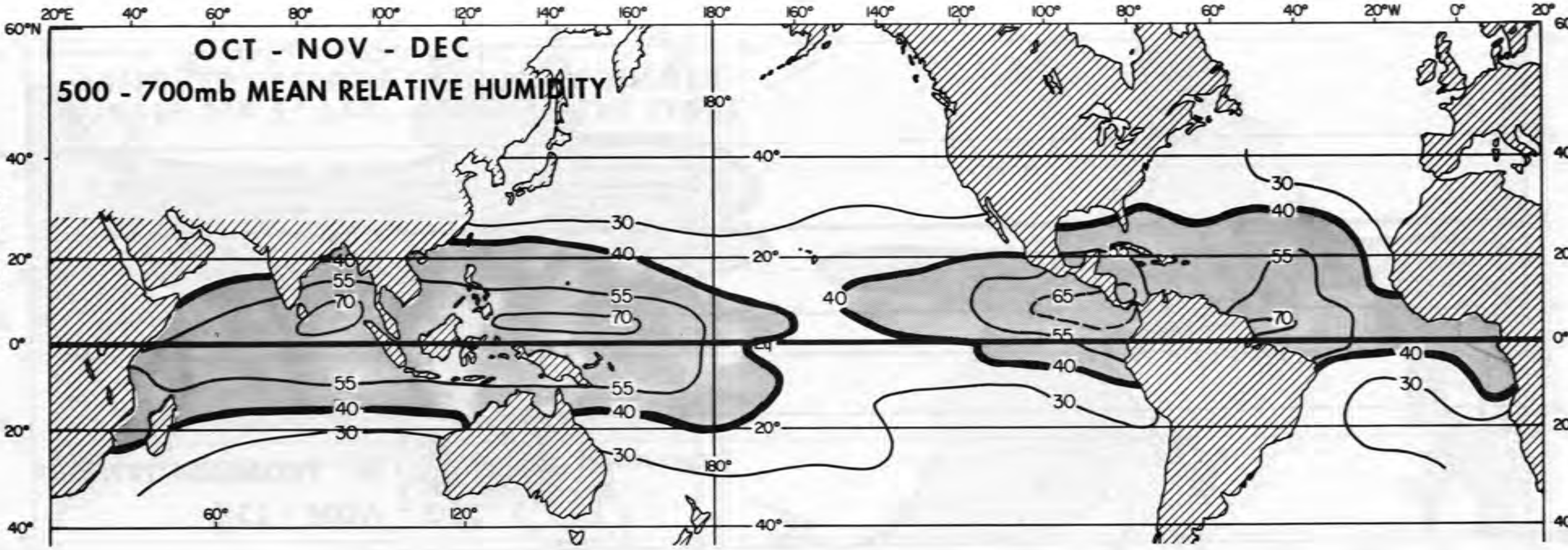
OCT - NOV - DEC
500 - 700mb MEAN RELATIVE HUMIDITY

Fig. 87

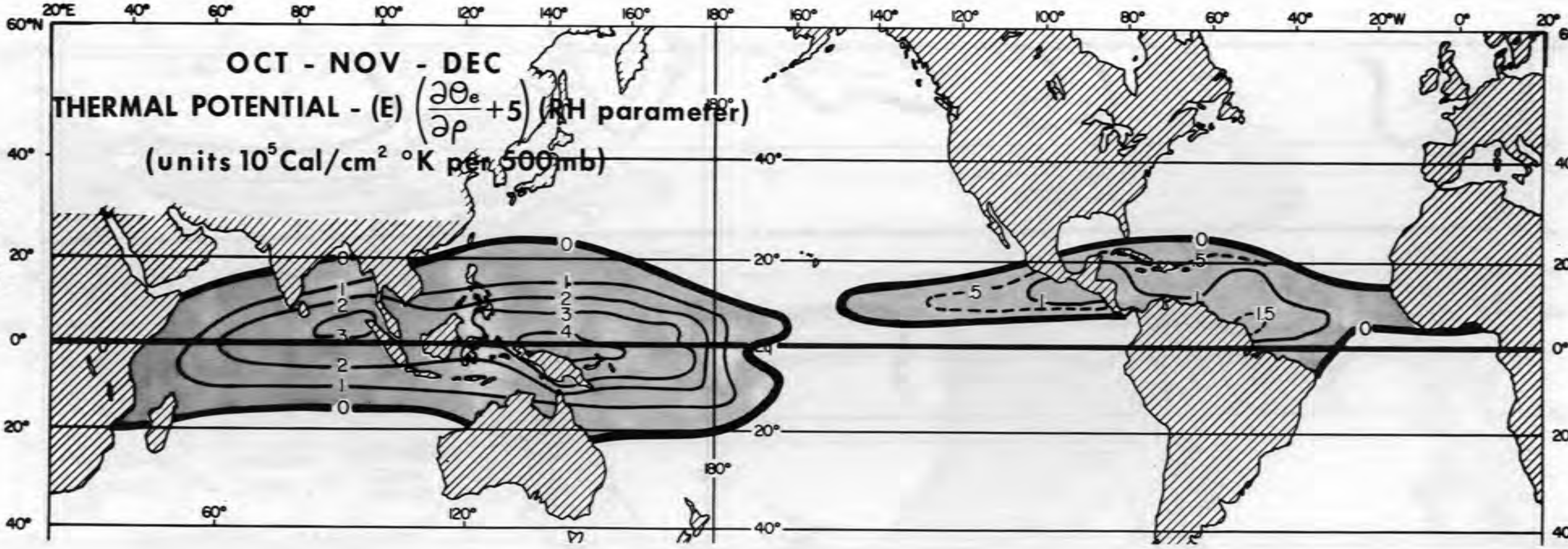
OCT - NOV - DEC
THERMAL POTENTIAL - (E) $\left(\frac{\partial \theta_e}{\partial p}+5\right)$ (RH parameter)
(units 10^5 Cal/cm^2 °K per 500mb)

Fig. 88

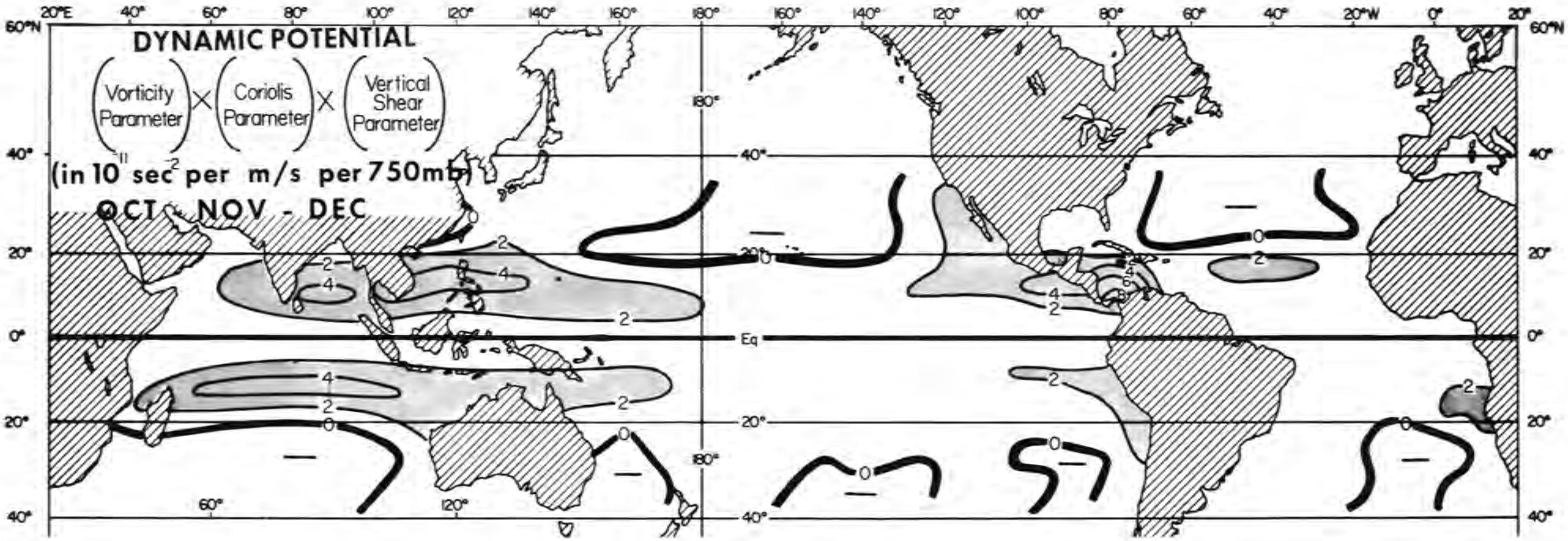
DYNAMIC POTENTIAL
(Vorticity Parameter) × (Coriolis Parameter) × (Vertical Shear Parameter)
(in 10^{-11} sec^{-2} per m/s per 750mb)
OCT - NOV - DEC

Fig. 89

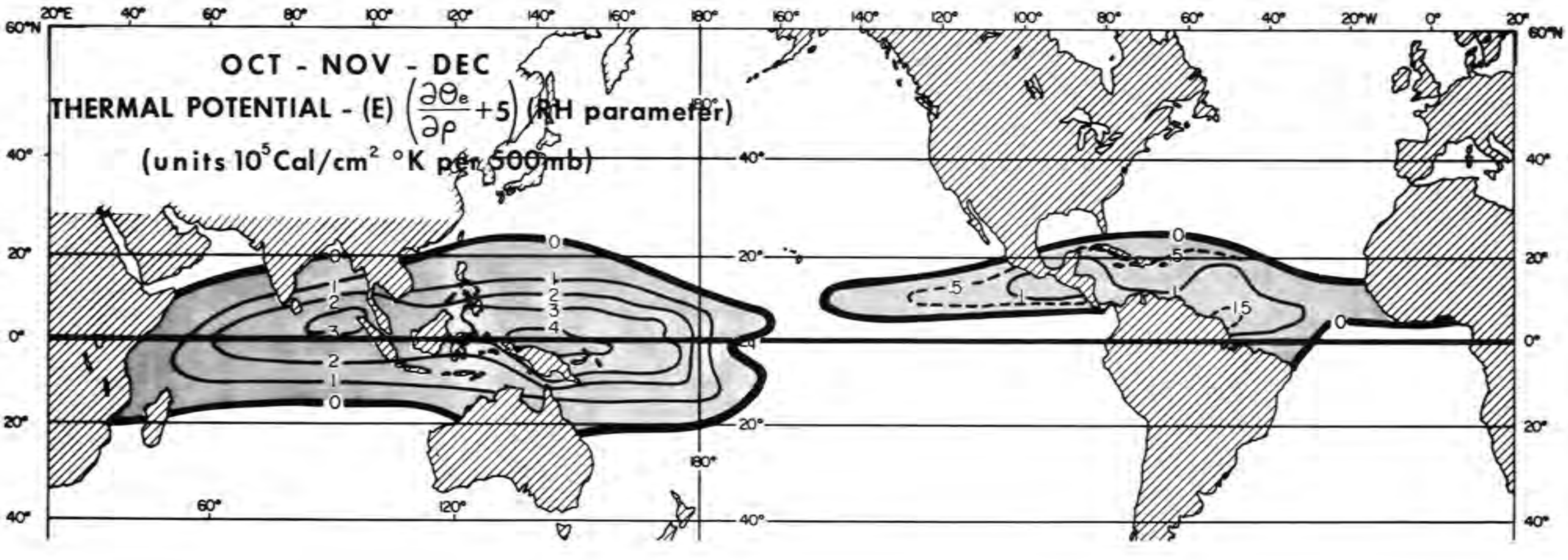
OCT - NOV - DEC
THERMAL POTENTIAL - (E) $\left(\frac{\partial \theta_e}{\partial p}+5\right)$ (RH parameter)
(units 10^5 Cal/cm^2 °K per 500mb)

Fig. 90

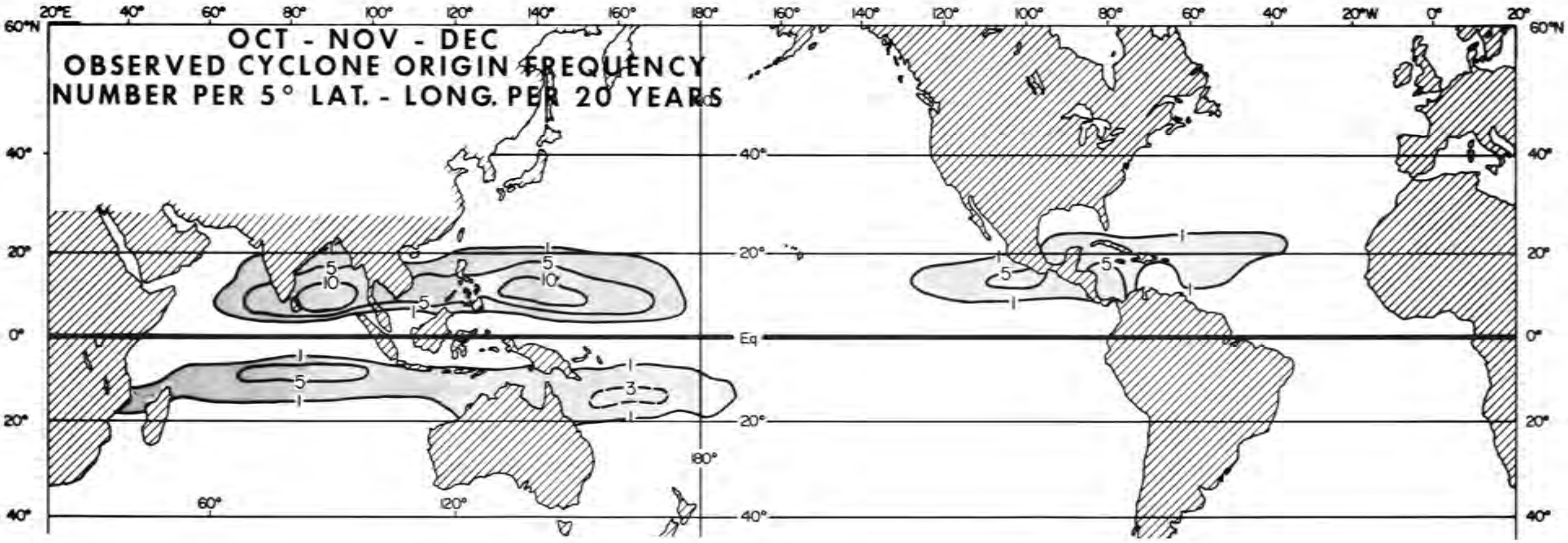
OCT - NOV - DEC
OBSERVED CYCLONE ORIGIN FREQUENCY
NUMBER PER 5° LAT. - LONG. PER 20 YEARS

Fig. 91

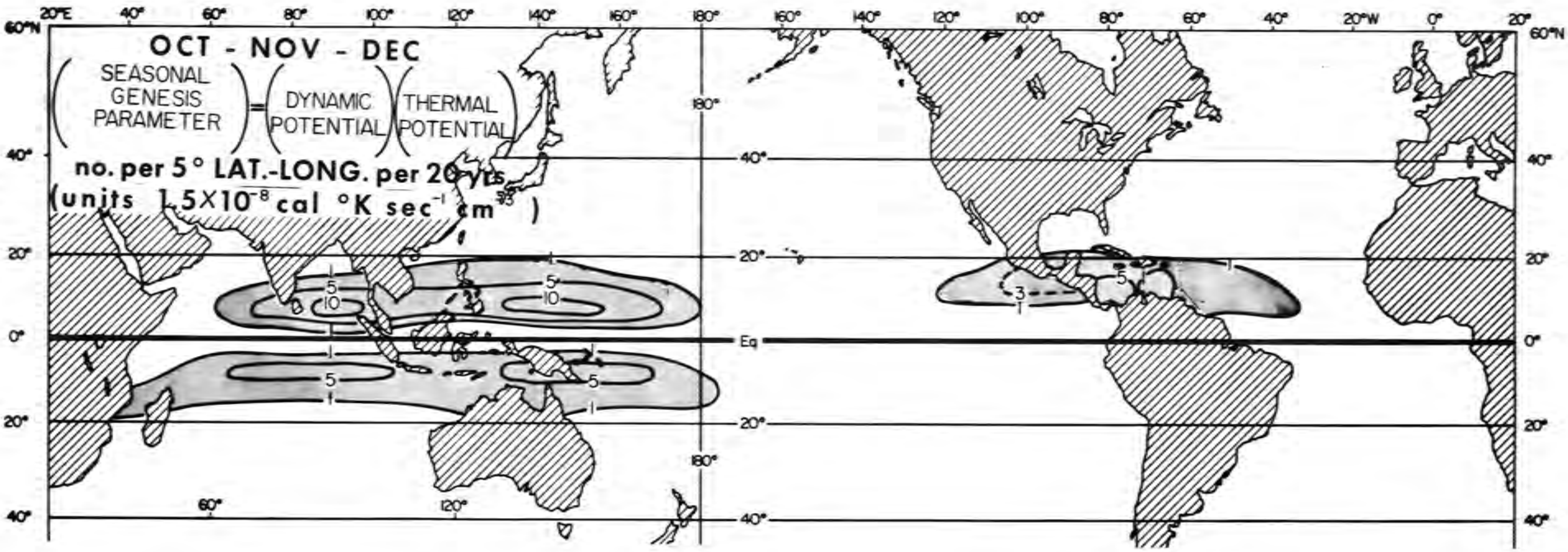
OCT - NOV - DEC
(SEASONAL GENESIS PARAMETER) = (DYNAMIC POTENTIAL)(THERMAL POTENTIAL)
no. per 5° LAT.-LONG. per 20 yrs
(units 1.5X10⁻⁸ cal °K sec⁻¹ cm⁻³)

Fig. 92

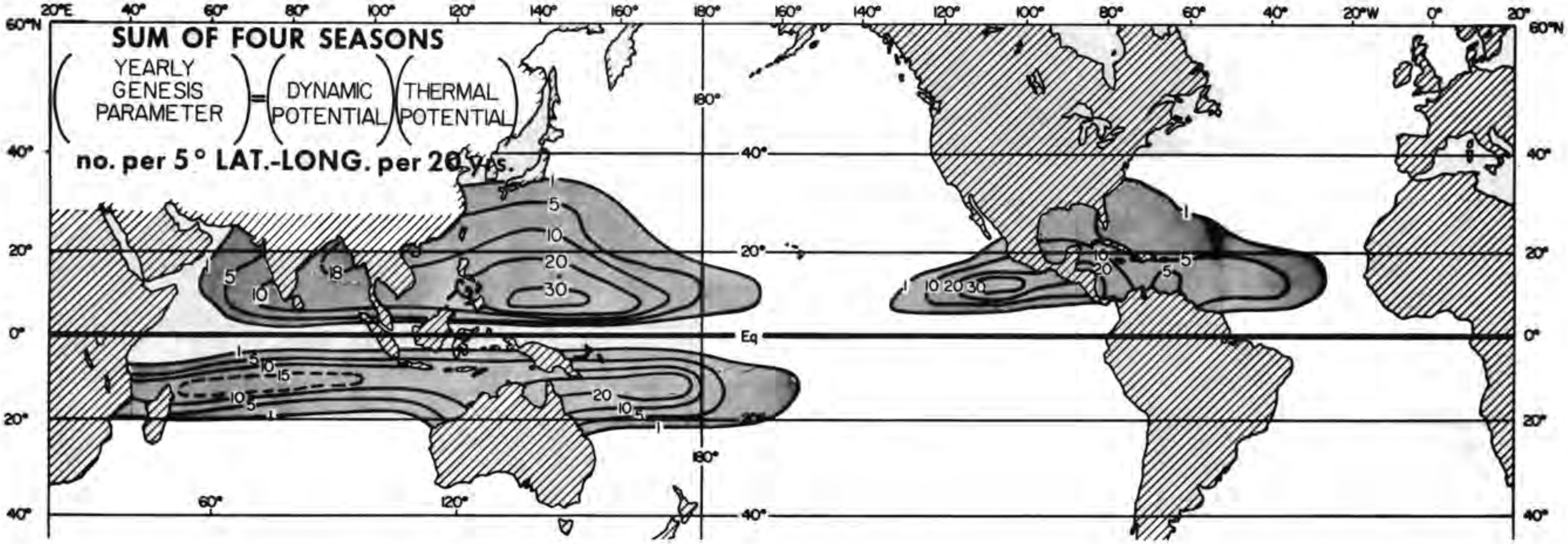
SUM OF FOUR SEASONS
YEARLY GENESIS PARAMETER = DYNAMIC POTENTIAL THERMAL POTENTIAL
no. per 5° LAT.-LONG. per 20 yrs.

Fig. 93

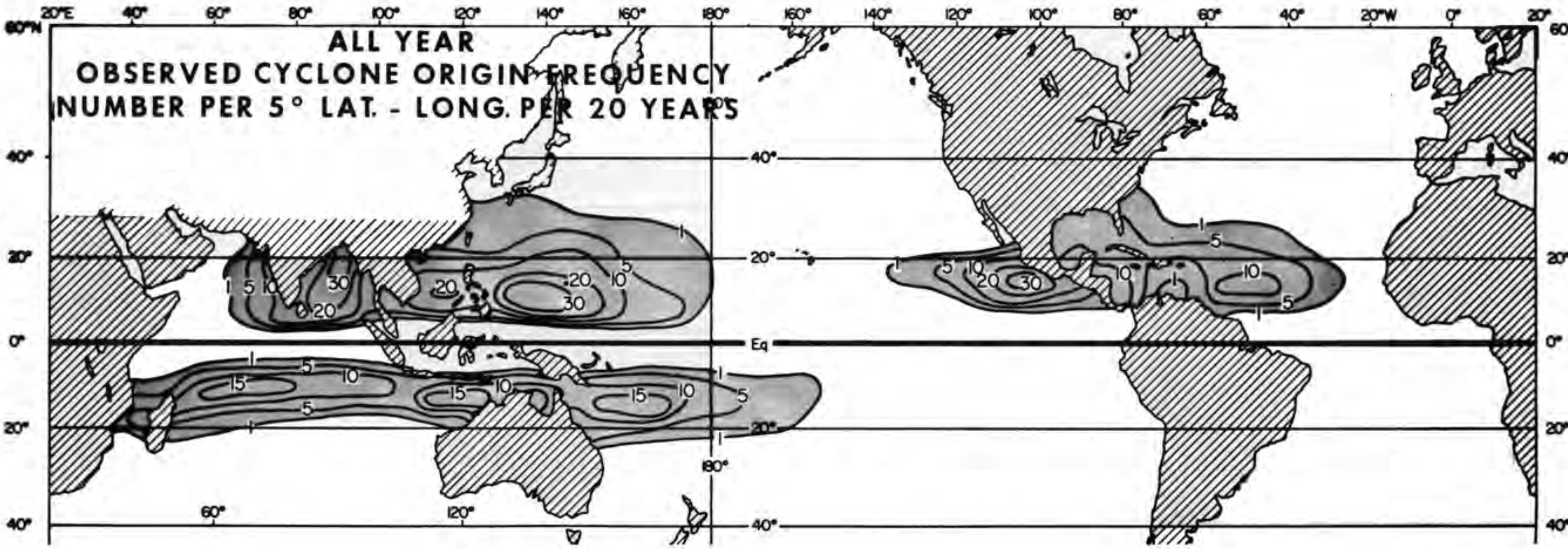
ALL YEAR
OBSERVED CYCLONE ORIGIN FREQUENCY
NUMBER PER 5° LAT. - LONG. PER 20 YEARS

Fig. 94

6. DISCUSSION

It is seen how closely the seasonal climatology of each area dictates the number of cyclones which form there even though the days of cyclone genesis (1-15 per 5° square per 20 years) make up but a very small percentage of the days of seasonal climatology. If it is assumed that cyclone genesis requires a favorable daily genesis potential to exist for three consecutive days over a 5° latitude-longitude square (or for 1 day periods in 3 adjacent up- and downstream 5° square one day apart), then the number of genesis days even in the regions of most active formation is no more than $\sim 2\frac{1}{2}\%$ of the non-genesis days. It is doubtful that these cyclones have a very large influence on the seasonal climatology based on several years. The seasonal climatology parameters are, to a large extent, independent of the cyclones. The cyclones are not independent of the climatology, however.

It is encouraging to learn that the frequencies and spatial distribution of tropical cyclone formation are so closely related to the seasonal climatology. Even though the dynamics of individual cyclone genesis are very non-linear and unquestionably very complicated, the frequency with which these individual genesis processes are activated is very strongly tied to the large-scale and long-term parameter averages. It was not expected that cyclone frequency could be so closely related to the long term climatological parameters.

It is not just the correlation of these six seasonal parameters with genesis frequency which is noteworthy, but also the physical rationale concerning the effects of these parameters on genesis which is important. It is possible that other climatological parameters can be found which are also related to cyclone frequency, but the author doubts if these other parameters, if detected, can be as well related to the previously discussed physical requirements of upper tropospheric enthalpy accumulation.

It is observed that cyclone genesis is a slow process of gradual cloud cluster upper tropospheric enthalpy increase which, on the average, requires about three days of favorable conditions. In some situations cyclones develop from cloud clusters in 1-2 days. In other cases it takes 4-5 days. Pre-cyclone cloud clusters move westward at a velocity of about 5° longitude per day ($\sim 12\frac{1}{2}$ knots) and occupy areas of about a 5° square. It can be assumed that cyclone formation requires favorable daily genesis conditions to exist over a 5° square for about 3 consecutive days or over three adjacent and progressive downwind 5° squares for one day each. In a statistical sense an interchange of space (5° square) and time (1 day) is assumed.

Since each 20 year individual seasonal climatology time period includes about 1800 days (3 month x 30 days x 20 years) or 600 consecutive 3-day periods (or 600 consecutive 3-day adjacent downwind 5° square period of one day each) we can calculate the percentage of time for which favorable cyclone genesis conditions are present. Table 7 shows the percentage of cyclone genesis days. Even for high frequency of genesis, these percentages are not large.

Daily Values of the Seasonal Genesis Parameter. Our observations of daily genesis parameter values associated with 40 individual cases of pre-cyclone cloud clusters (Williams and Gray, 1973, and recent undocumented studies) in the Western Pacific show that the early

Table 7

Number and Percent of Cyclone Genesis Days for 20 Seasons

Seasonal Cyclone Genesis Frequency per 5^o Square per 20 Years	No. of 5^o Seasonal 3 Day Consecutive Periods in 20 Years	Percent of 5^o Consecutive 3 Day Periods Which Produce Cyclone Genesis
15	600	2.50
10	600	1.66
5	600	0.83
1	600	0.17

stage pre-cyclone cluster 950 mb vorticity is about $\sim$ 10-15 x $10^{-6}sec^{-1}$ and that the 950 to 200 mb vertical wind shear averaged over the 5^o areas is no more than about 2-3 m/sec. Clusters which do not develop have typical vertical wind shears of $\sim$ 5-8 m/sec. The ocean thermal energy content and $\partial\Theta_e/\partial p$ are little different than climatological values. 500 to 700 mb relative humidity is larger than 70 percent. The typical magnitude of the Seasonal Genesis Parameter when applied to individual daily cases of cloud cluster growth to cyclone intensity is as shown in Table 8.

As the pre-cyclone disturbance gradually develops from a cloud cluster with 5^o square vorticity of 15 x $10^{-6}sec^{-1}$ to a cyclone with vorticity of 100 x $10^{-6}sec^{-1}$, the magnitude of the daily genesis potential increases from an initial day value of $\sim$ 15 to second and third day values of about 30 and 80 respectively. This table also lists estimated values of the daily genesis potential for the usual cloud cluster which does not develop into a cyclone. Note that the thermal or Cb potential is little altered in the genesis process. Given a sufficient thermal potential, it is the daily variations in low level vorticity and

Table 8

Typical 5^{o} Square Parameter Values of Daily Genesis Potential for Different Types of Cloud Clusters in the Western North Pacific

Type of Cluster System	Vorticity Parameter $\zeta_r + 5$ $10^{-6}sec^{-1}$	Coriolis Parameter f ($\sim 12^{o}$lat) $10^{-5}sec^{-1}$	Vertical Shear Parameter $1/(S_z + 3)$ 750 mb per m/sec	Dynamic Potential $10^{-11}sec^{-2}$ per m/sec per 200 mb	Ocean Energy Parameter E $10^{3}cal/cm^{2}$	Moist Stability Parameter $\frac{\partial\theta_e}{\partial p} + 5$ ^{o}K per 500 mb	Humidity Parameter $\overline{RH}$	Thermal Potential $10^{5}cal/cm^{2}$ ^{o}K per 500 mb	Daily Genesis Parameter (1.5×10^{-8} cal ^{o}K/sec cm^{3})
Typical Non-Developing Cloud Clusters	12	3	1/10	3	10	20	1.0	2	6
Developing Cluster 1st Day	18	3	1/7	8	10	20	1.0	2	16
Developing Cluster 2nd Day	30	3	1/6	15	10	20	1.0	2	30
Developing Cluster 3rd Day	55	3	1/4	40	10	20	1.0	2	80
Tropical Cyclone (Max. Wind 10 m/sec at 200 km radius)	100	3	1/3	100	10	20	1.0	2	200

tropospheric vertical wind shear which are the major short term determinants of genesis.

Daily values of the Genesis Potential for the developing clusters are usually larger than the seasonal values, but in some cluster situations they can be less than the seasonal values. Daily values of 950-200 mb vertical wind shear are often larger than climatological values of vertical shear when the climatological values are small. Where climatological vertical shear is small due to cancelling of larger magnitudes of daily easterly and westerly shear, the daily genesis parameter can be smaller than the seasonal parameter.

Individual cases of cyclone genesis require a local environment with favorable deviations from seasonal conditions. A crucial question emerges: <u>Can we directly relate the frequency of favorable deviations of the daily Genesis Potential to the Seasonal Genesis Potential</u>?

<u>Daily Correlation of Parameters.</u> The author believes that the individual daily variations of each of the six individual genesis parameters over 5° areas are largely uncorrelated. f does not vary with time. E changes only slowly with time and has little daily dependence upon wind or humidity factors. The 5° area daily variations of surface to 500 mb $\partial\Theta_e/\partial p$ are typically small. A separate study of the daily variations of 5° area average values of ζ_r and S_z parameters showed negligible correlation over many days. Daily variations of the relative humidity at individual locations is largely uncorrelated with all parameters except the low level vorticity, and this correlation is not very high. Thus, as a first approximation it may be assumed without very much error that the daily variations of these six genesis parameters over 5° areas are largely uncorrelated with each other. If the daily

correlation of parameters is negligibly small, then the correlation of the 3-day average parameter values should be similarly small. The five genesis parameters which undergo 3-day variations with time (f not considered) may be conveniently represented by the symbols A, B, C, D, E. Let the seasonal values of these parameters at any location be designated as $\overline{A}$, $\overline{B}$, $\overline{C}$, $\overline{D}$, $\overline{E}$, where the —— (bar) denotes a seasonal average. Let the deviation of the 5^{o} area three consecutive day average values at any location (or the 3-day downwind values at consecutive 5^{o} squares) from the seasonal averages be denoted by A', B', C', D', E', where the 3-day values (A, B, C, etc.) are also defined by the usual notation $A = \overline{A} + A'$, $B = \overline{B} + B'$, $C = \overline{C} + C'$, etc.

If the correlations of the 3-day parameter deviations averaged over a season are small, that is if the terms:

$$\frac{\overline{A'B'}}{\overline{A}\,\overline{B}},\ \frac{\overline{A'C'}}{\overline{A}\,\overline{C}},\ \frac{\overline{A'D'}}{\overline{A}\,\overline{D}},\ \frac{\overline{A'E'}}{\overline{A}\,\overline{E}},\ \frac{\overline{B'C'}}{\overline{B}\,\overline{C}},\ \frac{\overline{B'D'}}{\overline{B}\,\overline{D}},\ \frac{\overline{B'E'}}{\overline{B}\,\overline{E}},\ \frac{\overline{C'D'}}{\overline{C}\,\overline{D}},\ \frac{\overline{C'E'}}{\overline{C}\,\overline{E}},\ \frac{\overline{D'E'}}{\overline{D}\,\overline{E}}$$

are each of magnitude between $\pm$ 0-0.2, then the seasonal averages of the 3-day products will not be very different from the product of the seasonal averages, or

$$\overline{ABCDE} \approx \overline{A}\,\overline{B}\,\overline{C}\,\overline{D}\,\overline{E} \tag{13}$$

$\overline{ABCDE}$ is equal to the average of the 3-day values, or

$$\overline{ABCDE} = 1/600 \sum_{i=1}^{i=600} (ABCDE)_i \tag{14}$$

A study of the magnitude of the positive deviations of the 3-day Genesis Potential from its seasonal values in the Western Pacific show it to average about 9-10 $(\frac{1.5 \times 10^{-8} cal\,^{o}K}{cm^3 sec})$ units and to be largely independent of location and season. Assuming the 3-day average product of ABCDE to be randomly distributed for positive deviations of this parameter[5] with a standard deviation of $\sim$ 9-10 units which does not significantly vary with season or location one can see that a given threshold value for genesis (say, a 3-day average value of the Genesis Potential $\geq$ 30) can occur on only a small number of days per season. Given a standard deviation of 9-10 units, the number of days on which this is possible is specified by a factor of $\overline{ABCDE}$, or because of the relationship expressed by Eq. (13), by a factor of $\overline{A}\ \overline{B}\ \overline{C}\ \overline{D}\ \overline{E}$. Thus, <u>a direct relationship between the climatologically specified Seasonal Genesis Parameter and the actual genesis frequency should not be unexpected</u>.

It is assumed that if the 3-day genesis parameter is greater than 30 units (its second day value in its three-day growth) then enough upper tropospheric enthalpy accumulation will occur such that a cyclone will form and intensify. When the second day of the 3-day average of the Genesis Potential is less than 30, upper troposphere enthalpy increases are insufficient to allow cyclone formation. Even with the most favorable seasonal climatology, positive 3-day deviations of the Genesis Potential of 20-30 units can occur on only a few days. The rarity of cyclone genesis is to be expected.

---

[5]As negative values are not permitted for f, $1/(S_z + 3)$, E, and $\overline{RH}$, the negative deviations of the 3-day Genesis Potential are skewed around zero and not representative of a normal distribution. The positive deviations of the Daily Genesis Potential may be assumed to be normally distributed, however.

Figures 95 and 96 portray the number of 3-day periods per season for which the 3-day average Genesis Potential is above certain specified values for different Seasonal Genesis Parameters. Note the very infrequent number of 3-day periods when this potential is above 30. Note also how shifts in the seasonal genesis parameter from 1 to 5, 10 and 15 can increase the number of periods when the genesis potential is above 30 by a similar ratio. Because positive deviations of the Genesis Potential are largely independent of location and time of year, seasonal climatology plays a fundamental role in specifying the number of 3-day periods in which the genesis potential can be large enough to activate individual cyclone formation. It is seen that cyclone frequency, although occurring on only a very few days per season, is, nevertheless, directly related to the large scale and long term shifts in the tropical general circulation and thermal energy content. From the long time scale point of view, cyclone genesis frequency is seen as the statistical result of largely random 2-3 day parameter variations superimposed on a slowly varying seasonal climatology.

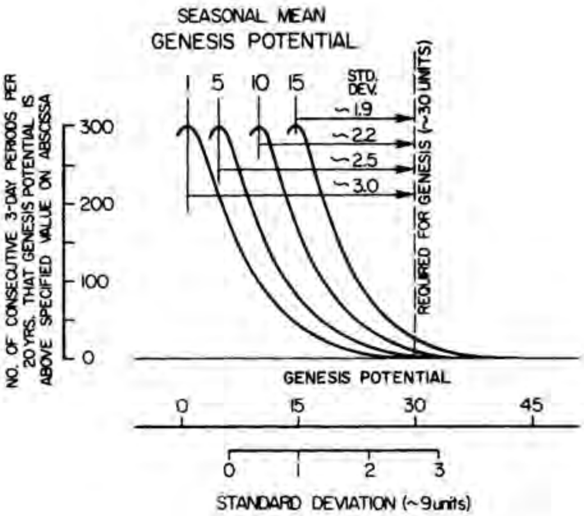

Fig. 95. Number of consecutive 3-day periods (ordinate) in which the 3-day genesis parameter is above the specified values on the abscissa for different values of seasonal forecast genesis frequency. A normal distribution for positive deviations of the 3-day daily genesis potential is assumed with the standard deviation of ∿9-10 units.

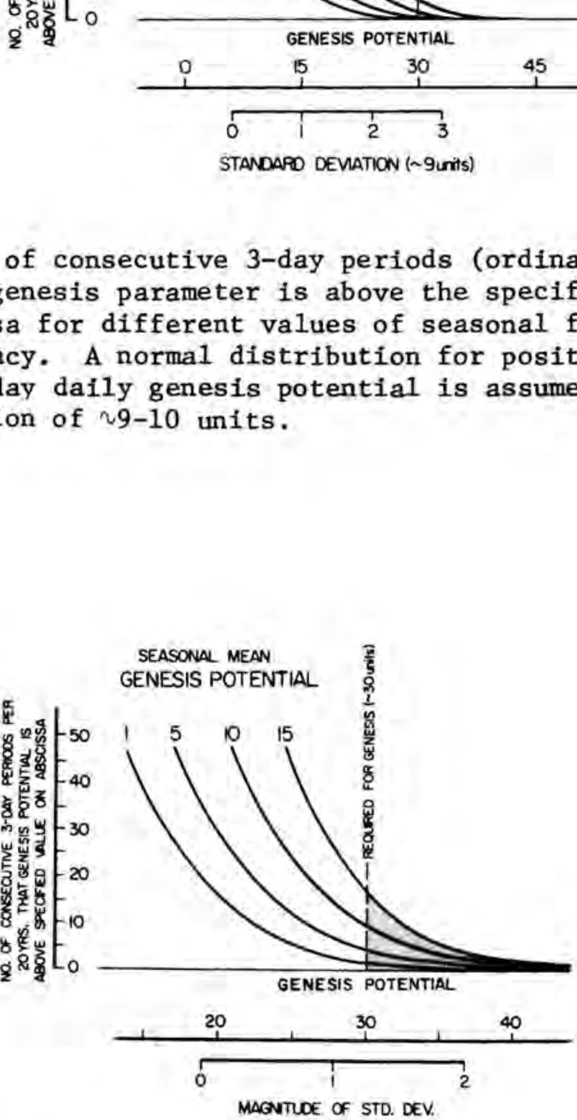

Fig. 96. Same as for Fig. 95 except for showing an expansion of the right portion of the figure where the required value of the 3-day daily genesis potential > 30 has been shaded.

ACKNOWLEDGEMENTS

This research has been supported by a National Science Foundation Research Grant Number (GA-32589X3). The author is much indebted for the excellent assistance rendered him in data reduction, in calculations, in drafting, and in overall manuscript preparation by Messrs. Ronald Phelps, Charles Solomon, and Scott Ryden and by Mrs. Barbara Brumit and Mrs. Genevra Metcalf.

REFERENCES

Anthes, R. A., 1972: Development of asymmetries in a three-dimensional numerical model of the tropical cyclone. Mon. Wea. Rev., 100, 461-476.

______, S. L. Rosenthal, and J. W. Trout, 1971a: Preliminary results from an asymmetric model of the tropical cyclone. Mon. Wea. Rev., 99, 744-758.

______, J. W. Trout, and S. L. Rosenthal, 1971b: Comparisons of tropical cyclone simulations with and without the assumption of circular symmetry. Mon. Wea. Rev., 99, 759-766.

Aspliden, C. I., 1971: On energy distribution in the tropical atmosphere. Ph.D. Dissertation, Florida State University, 232 pp.

______, et al., 1966: Satellite study, tropical North Atlantic, 1963, parts I and II. Research Reports, Florida State University, 153 and 98 pp.

Atkinson, G. D., 1971: Forecaster's guide to tropical meteorology, Unpublished Air Weather Service (MAC) Technical Report No. 240, 300 pp. (available from AWS, Scott AFB, Illinois).

______, 1973: Private communication. (Commander of the Joint Typhoon Warning Center, Guam).

Black, P. G., and W. D. Mallinger, 1972: The mutual interaction of Hurricane Ginger and the upper-mixed layer of the ocean. Appendix D, Project Stormfury Annual Report, 1971. National Hurricane Research Laboratory, Coral Gables, Florida.

Brand, S., 1971: The effects on a tropical cyclone of cooler surface waters due to upwelling and mixing produced by a prior tropical cyclone. J. Appl. Meteor., 10, 865-874.

Carrier, G. F., 1971: The intensification of hurricanes. J. Fluid Mech., 49, 145-158.

Ceselski, B. F., 1974: Cumulus convection in weak and strong tropical disturbances. J. Atmos. Sci., 31, 1241-1255.

Chang, C. P., 1970: Westward propagating cloud patterns in the tropical Pacific as seen from time-composite satellite photographs. J. Atmos. Sci., 27, 133-138.

Charney, J. C., and A. Eliassen, 1949: A numerical method for predicting the perturbations of the middle-latitude westerlies. Tellus, 1, 38-54.

______, and ______, 1964: On the growth of the hurricane depression. J. Atmos. Sci., 21, 68-75.

Cox, S. K., 1968: A radiation model in which the effects of clouds are simulated from moisture and temperature parameters. Annual Report on WBG-88, Department of Meteorology, University of Wisconsin, 2-50.

______, 1971: Infrared radiation models for the tropics. Proceedings of the Miami Workshop on Remote Sensing, NOAA, Boulder, Colorado, 161-178.

______, 1973: Radiation components of the energy budget for BOMEX. Department of Atmospheric Science Report No. 208. Colorado State University, 43 pp.

Dunn, G. E., 1940: Cyclogenesis in the tropical Atlantic. Bull. Am. Meteor. Soc., 21, 215-229.

______. 1951: Tropical cyclones. Compendium of Meteorology, American Meteorological Society, Boston, Mass., 887-901.

Fett, R. W., 1964: Aspects of hurricane structure: New model considerations suggested by TIROS and Project Mercury observations. Mon. Wea. Rev., 92, 43-60.

______, 1968: Typhoon formation within the zone of the intertropical convergence. Mon. Wea. Rev., 96, 106-117.

Fisher, E. L., 1958: Hurricanes and the sea-surface temperature field. J. Meteor., 15, 328-333.

Frank, N. L., 1969: The "Inverted V" cloud pattern - an easterly wave? Mon. Wea. Rev., 97, 130-140.

______, 1970a: Atlantic tropical systems of 1969. Mon. Wea. Rev., 98, 307-324.

______, 1970b: Energetics of cold lows. Proc. of the Symp. on Trop. Meteor., Honolulu, 2-11 June, 1970, Hawaii Inst. of Geophys.

______, 1971: Atlantic tropical systems of 1970, Mon. Wea. Rev., 99, 281-285.

______, 1972: Atlantic tropical systems of 1971, Mon. Wea. Rev., 100, 268-275.

______, 1973: Atlantic tropical systems of 1972, Mon. Wea. Rev., 101, 334-338.

______, and T. M. Johnson, 1969: Vortical cloud systems over the tropical Atlantic during the 1967 hurricane season. Mon. Wea. Rev., 97, 124-129.

______, and P. J. Hebert, 1974: Atlantic tropical systems of 1973, Mon. Wea. Rev., 102, 290-295.

Garstang, M., 1967: Sensible and latent heat exchange in low latitudes synoptic scale systems. Tellus, 19, 492-508.

Gray, W. M., 1968: Global view of the origin of tropical disturbances and storms. Mon. Wea. Rev., 96, 669-700.

______, 1972: A diagnostic study of the planetary boundary layer over the oceans. Department of Atmospheric Science, Colorado State University, Fort Collins. Atmos. Sci. Paper 179, 1-95.

______, 1973: Cumulus convection and large-scale circulations, Part I: Broadscale and meso-scale interactions. Mon. Wea. Rev., 101, 839-855.

Harrison, E. J., 1973: Three-dimensional numerical simulations of tropical storms utilizing nested finite grids. J. Atmos. Sci., 30, 1528-1543.

Heffernan, R. F., 1972: Hurricane heat potential of the North Atlantic and North Pacific Oceans. M.S. thesis of the Naval Postgraduate School, Monterey, California, 109 pp.

Holton, J., 1971: A diagnostic model for equatorial wave disturbances: The role of vertical shear of the mean zonal wind. J. Atmos. Sci., 28, 55-64.

Hubert, L. F., A. F. Krueger, and J. S. Winston, 1969: The double intertropical convergence zone - fact or fiction? J. Atmos Sci., 26, 771-773.

Jordan, C. L., 1958: Mean soundings of the West Indies area. J. of Meteor., 15, 91-92.

______, 1964: On the influence of tropical cyclones on the sea surface temperature field. Proc. Symp. Tropical Meteorology, Wellington, New Zealand Meteor. Service, 614-622.

Kuo, H. L., 1965: On formation and intensification of tropical cyclone through latent heat release by cumulus convection. J. Atmos. Sci., 22, 40-63.

Kurihara, Y., and R. E. Tuleya, 1974: Structure of a tropical cyclone developed in a three-dimensional numerical simulation model. J. Atmos. Sci., 31, 893-919.

Landis, R. C., and D. F. Leipper, 1968: Effects of Hurricane Betsy upon Atlantic ocean temperature, based upon radio transmitted data. J. Appl. Meteor., 7, 544-562.

LaSeur, N. E., 1962: On the role of convection in hurricanes. Proc. of the Second Tech. Conf. on Hurricanes, Miami, Fla., 1961, Nat. Hurr. Res. Proj. Report No. 50, 323-334. (Available from the U. S. Weather Bureau, Miami, Fla.)

Leipper, D. F., 1967: Observed ocean conditions and Hurricane Hilda, 1964. J. Atmos. Sci., 24, 182-196.

______, and J. Jensen, 1971: Changes in energy input from the sea into hurricanes. Bull. Am. Meteor. Soc., 52, 928.

______, and D. Volgenau, 1972: Hurricane heat potential of the Gulf of Mexico. J. Of Phy. Ocean., 2, 218-224.

Lopez, R. E., 1968: Investigation of the importance of cumulus convection and ventilation in early tropical storm development. Colorado State University, Atmos. Sci. Paper No. 124, Fort Collins, 86 pp.

______, 1973a: Cumulus convection and larger scale circulations. Part II: Cumulus and mesoscale interactions. Mon. Wea. Rev., 101, 856-870.

______, 1973b: A parametric model of cumulus convection. J. Atmos. Sci., 30, 1345-1373.

Malkus, J. S., and H. Riehl, 1960: On the dynamics and energy transformation in steady-state hurricanes, Tellus, 12, 1-20.

Mathur, M. B., 1972: Simulation of an asymmetric hurricane with a fine mesh multiple grid primitive equation model. Ph.D. dissertation, Florida State University, Tallahassee, Florida, 162 pp.

Miller, B. I., 1964: A study of the filling of hurricane Donna (1960) over land. Mon. Wea. Rev., 94, 389-406.

______, 1969: Experiment in forecasting hurricane development with real data. ESSA Tech. Memorandum ERLTM-NHRL 85, Miami, Fla. 23 pp.

O'Brien, J. J., 1967: The non-linear response of a two-layer, baroclinic ocean to a stationary, axially-symmetric hurricane: Part II. Upwelling and mixing induced by momentum transfer. J. of Atm. Sci., 24, 208-215.

______, and R. O. Reid, 1967: The non-linear response of a two-layer baroclinic ocean to a stationary, axially-symmetric hurricane: Part I. Upwelling induced by momentum transfer. J. of Atm. Sci., 24, 197-207.

Ooyama, K., 1969: Numerical simulation of the life cycle of tropical cyclones. J. Atmos. Sci., 26, 3-40.

Palmén, E. H., 1948: On the formation and structure of tropical cyclones, Geophysica, Helsinki, 3, 26-38.

______, 1957: A review of knowledge on the formation and development of tropical cyclones, Proc. Tropical Cyclone Symp., Brisbane, December 1965, Wilke & Co., Ltd., Melbourne, 213-231.

Perlroth, I., 1967: Hurricane behavior as related to oceanographic environmental conditions. Tellus, 19, 258-268.

______, 1969: Effects of oceanographic media on equatorial Atlantic hurricanes. Tellus, 21, 230-244.

Ramage, C., 1974: Monsoonal influences on the annual variation of tropical cyclone development over the Indian and Pacific Oceans. Mon. Wea. Rev., 102, 745-753

Riehl, H., 1954: Tropical Meteorology, McGraw-Hill, New York, 392 pp.

______, 1957-1962: Much personal communication during this period.

Rosenthal, S. L., 1970: A circularly symmetric primitive equation of tropical cyclone development containing an explicit water vapor cycle. Mon. Wea. Rev., 98, 643-663.

Ruprecht, E., and W. M. Gray, 1974: Analysis of satellite-observed tropical cloud clusters. Colorado State University, Fort Collins, Atmos. Sci. Paper 219, 91 pp.

Sadler, J. C., 1967a: On the origin of tropical vortices. Working Panel on Trop. Dyn. Meteor. Naval Post Graduate School, Monterey, Calif., 39-75.

______, 1967b: The tropical tropospheric trough as a secondary source of typhoons and a primary source of tradewind disturbances. Final Rept. Cont. AF19 (628)3860, A. F. Cambridge Res. Lab., Bedford, Mass., Rept. 67-12, 44 pp.

______, 1974a: A role of the tropical upper tropospheric trough in early seasonal typhoon development. Tech. Paper No. 9-74, ENVPREDRSCHFAC, U. S. Navy Environmental Prediction Research Facility Report. 54 pp.

______, 1974b: Personal Communication.

Sartor, J., 1968: Monthly climatological wind fields associated with tropical storm genesis in the West Indies. Colorado State Univ., Ft. Collins, Atmospheric Science Research paper, 34 pp.

Simpson, R. H., 1971: The decision process in hurricane forecasting. Technical Memorandum NWS SR 53, National Weather Service, Southern Region, U. S. Department of Commerce, Miami, Florida.

______, and H. Riehl, 1958: Mid-tropospheric ventilation as a constraint on hurricane development and maintenance. Proc. of the Tech. Conf. on Hurricanes, Miami Beach, Fla., Nov. 10-22, 1958. D4-1 to D4-10.

Sundquist, H., 1970: Numerical simulation of the development of tropical cyclones with a ten-layer model. Part I. Tellus, 22, 359-390.

Wachtmann, R. F., 1968: Role of angular momentum transport in tropical storm dissipation over tropical oceans. Colorado State University, Fort Collins, Atmospheric Science Research Paper, 46 pp.

Wallace, J. M., 1970: Time-longitude sections of tropical cloudiness (December 1966-November 1967), ESSA Technical Report, NESC 56, National Environmental Satellite Center, Suitland, Md., 37 pp.

Whitaker, W. D., 1967: Quantitative determination of heat transfer from sea to air during passage of hurricane Betsy. Master's Thesis, Texas A&M University, College Station, Texas. 65 pp.

Williams, K. T., and W. M. Gray, 1973: A statistical analysis of satellite-observed trade wind cloud clusters in the western north Pacific. Tellus, 21, 323-336.

Yamasaki, M., 1968: Numerical simulation of tropical cyclone development with the use of primitive equations. J. Meteor. Soc. Jap., 46, 178-201.

Yanai, M., 1961: A detailed analysis of typhoon formation. J. Meteor. Soc. Japan, 39, 187-214.

______, 1963: A preliminary survey of large-scale disturbances over the tropical Pacific region. Proc. 3rd Conf. on Hurricanes and Tropical Meteor., Mexico City. Geofisica, 3, 73-84.

______, 1964: Formation of tropical cyclones, Reviews Geophys., 2, 367-414.

______, 1968: Evolution of a tropical disturbance in the Caribbean Sea region. J. of Meteor. Soc. of Japan, Series II, 46, 86-108.

______, S. Esbensen, and J. H. Chu, 1973: Determination of bulk properties of tropical cloud clusters from large-scale heat and moisture budgets. J. Atmos. Sci., 30, 611-617.

Zipser, E. J., 1964: On the thermal structure of developing tropical cyclones. Nat'l Hurr. Res. Proj. Report No. 67, 23 pp. (Available from the U.S. Weather Bureau, Miami, Florida),

APPENDIX

Data Sources for Various Calculations.

1. Seasonal vorticity was calculated from the monthly gradient level streamline charts of G. D. Atkinson and J. C. Sadler's 1970 report entitled "Mean Cloudiness and Gradient Wind Charts over the Tropics", (Air Weather Service Technical Report No. 215, Vol. II). Vorticity was calculated for each month and then averaged to obtain seasonal mean values.

2. Vertical shear of the horizontal wind from 950 to 200 mb was calculated from the low level data source listed above and from specially constructed 200 mb flow fields for the months of February, May, August, and November which were accomplished by the author at Colorado State University. The specially constructed 200 mb maps were made from the NOAA Monthly Climatic Data for the World where 200 mb monthly vector winds are listed. It was assumed that the February, May, August, and November 200 mb wind vectors were typical of those of the January-March, April-June, July-September, and October-December periods respectively. The vertical shear charts represent the magnitude of the mean wind vector differences between the 200 and 950 mb levels.

3. The oceanic thermal energy calculations were made from the ocean temperature depth data of the North Pacific as reported by Robinson and Bauer (1971). The other oceanographic temperature depth information was obtained from special printout data supplied to the author at cost by the National Oceanographic Data Center (Suitland, MD). This information contained special 5^{o} latitude-longitude seasonal bathythermograph averages for all ocean areas except the North Pacific.

These special listings included all bathythermograph data which the Oceanographic Data Center had through 1972. Most 5^{o} squares had ample sampling. Some 5^{o} squares in the Southern Hemisphere had only a dozen or so recorded seasonal temperature soundings. Nevertheless, this is the best information which is available. These records contain mean ocean temperatures and standard deviations of temperature and salinity by 10 m depth intervals. Although some 5^{o} squares are not well sampled, the seasonal energy calculations from this data are believed to be generally representative.

4. Θ_e gradients between the surface and 500 mb were calculated from monthly values of temperature and moisture from the NOAA Monthly Climatic Data of the World Listings for the months of February, May, August, and November. These months were taken as representative of the January-March, April-June, July-September, and October-December seasonal averages.

5. Relative humidity at 500 and 700 mb was obtained from the monthly mean of information of the NOAA Monthly Climatic Data of the World which was adjusted and smoothed to fit as well as possible the upper air moisture data contained in the United States Navy Marine Atlas of the World, Vols. I-V and the 1969 report by J. J. Taljaard, H. VanLoon, H. L. Crutcher and R. L. Jenne titled "Climate of the Upper Air, Southern Hemisphere, Vol. I, Temperature, Dew Point, and Height by Month at Selected Pressure Levels". Some degree of smoothing and reconciliation of these data sources was required. Special attention had to be paid to biases introduced by different sondes and diurnal moisture measuring errors. Figures 42, 57, 72 and 87 represent the author's best rectified values.

6. Initial tropical cyclone genesis location data was obtained from the author's previous global data on tropical cyclone origin and from updated information listed in the combined U.S. Navy Environmental Prediction Research Facility and the NOAA National Weather Records Center, Asheville, NC, printout tape of tropical cyclone date, position, intensity, etc. This tape was kindly furnished to the author by Mr. Samson Brand of the Navy Environmental Prediction Facility. The twenty year period of 1952-1971 was used in this study. The tropical cyclone origin points in the Northern Bay of Bengal may be excessive. Developing cyclones in this region often move inland before they become very intense. Some confusion in cyclone classification may be present. The author has no reason to question the basic reliability of the cyclone origin data from the other oceans.

7. Information on the characteristics of satellite-observed tropical cloud clusters and pre-cyclone disturbances was taken from previous and current Colorado State University studies on this subject by the author and his colleagues. Some of this cloud cluster information is contained in the reports of Williams and Gray (1973) and Ruprecht and Gray (1974). The tropical cloud cluster movies of Bohan (1968) are also helpful.

Final Note to Reader. Any of you who have handled large amounts of meteorological data know of the many difficulties in reconciling different data sources and coming to grips with fragmentary or non-existent information as is available over parts of the tropical oceans. The observational information contained in this report undoubtedly has some degree of inaccuracy. This is unavoidable. These possible data inaccuracies are, however, not felt to be of sufficient importance as to significantly alter any of the ideas or conclusions presented. Much effort was expended to come up with the best possible parameter analyses.

BIBLIOGRAPHY OF GENERAL TROPICAL DATA SOURCES

Atkinson, G. D., 1971: Forecaster's guide to tropical meteorology. Unpublished Air Weather Service (MAC) Technical Report No. 240, 300 pp. (Available from Hq., AWS, Scott AFB, IL).

________, and J. C. Sadler, 1970: Mean-cloudiness and gradient-level-wind charts over the tropics. Tech. Rept. 215, II, published by U.S. Air Weather Service (MAC).

Bohan, W. A., 1968: Tropical Pacific cloud patterns. ESSA Digital Product, 1967 (WAB 196), 16-mm film prepared by Walter S. Bohan Co., Park Ridge, IL.

Chief of Naval Operations, 1966: Components of the 1000 mb (or surface winds) winds of the northern hemisphere. NAVAIR 50-1C-51.

Crutcher, H. L., 1961: Meridional cross-sections - upper winds over the northern hemisphere. Tech. Paper No. 41, U. S. Dept. of Commerce, Superintendent of Documents, U. S. Government Printing Office, Washington, DC, 307 pp.

__________, and J. M. Meserve, 1970: Selected level heights, temperatures and dew points for the northern hemisphere. NAVAIR 50-1C-52, Navy Weather Service Command.

__________, and R. G. Quale, 1974: Mariners' worldwide climatic guide to tropical storms at sea. NOAA/EDS National Climatic Center and Naval Weather Service Publication (NAVAIR 50-1C-61). (Available from NOAA, Asheville, NC).

Fleet Weather Central/Joint Typhoon Warning Center, (FWC/JTWC) Guam. Annual Typhoon reports of 1946-1973. Summaries of aircraft reconnaissance reports, tropical cyclone tracks, forecasts, etc.

Gray, W. M., 1968: Global view of the origin of tropical disturbances and storms. Mon. Wea. Rev., 96, 669-700.

Krishnamurti, T. N., 1971: Observational study of the tropical upper tropospheric motion field during the northern hemisphere summer. J. of Appl. Meteor., 10, 1066-1096.

__________, and E. B. Rodgers, 1970: 200 mb wind field, June, July, August, 1967. Rept. No. 70-2. Dept. of Meteorology, Florida State University, 114 pp.

Malkus, J., 1960: The air and sea in interaction. Woods Hole Oceanographic Institution, 350 pp.

BIBLIOGRAPHY OF GENERAL TROPICAL DATA SOURCES (cont'd)

Robinson, M. K., 1973: Atlas of monthly mean sea surface and sub-surface temperature and depth of the thermocline, Gulf of Mexico and Caribbean Sea. Research Rept. of the Scripps Institute of Oceanography, Univ. of California, San Diego, CA, 105 pp.

__________ and R. A. Bauer, 1971: Atlas of monthly mean sea surface and subsurface temperature and depth of the top of the thermocline, North Pacific Ocean. Monterey, Fleet Numerical Weather Central, 72 charts.

Ruprecht, E. and W. M. Gray, 1974: Analysis of satellite-observed tropical cloud clusters. Colo. State Univ., Dept. of Atmospheric Science Paper No. 219, 91 pp.

Newell, R. E., et al., 1972: The general circulation of the tropical atmosphere. The M.I.T. Press, Cambridge, MA., 258 pp.

Simpson, J., 1973: The global energy budget and the role of cumulus clouds. NOAA Technical Memorandum FRL WMPO-8, 175 pp.

Taljaard, J. J., H. Van Loon, H. L. Crutcher, and R. J. Jenne, 1969: Climate of the upper air, Part 1, Southern hemisphere, Vol. 1, temperature, dew points and height. NAVAIR 50-1C-55, Navy Weather Service Command, Washington, DC.

U. S. Navy Marine Climatic Atlas of the World. Selected level temperatures and dew points for the northern hemisphere (NAVAIR 50-1C-52) 1 September 1966 (published by direction of Chief of Naval Operations) Superintendent of Documents, U.S. Government Printing Office, Washington, DC.

U. S. Navy Oceanographic Marine Climatic Atlas of the World, 1957-1959: Volumes II (North Pacific), III (Indian Ocean), IV (South Atlantic Ocean), V (South Pacific Ocean) and VII (Antarctic). Washington, DC.

U. S. Navy Oceanographic Atlas of the North Atlantic Ocean, Pub., 700, Section IV, 1963: U. S. Navy Oceanographic Office, Washington, DC, 235 pp.

U. S. Weather Bureau (NOAA) Monthly Climatic Data for the World, 1960-1968.

Williams, K. and W. M. Gray, 1973: A statistical analysis of satellite-observed trade wind cloud clusters in the Western North Pacific. Tellus, 21, 313-336. (Also see more expanded CSU Dept. of Atmospheric Science 1970 Project Report No. 161).

BIBLIOGRAPHIC DATA SHEET	1. Report No. CSU-ATSP-234	2.	3. Recipient's Accession No.
4. Title and Subtitle TROPICAL CYCLONE GENESIS			5. Report Date March, 1975 6.
7. Author(s) William M. Gray			8. Performing Organization Rept. No. CSU-ATSP-234
9. Performing Organization Name and Address Atmospheric Science Department Colorado State University Fort Collins, CO 80523			10. Project/Task/Work Unit No. 11. Contract/Grant No. NSF GA-32589X3
12. Sponsoring Organization Name and Address National Science Foundation Washington, D.C. 20550			13. Type of Report & Period Covered Project Report 14.

15. Supplementary Notes

16. Abstracts

A new global observational and theoretical study of tropical cyclone genesis is made. This is an extension of the author's previous study (Gray, 1968) on this subject. Cyclone initial genesis locations have been stratified by season for the 20-year period of 1952-1971. Wind, temperature and moisture information are averaged by season and by 5-degree latitude-longitude Marsden squares. It is observationally shown and physical reasons are given why seasonal cyclone genesis frequency is related to the product of the seasonally averaged parameters of: 1) low level relative vorticity, 2) Coriolis parameter, 3) inverse of the vertical shear of the horizontal wind from lower to upper troposphere, 4) ocean's thermal energy to 60 meters' depth, 5) moist stability from the surface to 500 mb, and 6) middle troposphere relative humidity. A seasonal forecast potential of cyclone genesis frequency is derived. This forecast potential very well specifies the location and frequency of global cyclone genesis. A general theory on cyclone frequency is advanced.

17. Key Words and Document Analysis. 17a. Descriptors

Tropical Cyclone Formation 551.515.53
Tropical Circulations 551.515.52
Tropical Cumulus Convection

17b. Identifiers/Open-Ended Terms

17c. COSATI Field/Group

18. Availability Statement	19. Security Class (This Report) UNCLASSIFIED	21. No. of Pages 121
	20. Security Class (This Page) UNCLASSIFIED	22. Price